# Interdecadal Changes in the Hydrometeorological Regime of the Pacific Northwest and in the Regional-to-Hemispheric Climate Regimes, and Their Linkages

Interdecadal Changes in the Hydrometeorological Regime of the Pacific Northwest and in the Regional-to-Hemispheric Climate Regimes, and Their Linkages

By J. J. Vaccaro

U.S. GEOLOGICAL SURVEY

Water-Resources Investigations Report 02-4176

Tacoma, Washington
2002

CONTENTS

FIGURES

TABLES

CONVERSION FACTORS, VERTICAL DATUM, AND ABBREVIATIONS

CONVERSION FACTORS

Multiply	By	To obtain
centimeter (cm)	0.3937	inch
meter (m)	3.281	foot
kilometer (km)	0.6214	mile
square kilometer (km^2)	0.3861	square mile
cubic meter per second (m^3/s)	70.07	acre-foot per day

Temperature in degrees Fahrenheit (^{o}F) may be converted to degrees Celsius (^{o}C) as follows:

$$^oC=(^oF-32)/1.8.$$

VERTICAL DATUM

Sea level: In this report, "sea level" refers to the National Geodetic Vertical Datum of 1929 (NGVD of 1929)—a geodetic datum *derived* from a general adjustment of the first-order level nets of both the United States and Canada, formerly called Sea Level Datum of 1929.

ABBREVIATIONS

CNP   Central North Pacific

HM   Hydrometeorological

NAO   North Atlantic Oscillation

PNA   Pacific/North America

PNW   Pacific Northwest centers of the Pacific/North America Index

swc   Snow water content

SO   Southern Oscillation

SOI   Southern Oscillation Index

SST   Sea-surface temperature

Interdecadal Changes in the Hydrometeorological Regime of the Pacific Northwest and in the Regional-to-Hemispheric Climate Regimes, and Their Linkages

By J.J. Vaccaro

ABSTRACT

Selected hydrometeorological (HM) data for the Pacific Northwest, and regional-to-hemispheric atmospheric-circulation data and sea-surface temperature (SST) data for the North Pacific, are examined for three successive interdecadal periods that are subsets of the instrumental record in order to estimate if their characteristics have changed. The HM data included monthly precipitation totals for 50 sites in western Washington and 29 climate divisions of the Pacific Northwest, and streamflow averages for 112 sites in Washington, Oregon, and Idaho. The atmospheric data included the Southern Oscillation Index (SOI), an index of the Pacific/North America (PNA) circulation pattern, measures of the westerly and northerly components of geostrophic flow, and a subset of the Northern Hemisphere 700-millibar geopotential height data; this subset of 162 grid points includes the area between 15° and 75°N, 110°W and 130°E. The SST data are for a 5°-grid between 20°N and 60°N, 110°W and 130°E. The atmospheric and SST data were examined not only because the HM regime is linked to regional-to-hemispheric climate regimes, but also to estimate the extent of climate shifts displayed by these data.

Three subsets of the record were identified as pre-1947 (PRE), 1947-76 (BASE), and post-1976 (POST) water years, based on an analysis of the HM data and previous studies. For each subset, means were calculated for the water year (October-September), the runoff season (March-August), the winter season (October-February), and a baseflow season (August-September). Differences in means and in ratios of the means between the BASE period and the PRE and POST periods were examined for changes.

Winter-season mean precipitation during both the PRE and POST periods was smaller than the BASE period, indicating a spatially consistent and distinct change in the HM regime during winter during the PRE and POST periods. For the runoff season, mean precipitation at most sites, in comparison to the BASE period, was smaller during the PRE period and larger during POST period, indicating that different HM regimes occurred during the runoff season for the PRE and POST periods. Water-year mean precipitation was less for both the PRE and POST periods because of decreases in winter-season precipitation; however, the water-year values for the POST period were not as small as those of the PRE period because more precipitation was concentrated in the runoff season.

During both the PRE and POST periods, the mean water-year discharge was less than the BASE period for all but 15 of the 112 sites. Fourteen of the 15 sites were in a well-defined region (southern Idaho and southeastern Oregon), and 13 of the 14 had larger means only during the POST period. Winter-season streamflow was less for all but 11 sites during both PRE and POST periods; the largest decreases in the mean, more than 30 percent, were for an area in central Oregon. Except for the sites that had larger mean water-year discharge, runoff-season means also were less than those during the BASE period.

Changes in the SOI and PNA index from the BASE period were generally similar to and consistent with those of the majority of the hydrologic data; dissimilarities were in well-defined regions and are attributed to the evolutionary nature of the regime shifts. Negative values of the SOI for the POST period were more persistent than those that have occurred during both the PRE and BASE periods. The changes in the PNA index and the geostrophic flow components during the POST period are consistent with drier and warmer conditions in the Pacific Northwest. The 700-millibar data display trends and differences between the BASE and POST periods; differences in composite anomalies for selected winter months between these periods show a well-defined PNA pattern. For many areas of the North Pacific, the record of SSTs shows a significant long-term trend of both increasing and decreasing temperatures, reflecting well-defined patterns, over the period from 1947 to present, and there have been large changes in monthly values between the BASE and POST periods, most related to differences in the spatial patterns. Other long-term geophysical time-series also display distinct shifts, especially at the 1946-47 boundary.

The changes in atmospheric and SST data are clearly linked to and have influenced the changes in the HM regime. Together, these changes suggest that the HM regime in the post-1976 period was different than anything reflected in the record analyzed in this study—a regime with less water-year precipitation and streamflow in all but one region, and secondarily, more runoff-season precipitation over part of the Pacific Northwest.

Of the two major interdecadal-regime boundaries, the 1946-47 boundary appears to have been hemispheric in nature, and is documented in Arctic ice-concentration data and two sea-level pressure indices. On the other hand, the 1976-77 boundary (known as the 1977 climate shift) appears to be mainly contained in North Pacific information, suggesting the influence of the ocean-atmosphere system over the tropics and North Pacific in mediating the 1977 climate shift. Understanding the causes of these two major shifts will provide valuable information for the planning and management of water resources in the Pacific Northwest.

INTRODUCTION

The study and interpretation of natural climate variability is important for improving the understanding of the potential effects of climate change on precipitation, temperature, and streamflow. Climatic variability and its subsequent effects on the forcing and feedback with regional hydrometeorological (HM) regimes have large implications for water-resource planning and operations. Natural climate variability and its effects can be studied at interannual-to-interdecadal time scales by analyses of information from such sources as ice and coral cores, varved sediments, and tree rings, or by retrospective analyses of instrumental records. Some analyses have identified "shifts" in the mean climate that are part of the natural variability. Although large shifts such as those associated with the Pleistocene-to-Holocene climate change are important for understanding natural variability, much smaller changes can have a large impact on regional water resources, especially considering the 5-to-20 year time frame of many water resource planning horizons and the nearly total utilization of water resources in some areas. These smaller climate changes, their spatial extent, and their linkages to the regional hydrometeorological regime in the Pacific Northwest are addressed in this report; for this study, the Pacific Northwest is defined to include the States of Idaho, Oregon, and Washington (fig. 1).
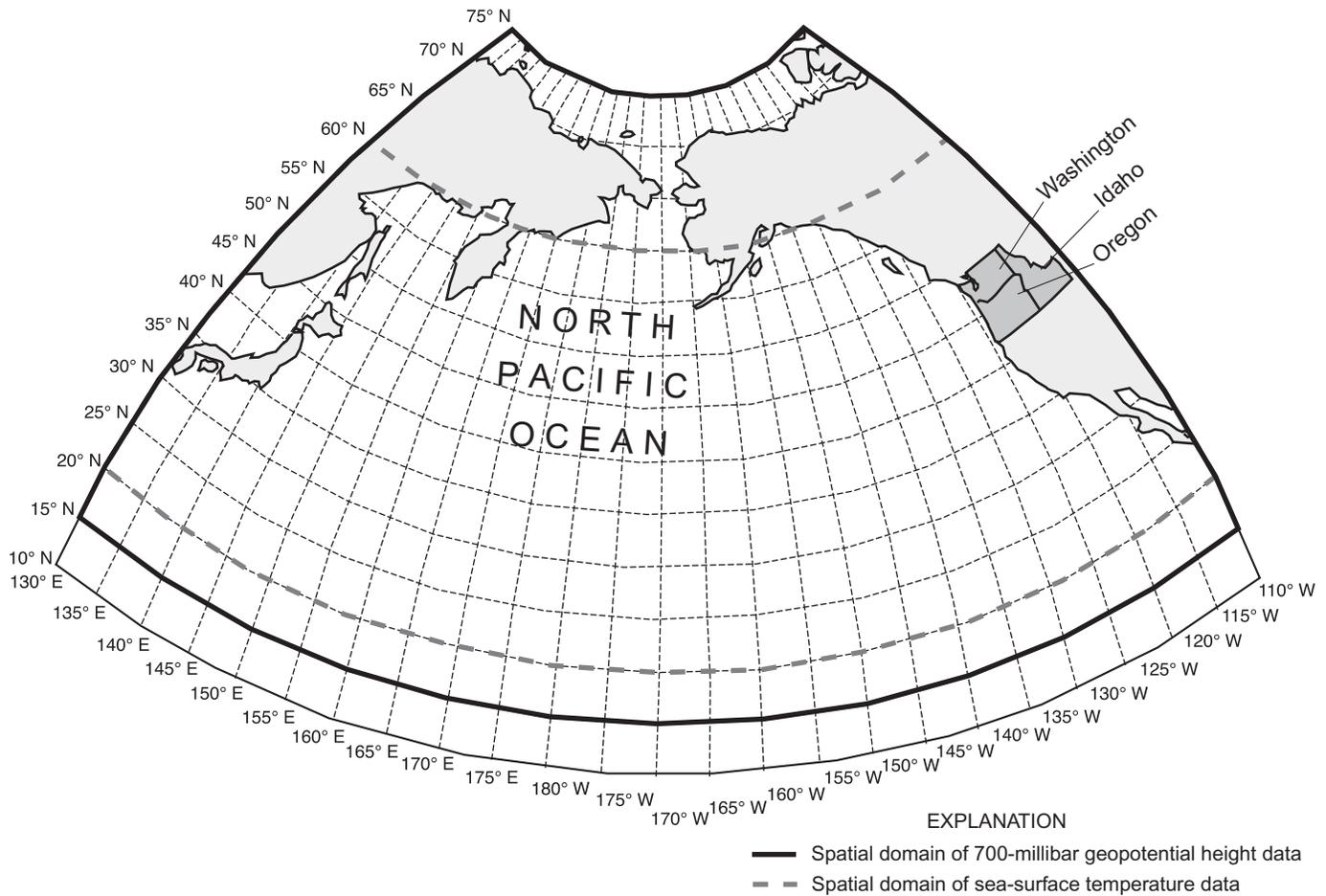
Figure 1. Relation of the location of the States in the Pacific Northwest study area to the North Pacific Ocean, and the spatial domain for the sea-surface temperature data and the subset of the 700-millibar geopotential height data.

The initial impetus for this study was the discovery of large, climatically forced, interannual variability in ground-water recharge in eastern Washington and Oregon and parts of northern Idaho (Bauer and Vaccaro, 1986, 1990; Vaccaro, 1992b). Time-series of recharge indicated not only the large interannual variability but also shifts in recharge, distinguished by long periods of generally below- or above-average values along with attendant interannual variability in the periods. These indications led to an analysis of precipitation characteristics in western Washington to determine if shifts were present that may affect long-term variations in ground-water recharge and streamflow in this region (Vaccaro, 1992a).

This report first presents a retrospective analysis of selected HM data for the Pacific Northwest, a region typified by dry, warm summers and by cold winters when most of the precipitation occurs. The objective of this analysis was to determine if there have been changes (shifts) in the HM regime on the interdecadal scale that may be important in the planning and management of water resources in the Pacific Northwest. Shifts were analyzed by determining differences in characteristics of the data between three subsets of the instrumental record that define three reasonably long interdecadal periods. The boundaries of the subsets are defined by the years 1946-47 and 1976-77, and differences in characteristics are referenced to the 1947-76 subset.

Because the HM regime in the Pacific Northwest is ultimately forced by and clearly linked to atmospheric-oceanic circulation (Namias, 1976b; Wallace and Gutzler, 1981; Yarnal and Diaz, 1986; Ropelewski and Halpert, 1986; Cayan and Peterson, 1989; Redmond and Koch, 1991; Cayan and Webb, 1992), selected atmospheric information and North Pacific sea-surface temperature (SST) data were also analyzed to determine if they exhibit shifts, to estimate if their variability is similar to the variability of the HM data, and to assess potential linkages but not cause-effect relations. The analysis of the atmospheric and SST information is more extensive than that of the HM data because of the importance of those data on a spatial scale that is much larger than the Pacific Northwest and because of the large amount of information analyzed.

In subsequent sections, the data series that are analyzed are described first, and relevant background information related to the atmospheric and SST data is briefly discussed. The general methods of analysis are then discussed. Next, the results of the analysis are presented, beginning with the HM data, followed by the atmospheric information, and ending with the SST information. Presentation of results is descriptive in nature, that is, estimated changes are described, discussed, and documented. The HM results are primarily described for each HM data set, and the relations between the data sets are of secondary importance, that is, each analysis can be considered separate with the primary purpose being to document interdecadal shifts in a particular data set. The overall findings are then described and potential linkages between the HM regime and the atmospheric and SST information are presented. Related information is then discussed; this information includes long-term data series (two sea-level pressure series and Arctic sea-ice concentration data) that were analyzed independently of the other data series. This later discussion is based on estimating the presence or absence of shifts in these long-term series in order to obtain some concept of the potential spatial extent (Pacific Northwest to Northern Hemisphere) of climate shifts and potential linkages. This additional analysis was done principally because of the practical importance of regime shifts and secondarily to independently check the reasonableness of the results, including the existence and timing of shifts, and to provide additional information for the earlier period of record (the first half of the twentieth century).

DATA

Hydrometeorological

Two sets of HM data were analyzed in this study—(1) monthly and annual precipitation totals for 48 sites in western Washington State and two sites in a small part of neighboring British Columbia, Canada, (fig. 2) and (2) monthly and annual streamflow averages for 112 sites in the States of Washington, Oregon, and Idaho. Precipitation in western Washington should be a reasonable measure of the net moisture input to the Pacific Northwest, and streamflow is the measured part of the output. Galdwell (1970), in a seminal study of streamflow generation in western Washington, showed that streamflow variability is "more climatically controlled than physically controlled." Thus, changes in the characteristics of the precipitation regime should be reflected in streamflow characteristics, primarily in western Washington and secondarily in other regions where streamflow variability is coherent (or in phase) with the precipitation variability; the coherency of regions in the Pacific Northwest based on precipitation and streamflow has been verified by Kresch (1994).
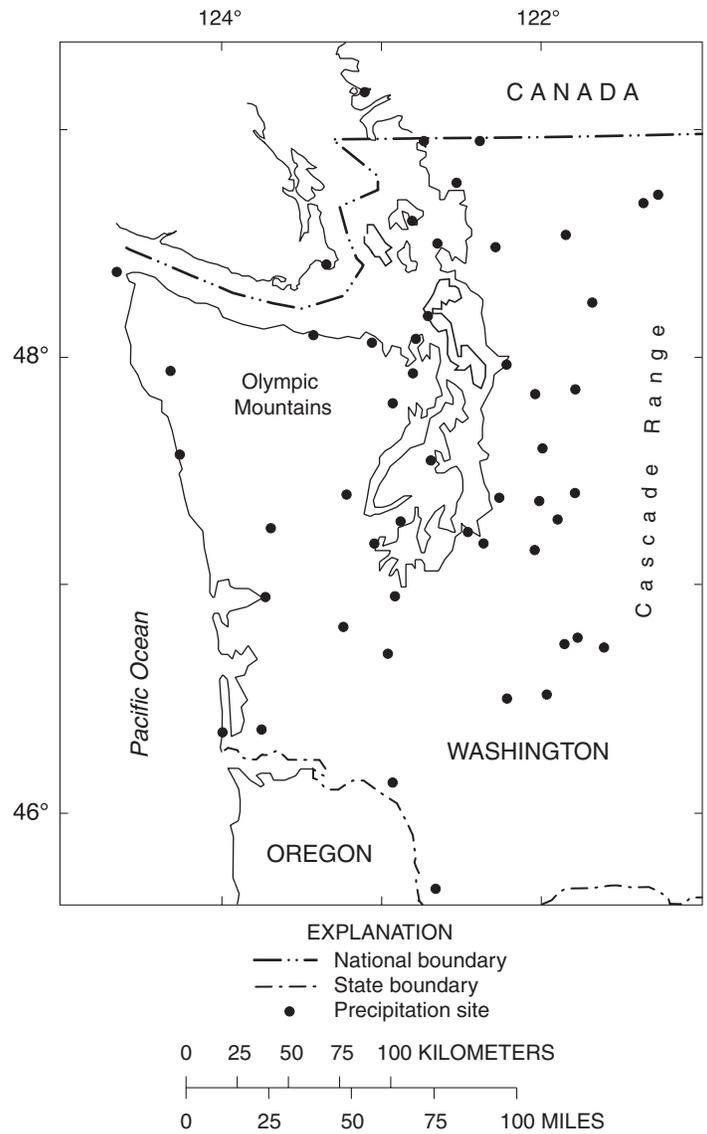
Figure 2. Location of the precipitation data sites.

Because the precipitation-data set is limited to individual sites in western Washington State and neighboring British Columbia, Canada, one additional data set that includes information for the complete region was briefly analyzed. This data set is the monthly mean precipitation for 29 climate divisions determined by the National Weather Service for Washington (10 divisions), Oregon (9 divisions), and Idaho (10 divisions); the climate divisions can be viewed at: http://lwf.ncdc.noaa.gov/oa/climate /onlineprod/drought/statelist.html. The analysis of this data set allows for testing the results of the site data, estimating the spatial coherency of the results, and identifying differences in the precipitation characteristics within the Pacific Northwest.

Precipitation

Precipitation data were obtained from three sources—digital data from the National Weather Service (written commun., 1989), published information for Washington (U. S. Department of Agriculture, 1916-1940, 1936; U. S. Department of Commerce, 1940-1988, 1956), and published information from Environment Canada (complete records). The western Washington data were checked and adjusted, if necessary, to assure and improve their quality. Data for one of the Canadian sites (Victoria) were used "as is" because of the quality of the records; the remaining two sites (located close to each other—Vancouver, Steveston) were averaged to obtain a smoothed effective series. This precipitation-data set was created as part of a regional ground-water study (Vaccaro, 1992a) and was initially analyzed as part of that study to identify occurrences of shifts and regions of similar precipitation variability and thus similar ground-water recharge variability and streamflow variability in western Washington.

Station histories of the western Washington sites were first checked for relocation of sites, dates of which were recorded. Months with missing digital data were compared to the published monthly data to determine if the values were actually missing. For all years with complete data, annual values were calculated and then verified with published annual values; for years with differences, monthly values were checked. Data were then analyzed, using simple statistical and graphical methods, for inhomogenieties due to station relocations. Monthly correlations /regressions, distance-weighted interpolation, and ratios between sites were calculated and used either to fill in missing data or to adjust monthly values due to station relocations. This technique was continued until (1) all data series with missing data (less than about 1 percent of the more than 38,000 monthly totals) were filled-in and (2) all data with inhomogenieties (based on station relocation) were eliminated.

The resulting data set is of reasonable high quality, has a good spatial distribution, and is representative of a large range in climatological regimes. Data for all sites include at least water years 1931-88 (a water year is the 12-month period October 1 to September 30 of the named year). Mean water-year precipitation at the sites ranges from 41 to 332 centimeter (cm), and the altitudes of the sites range from 2 to 1,654 meters (m). On the average, 66 percent of the water-year precipitation falls during the October-February period. Location of the sites are shown on figure 2, and typical mean monthly distributions of precipitation for selected sites are shown on figure 3. This data set, from the 50 sites, is referred to as the western Washington data set in this report.

The climate division data were analyzed for the years 1931-94. The starting year of 1931 was selected to correspond to the starting year of the above precipitation data and because prior to 1931 there were fewer sites used to calculate means for the divisional data. The ending year of 1994 was selected, in contrast to the 1988 end date for the precipitation data, to determine if regime changes are also identifiable in (persist through) this later period of record. Mean water-year precipitation for the climate divisions ranges from about 20 cm in southern Idaho to 250 cm in coastal Washington.
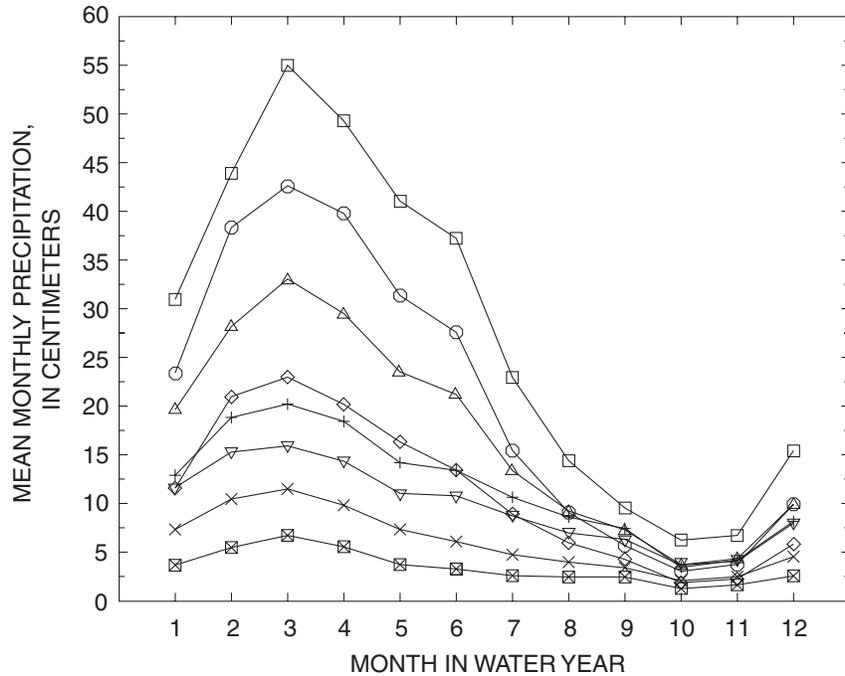
Figure 3. Mean monthly distribution of precipitation for selected sites.

Streamflow

Monthly and water-year streamflow data for 100 sites were obtained from the U. S. Geological Survey; 92 of the sites had records that extended from water year 1947 through water year 1992 (table 1). All but two of the sites measure unregulated flow. Data for an additional 12 sites were obtained from the U. S. Bureau of Reclamation (R. A. Larson, written commun., 1995); these sites are in a 14,374 square-kilometer (km^2) basin that supports one of the most extensive surface-water-irrigated agriculture activities in the three-State region. The records, as unregulated values, for these 12 sites extend from water year 1929 through water year 1989. A summary of selected streamflow information for the 112 sites (average record length of 64 years) is given in table 1, and the locations of the sites are shown on figure 4.

The streamflow data represent discharge from a diverse assemblage of physical settings and climatological regimes (table 1). The basins typify those ranging from glacier- and snowmelt-driven systems (maximum ratio of mean runoff-season (March-August) discharge to annual discharge is 1.60) to ground-water-driven systems (with a minimum ratio of mean runoff-season discharge to annual discharge of 0.55). Annual peak flows at various sites occur from October through July, further showing the range in settings. Typical long-term average hydrographs of daily discharge for a glacier-, a snowmelt-, and a ground-water-driven stream are shown on figure 5.

Table 1. Selected information for streamflow sites analyzed in this study

[**Site identifier:** location shown on figure 3; **Runoff,** mean of the mean monthly values for March through August; **Winter**, mean of the mean monthly values for October through February; **Baseflow**, mean of the mean monthly values for August and September; **Abbreviations**: km^2, square kilometer; m, meter; $m^3s^{-1} km^{-2}$, cubic meter per second per square kilometer; –, no altitude listed]

Site identi-fier	Period of record	Name	USGS station No.	Drainage area (km^2)	Altitude of gage (m)
1	1931-92	Thunder Creek	12175500	268	67
2	1921-92	Skagit River	12178000	3,008	122
3	1929-92	Sauk River above White.	12186000	389	283
4	1929-92	Sauk River near Sauk	12189500	1,827	81
5	1939-92	North Fork Nooksack River	12205000	268	379
6	1929-92	North Fork Stillaguamish River	12167000	670	27
7	1929-92	Skykomish River	12134500	1,369	63
8	1930-92	Snoqualmie River	12149000	1,543	0
9	1946-92	Cedar River	12115000	202	475
10	1946-92	Rex River	12115500	33	487
11	1946-90	Green River	12104500	245	451
12	1932-92	Puyallup River	12093500	440	107
13	1943-92	Nisqually River	12082500	340	441
14	1929-92	Chehalis River	12027500	2,291	37
15	1930-92	Satsop River	12035000	765	0
16	1919-92	Elwha River	12045500	688	60
17	1937-92	Dungeness River	12048000	399	173
18	1939-92	Duckabush River	12054000	168	73
19	1925-92	North Fork Skokomish River	12056500	145	232
20	1931-84	South Fork Skokomish River	12060500	194	31
21	1934-92	Quinault River	12039500	675	56
22	1930-92	Naselle River	12010000	140	7
23	1930-92	Cispus River	14232500	821	372
24	1930-93	East Fork Lewis River	14222500	320	108
25	1929-93	Kettle River	12401500	5,632	559
26	1923-93	Colville River	12409000	2,577	426
27	1892-93	Spokane River	12422500	10,982	517
28	1947-93	Little Spokane River	12431000	1,702	484
29	1943-93	Crab Creek	12465000	2,667	422
30	1927-93	Stehekin River	12451000	821	334
31	1929-93	Wenatchee River	12459000	2,560	313
32	1940-93	American River	12488500	202	822
33	1929-93	Klickitat River	14113000	3,320	88
34	1936-92	White Salmon River	14123500	988	34
35	1916-93	Big Wood River	13139510	1,638	1,613

Table 1. Selected information for streamflow sites analyzed in this study—*Continued*

Site identi-fier	Mean (m^3s^{-1})				Mean unit discharge ($m^3s^{-1}\ km^{-2}$)				Percent of annual (as ratio)		
	Annual	Runoff	Winter	Base-flow	Annual	Runoff	Winter	Base-flow	Runoff	Base-flow	Winter
1	10.0	14.3	5.0	13.8	0.037	0.053	0.018	0.051	1.43	0.50	1.38
2	125.2	146.1	109.4	89.9	0.041	0.048	0.036	0.030	1.17	0.87	0.72
3	31.9	37.7	28.7	15.3	0.081	0.096	0.073	0.039	1.18	0.90	0.48
4	123.2	143.3	111.6	70.7	0.067	0.077	0.060	0.038	1.16	0.91	0.57
5	22.1	27.0	17.1	19.9	0.081	0.099	0.063	0.073	1.23	0.77	0.90
6	53.9	45.3	71.2	16.6	0.079	0.067	0.105	0.025	0.84	1.32	0.31
7	111.2	122.6	112.2	39.0	0.080	0.088	0.081	0.028	1.10	1.01	0.35
8	106.1	99.7	127.2	35.9	0.068	0.064	0.081	0.023	0.94	1.20	0.34
9	7.4	7.7	8.1	1.8	0.036	0.038	0.040	0.009	1.04	1.10	0.25
10	2.9	2.7	3.5	0.7	0.086	0.080	0.104	0.021	0.94	1.22	0.25
11	10.8	11.7	11.6	1.9	0.044	0.047	0.047	0.008	1.08	1.07	0.17
12	20.1	19.9	21.9	14.4	0.045	0.045	0.049	0.032	0.99	1.09	0.71
13	21.7	23.1	21.9	14.1	0.063	0.067	0.064	0.041	1.06	1.01	0.65
14	78.9	48.1	130.7	8.1	0.034	0.021	0.056	0.003	0.61	1.66	0.10
15	57.0	36.1	91.5	10.9	0.074	0.047	0.118	0.014	0.63	1.61	0.19
16	42.4	43.0	46.6	20.3	0.061	0.062	0.067	0.029	1.02	1.10	0.48
17	11.3	12.8	10.4	6.3	0.028	0.032	0.026	0.016	1.14	0.93	0.56
18	11.7	11.4	13.6	4.4	0.068	0.067	0.080	0.026	0.98	1.16	0.37
19	14.3	13.0	17.9	4.3	0.097	0.088	0.121	0.029	0.91	1.25	0.30
20	21.1	14.5	32.2	4.7	0.107	0.074	0.163	0.024	0.69	1.52	0.22
21	81.9	65.6	112.7	27.1	0.120	0.096	0.165	0.040	0.80	1.38	0.33
22	12.0	7.0	20.2	1.9	0.084	0.049	0.142	0.014	0.58	1.68	0.16
23	37.4	43.2	35.5	14.1	0.045	0.052	0.043	0.017	1.15	0.95	0.38
24	20.9	15.2	31.4	2.8	0.064	0.047	0.097	0.009	0.73	1.50	0.13
25	43.0	77.3	8.1	11.2	0.008	0.014	0.001	0.002	1.80	0.19	0.26
26	8.4	11.9	5.2	2.5	0.003	0.005	0.002	0.001	1.43	0.63	0.30
27	191.0	269.6	125.3	50.5	0.017	0.024	0.011	0.005	1.41	0.66	0.26
28	8.6	10.3	7.3	3.9	0.005	0.006	0.004	0.002	1.20	0.84	0.46
29	1.8	2.0	2.0	0.3	0.001	0.001	0.001	0.000	1.08	1.11	0.17
30	39.9	63.8	15.1	27.6	0.048	0.077	0.018	0.033	1.60	0.38	0.69
31	86.7	132.6	44.0	32.7	0.033	0.051	0.017	0.013	1.53	0.51	0.38
32	6.6	9.8	3.6	2.1	0.032	0.048	0.018	0.010	1.50	0.55	0.32
33	43.8	51.2	39.9	21.9	0.013	0.015	0.012	0.007	1.17	0.91	0.50
34	31.7	34.8	30.9	18.6	0.032	0.035	0.031	0.019	1.10	0.98	0.59
35	12.7	20.4	4.8	6.6	0.008	0.012	0.003	0.004	1.61	0.38	0.52

Table 1.   Selected information for streamflow sites analyzed in this study—*Continued*

Site identi-fier	Period of record	Name	USGS station No.	Drainage area (km^2)	Altitude of gage (m)
36	1945-93	North Fork Big Lost River	13120000	291	2,078
37	1912-93	Boise River	13185000	2,124	992
38	1931-92	Boundary Creek	12321500	248	539
39	1919-92	Falls River	13047500	834	1,703
40	1920-93	Goose Creek	13082500	1,620	1,453
41	1929-93	Johnson Creek	13313000	545	1,419
42	1946-93	Lake Fork Payette River	13240000	122	1,566
43	1958-93	Little Lost River	13118700	1,126	1,792
44	1930-93	Lochsa River	13337000	3,020	442
45	1955-93	Marsh Creek	13075000	903	1,405
46	1951-93	Mores Creek	13200000	1,021	950
47	1930-93	Moyie River	12306500	1,459	798
48	1951-93	North Fork Coeur d'Alene River	12411000	857	757
49	1940-93	North Fork Coeur d'Alene River	12413000	2,291	640
50	1920-93	Portneuf River	13073000	1,459	1,499
51	1920-93	Salmon River at Salmon	13302500	9,625	1,192
52	1920-93	Salmon River at Whitebird	13317000	34,688	430
53	1930-93	Selway River	13336500	4,889	469
54	1946-93	South Fork Boise River	13186000	1,625	1,285
55	1921-93	St. Joe River	12414500	2,636	661
56	1934-93	Teton River	13055000	2,278	1,514
57	1920-93	Trapper Creek	13083000	135	1,469
58	1940-93	Weiser River	13258500	1,548	806
59	1940-93	Alsea River	14306500	855	14
60	1946-93	Elk Creek	14338000	330	455
61	1941-93	Johnson Creek	14211500	66	69
62	1932-93	Little North Santiam River	14182500	286	199
63	1936-93	Long Tom River	14166500	227	118
64	1920-93	Little Sandy River	14141500	56	219
65	1941-93	Luckiamute River	14190500	614	52
66	1948-93	Mckenzie River	14158500	235	919
67	1936-93	Molalla River	14198500	248	241
68	1940-93	Nehalem River	14301000	1,707	9
69	1936-93	North Fork of Middle Fork Willamette	14147500	629	313
70	1929-93	North Santiam River	14178000	552	484
71	1924-93	Rogue River	14328000	798	798
72	1936-93	Row River	14154500	540	260
73	1940-93	South Umpqua River at Tiller	14308000	1,149	302
74	1942-93	South Umpqua River nr Brock.	14312000	4,275	140
75	1934-93	Salmon Creek	14146500	299	445

Table 1. Selected information for streamflow sites analyzed in this study—*Continued*

Site identi-fier	Mean (m^{3}s^{-1})				Mean unit discharge (m^{3}s^{-1} km^{-2})				Percent of annual (as ratio)		
	Annual	Runoff	Winter	Base-flow	Annual	Runoff	Winter	Base-flow	Runoff	Base-flow	Winter
36	2.9	4.9	0.8	1.7	0.010	0.017	0.003	0.006	1.69	0.28	0.58
37	33.6	54.8	12.7	11.7	0.016	0.025	0.006	0.005	1.63	0.38	0.35
38	5.6	9.6	1.7	1.2	0.022	0.038	0.007	0.005	1.70	0.31	0.21
39	22.1	31.0	12.8	15.5	0.026	0.037	0.015	0.018	1.40	0.58	0.70
40	1.3	1.9	0.8	0.3	0.001	0.001	0.000	0.000	1.45	0.62	0.25
41	9.7	16.7	2.6	3.0	0.018	0.030	0.005	0.005	1.73	0.27	0.31
42	4.0	7.0	1.0	0.8	0.032	0.056	0.008	0.006	1.75	0.26	0.20
43	1.9	2.8	0.9	1.7	0.002	0.002	0.001	0.001	1.45	0.48	0.88
44	80.1	132.3	30.1	17.3	0.026	0.043	0.010	0.006	1.65	0.38	0.22
45	2.5	2.6	2.5	1.9	0.003	0.003	0.003	0.002	1.02	1.01	0.74
46	8.1	12.9	3.8	1.2	0.008	0.012	0.004	0.001	1.59	0.47	0.15
47	19.5	34.2	5.2	3.4	0.013	0.023	0.004	0.002	1.75	0.27	0.17
48	19.8	29.1	12.1	3.3	0.023	0.034	0.014	0.004	1.47	0.61	0.17
49	53.6	76.5	35.3	9.2	0.023	0.033	0.015	0.004	1.43	0.66	0.17
50	5.6	6.9	4.4	4.7	0.004	0.005	0.003	0.003	1.22	0.78	0.83
51	54.7	76.6	33.2	32.5	0.006	0.008	0.003	0.003	1.40	0.61	0.59
52	311.8	494.6	129.3	137.0	0.009	0.014	0.004	0.004	1.59	0.41	0.44
53	105.2	177.0	35.6	23.6	0.021	0.036	0.007	0.005	1.68	0.34	0.22
54	21.7	36.4	7.0	7.4	0.013	0.022	0.004	0.005	1.68	0.32	0.34
55	66.2	104.0	31.4	15.2	0.025	0.039	0.012	0.006	1.57	0.47	0.23
56	23.2	32.8	12.6	20.2	0.010	0.014	0.005	0.009	1.41	0.54	0.87
57	0.4	0.5	0.3	0.3	0.003	0.004	0.002	0.002	1.25	0.77	0.67
58	18.0	27.3	10.0	2.4	0.011	0.017	0.006	0.002	1.52	0.56	0.14
59	41.6	26.0	68.4	3.5	0.048	0.030	0.079	0.004	0.63	1.64	0.08
60	6.2	4.6	9.5	0.2	0.019	0.014	0.028	0.001	0.73	1.53	0.03
61	1.5	0.8	2.6	0.1	0.022	0.012	0.039	0.001	0.55	1.74	0.04
62	21.3	16.4	30.9	2.5	0.073	0.057	0.106	0.008	0.77	1.45	0.12
63	6.4	4.3	10.2	0.5	0.028	0.019	0.044	0.002	0.67	1.60	0.08
64	4.1	3.4	5.6	0.9	0.072	0.059	0.098	0.016	0.83	1.36	0.22
65	24.4	14.3	41.4	1.3	0.039	0.023	0.067	0.002	0.59	1.70	0.05
66	13.0	14.3	12.5	7.9	0.054	0.060	0.052	0.033	1.10	0.97	0.61
67	15.0	11.6	21.8	1.8	0.060	0.046	0.087	0.007	0.77	1.45	0.12
68	74.7	43.7	126.6	5.1	0.043	0.025	0.073	0.003	0.59	1.69	0.07
69	22.3	21.2	27.3	4.8	0.035	0.033	0.043	0.008	0.95	1.22	0.22
70	28.3	29.2	30.6	12.9	0.051	0.052	0.055	0.023	1.03	1.08	0.46
71	25.4	27.4	26.0	12.5	0.031	0.034	0.032	0.016	1.08	1.02	0.49
72	16.8	13.2	24.4	1.2	0.031	0.024	0.045	0.002	0.79	1.45	0.07
73	29.0	23.6	41.3	2.2	0.025	0.020	0.035	0.002	0.81	1.42	0.08
74	80.1	55.5	125.8	4.0	0.019	0.013	0.029	0.001	0.69	1.57	0.05
75	12.0	12.0	13.6	4.3	0.039	0.039	0.045	0.014	1.00	1.14	0.36

Site identi-fier	Period of record	Name	USGS station No.	Drainage area (km^2)	Altitude of gage (m)
76	1920-93	Sandy River	14137000	670	222
77	1929-93	South Fork Coquille River	14325000	432	60
78	1926-93	Siletz River	14305500	517	31
79	1936-93	South Santiam River	14185000	445	231
80	1935-93	South Yamhill River	14192500	340	71
81	1906-93	Umpqua River	14321000	9,420	27
82	1932-93	Wilson River	14301500	412	21
83	1926-93	Catherine Creek	13320000	268	939
84	1907-93	Deschutes River	14103000	26,880	51
85	1938-93	Donner Und Blitzen	13396000	512	1,296
86	1945-93	Grande Ronde River	13333000	8,371	483
87	1929-93	Imnaha River	13292000	1,592	591
88	1905-93	John Day River at Mcdonald	14048000	19,404	119
89	1930-93	John Day River at Service	14046500	13,030	497
90	1927-93	Malheur River	13214000	2,329	1,060
91	1922-93	Metolius River	14091500	808	601
92	1930-93	Middle Fork John Day River	14044000	1,318	775
93	1929-93	North Fork John Day River	14046000	6,451	597
94	1937-93	North Fork Malheur River	13216500	908	1,020
95	1950-93	Owyhee River	13181000	20,480	1,019
96	1922-93	Sprague River	11501000	4,044	1,280
97	1926-93	Squaw Creek	14075000	115	1,063
98	1934-93	Umatilla River above Meac.	14020000	335	565
99	1905-93	Umatilla River nr Umatilla	14033500	5,862	100
100	1918-93	Williamson River	11502500	7,680	1,264
101	1926-89	Yakima River near Martin	12474500	140	738
102	1926-89	Kachess River	12476000	161	666
103	1926-89	Yakima River near Easton	12477000	481	666
104	1926-89	Cle Elum River	12479000	519	640
105	1926-89	Yakima River at Cle Elum	12479500	1,267	579
106	1926-89	Yakima River at Umtanum	12484500	4,080	396
107	1926-89	Bumping River	12488000	181	1,014
108	1926-89	Tieton River	12491500	478	817
109	1926-89	Naches River	12494000	2,408	472
110	1926-89	Yakima River at Parker	12505000	9,369	270
111	1926-89	Yakima River at Prosser	12509500	13,908	183
112	1926-89	Yakima River at Kiona	12510500	<u>14,374</u>	<u>138</u>
Average				2,844	544

Table 1. Selected information for streamflow sites analyzed in this study—*Continued*

Site identifier	Mean (m³s⁻¹)				Mean unit discharge (m³s⁻¹ km⁻²)				Percent of annual (as ratio)		
	Annual	Runoff	Winter	Base-flow	Annual	Runoff	Winter	Base-flow	Runoff	Base-flow	Winter
76	38.0	36.0	45.9	11.9	0.056	0.053	0.068	0.017	0.95	1.21	0.31
77	22.2	14.2	36.2	1.1	0.051	0.032	0.083	0.003	0.64	1.63	0.05
78	42.2	25.6	69.8	4.6	0.081	0.049	0.133	0.009	0.61	1.66	0.11
79	23.0	19.0	32.1	2.5	0.051	0.042	0.071	0.006	0.82	1.40	0.11
80	17.1	9.7	29.4	0.9	0.050	0.028	0.085	0.003	0.57	1.72	0.05
81	209.1	165.2	299.1	33.6	0.022	0.017	0.031	0.004	0.79	1.43	0.16
82	33.1	19.8	55.0	3.7	0.079	0.047	0.132	0.009	0.60	1.66	0.11
83	3.3	5.5	1.2	0.9	0.012	0.020	0.004	0.003	1.65	0.37	0.28
84	163.7	166.7	168.8	123.7	0.006	0.006	0.006	0.005	1.02	1.03	0.76
85	3.5	5.5	1.7	1.3	0.007	0.011	0.003	0.002	1.54	0.49	0.35
86	85.5	124.8	51.3	23.0	0.010	0.015	0.006	0.003	1.46	0.60	0.27
87	14.3	23.3	5.6	4.8	0.009	0.014	0.003	0.003	1.63	0.39	0.33
88	58.6	86.9	35.9	5.4	0.003	0.004	0.002	0.000	1.48	0.61	0.09
89	54.5	80.6	33.4	5.2	0.004	0.006	0.003	0.000	1.48	0.61	0.10
90	5.4	7.8	3.5	0.4	0.002	0.003	0.001	0.000	1.46	0.65	0.07
91	42.0	43.4	41.0	39.1	0.051	0.053	0.050	0.048	1.03	0.98	0.93
92	7.2	11.3	3.6	0.9	0.005	0.008	0.003	0.001	1.57	0.50	0.12
93	36.4	56.0	19.6	3.6	0.006	0.009	0.003	0.001	1.54	0.54	0.10
94	3.8	5.6	2.1	1.3	0.004	0.006	0.002	0.001	1.49	0.55	0.35
95	27.5	41.8	15.3	4.2	0.001	0.002	0.001	0.000	1.52	0.56	0.15
96	16.3	20.8	12.9	6.5	0.004	0.005	0.003	0.002	1.28	0.79	0.40
97	2.9	3.7	2.0	2.7	0.025	0.032	0.017	0.023	1.29	0.70	0.92
98	6.4	7.9	5.6	1.3	0.019	0.023	0.016	0.004	1.24	0.88	0.21
99	13.7	15.7	14.0	0.9	0.002	0.003	0.002	0.000	1.15	1.02	0.07
100	29.4	34.8	25.7	15.7	0.004	0.004	0.003	0.002	1.18	0.87	0.53
101	9.5	11.4	8.5	2.4	0.066	0.080	0.060	0.017	1.21	0.90	0.26
102	8.2	10.3	7.1	1.4	0.050	0.063	0.043	0.008	1.25	0.86	0.17
103	25.3	30.9	22.4	5.4	0.052	0.063	0.046	0.011	1.22	0.89	0.21
104	26.1	37.2	16.6	8.3	0.050	0.071	0.031	0.016	1.43	0.64	0.32
105	57.0	75.3	43.5	16.2	0.044	0.059	0.034	0.013	1.32	0.76	0.28
106	77.5	102.8	58.2	22.9	0.019	0.025	0.014	0.006	1.33	0.75	0.30
107	8.1	11.4	5.4	2.5	0.044	0.062	0.029	0.014	1.40	0.66	0.31
108	14.3	19.3	9.7	8.3	0.029	0.040	0.020	0.017	1.35	0.68	0.58
109	47.7	69.0	28.9	16.7	0.020	0.028	0.012	0.007	1.44	0.61	0.35
110	131.8	177.8	95.7	38.0	0.014	0.019	0.010	0.004	1.35	0.73	0.29
111	131.8	177.8	95.7	38.0	0.009	0.013	0.007	0.003	1.35	0.73	0.29
112	152.6	196.2	120.7	47.0	0.010	0.013	0.008	0.003	1.29	0.79	0.31
Average	39.7	47.7	35.8	13.4	0.034	0.035	0.037	0.011	1.21	0.92	0.36
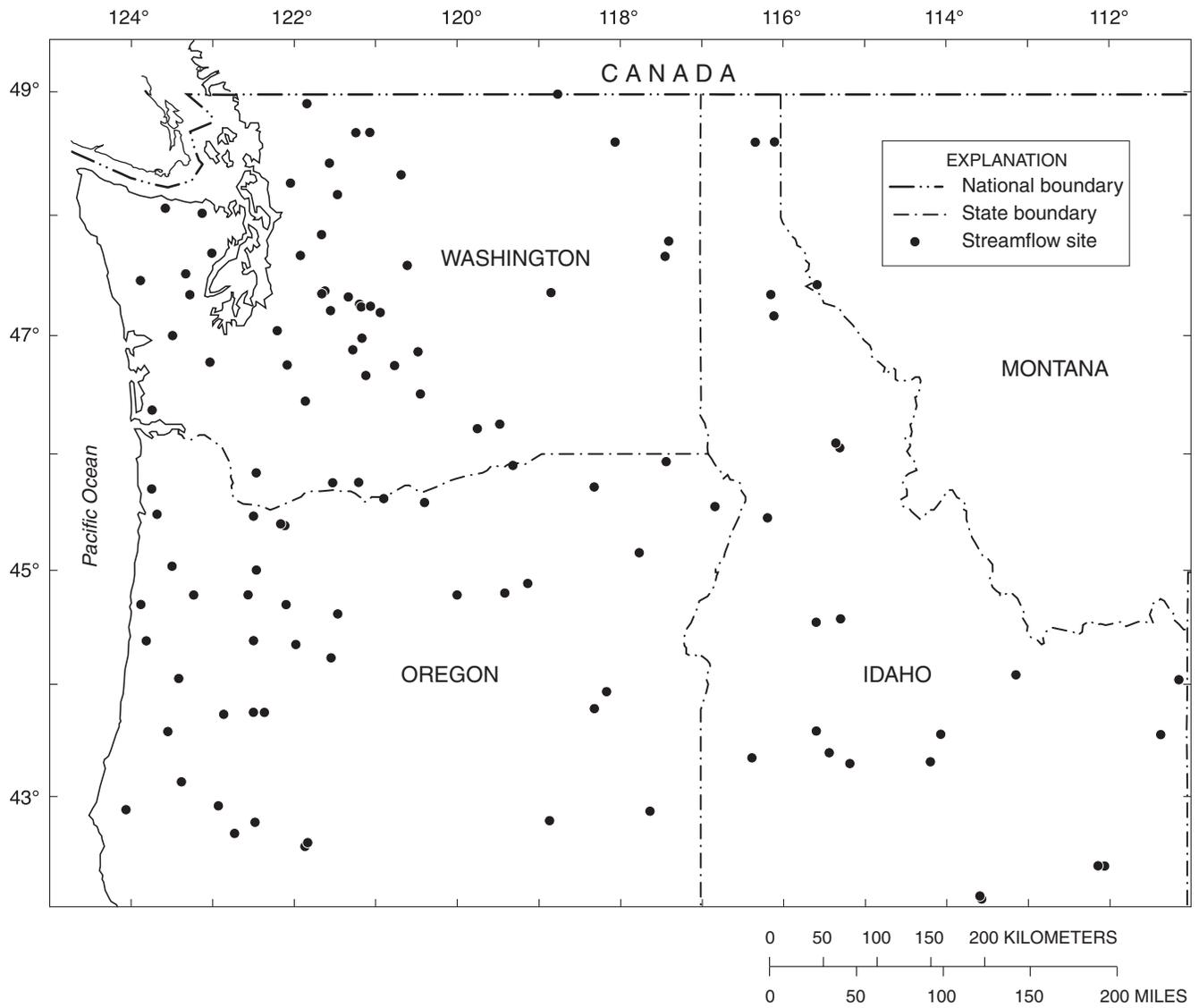
Figure 4. Location of the streamflow data sites.
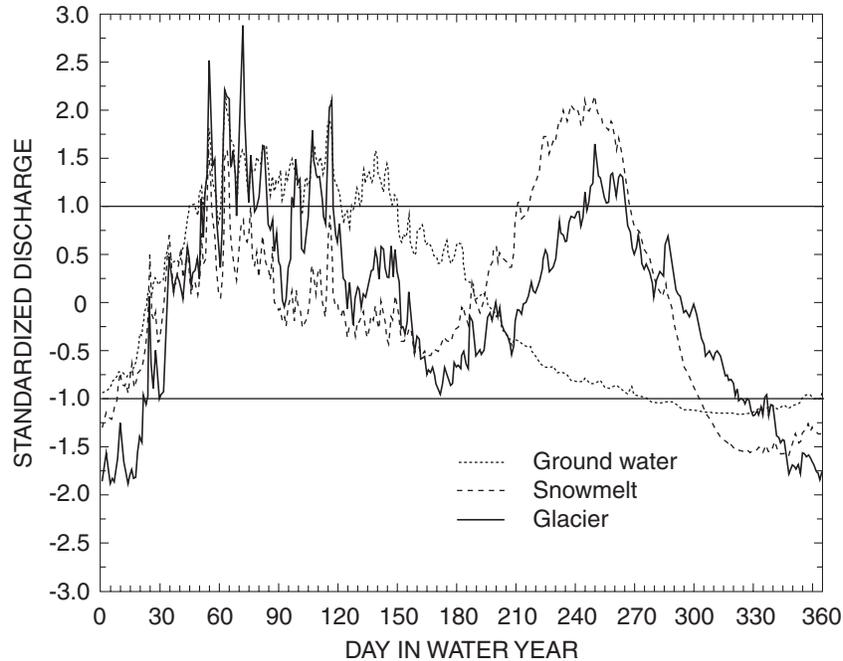
Figure 5. Typical long-term hydrographs for streams in the Pacific Northwest.

The hydrographs are representative of glacier-driven streams (site 12, table 1), snowmelt-driven streams (site 7, table 1), and ground-water-driven streams (site 22, table 1). Each value plotted is the mean daily discharge for the period of record for each stream. Horizontal lines indicate one standard deviation.

Atmospheric and Sea-Surface Temperature

The atmospheric information includes the Southern Oscillation Index (SOI)—an index of the Southern Oscillation (SO)—of the National Oceanic and Atmospheric Administration, Climate Analysis Center (Ropelewski and Jones, 1987) and diamond-grid, monthly 700-millibar (mb) geopotential heights and anomalies for the Northern Hemisphere (D.R. Cayan, U.S. Geological Survey, 1993, written commun.). The heights of the 700-mb pressures effectively portray circulation in the mid-troposphere, typically about 3 kilometers (km) high in the North Pacific region. The SST data set consists of 5°-gridded monthly means and anomalies for the area 20°N-60°N, 110°W-130°E (D. R. Cayan, U.S. Geological Survey, 1993, written commun.); figure 1 shows the spatial domain for the SST data. The water years of record analyzed in this study for the SOI, SSTs, and the 700-mb data are 1933-94, 1947-92, and 1947-91, respectively; the SST record starts in January 1947, and the 700-mb record in December 1946. Monthly anomalies for the 700-mb and

SST data sets were calculated by Cayan (U.S. Geological Survey, 1993, written commun.) using a base period of calendar years 1947-72.

The SOI is calculated as the standardized difference between standardized monthly values of sea-level pressure at Tahiti and Darwin, Australia; standardized values are obtained by subtracting the mean from each value and then dividing by the standard deviation, yielding a mean of zero and a standard deviation of one. The SOI is a measure of the strength of the equatorial atmospheric circulation, which is largely driven by the differences between persistent low- and high-pressure cells present in the region (Julian and Chervin, 1978; Horel and Wallace, 1981). Generally, high pressures at Darwin and low pressures at Tahiti result in easterly flow (a positive SOI). When the difference diminishes (a small or negative SOI), the easterly flow also diminishes and may even become westerly; these changes are associated with changes in warm and cool SSTs in the equatorial Pacific.

A large negative SOI is generally associated with the well known El Niño/Southern Oscillation phenomenon or a warm event, which generally elicits extratropical responses in circulation and affects SSTs over much of the North Pacific (Bjerknes, 1969; Namias, 1976a) due to the changes in the equatorial energy distribution. A large positive SOI is generally associated with a La Niña or a cool event. For a detailed analysis of the Southern Oscillation phenomenon and its effects (including those on circulation, SSTs, biota, and HM regimes), see American Geophysical Union (1987) and Diaz and Markgraf (1992).

One mid-latitude response associated with a negative SOI is the Pacific/North America (PNA) circulation pattern (Bjerknes, 1969; White and Walker, 1973; Wallace and Gutzler, 1981), which is a dominant winter mode of interannual variability in the Northern Hemisphere and, in particular, the Pacific Northwest (Namias, 1981; Wallace and Gutzler, 1981; Horel and Wallace, 1981; Barnston and Livezey, 1987). In turn, a reverse-PNA pattern is generally associated with a positive SOI. A strong PNA (negative SOI) is generally associated with drier and warmer conditions in the Pacific Northwest, and a strong PNA (positive SOI) with colder and wetter conditions (Yarnal and Diaz, 1986; Cayan and Peterson, 1989; Redmond and Koch, 1991; Cayan and Webb, 1992; Kahya and Dracup, 1992). During an occurrence of both a strong PNA pattern and a warm event, there generally is a large change in the mean position of the jet stream over the North Pacific, as it splits into northeastward and southeastward components. The PNA pattern typically is reinforced by changes in the tropical SSTs, whereas the reverse-PNA pattern is dynamically related to changes in circulation in the mid-latitude regions and not to tropical forcing (Yarnal and Diaz, 1986). Namias (1975) describes the rapid transition in 1957 from a strong PNA pattern in November to a strong reverse-PNA pattern in December that he attributes to the development of a mid-latitude eastern Asiatic trough. This explanation is consistent with the dynamical model of Yarnal and Diaz (1986), which also identifies why there is coherency between the reverse-PNA pattern and cool events.

The degree to which the atmospheric mid-latitude response and SSTs are affected by the SO appears to depend on the extent and magnitude of the movement of warm SSTs from the western equatorial Pacific to the eastern equatorial Pacific, resulting from decreased easterly flow along the equator that is associated with a negative SOI. The change in the equatorial SSTs affects the tropical energy distribution, which in turn affects the transport of energy to mid-latitude regions and thus elicits large changes in mid-latitude atmospheric circulation. The International dateline defines a region in which, in the mean, the sea surface slopes downward to the east and is relatively flat to the west where the western Pacific contains the world's ocean's largest pool of warm water (Wyrtki, 1984). The effects on the mid-latitude response and equatorial SSTs start to become more influential as the warm water moves eastward and reaches beyond about 180°W, and, conversely, the effects decrease as the warm water dissipates and is replaced by colder water (see Wyrtki, 1985; Cane and Zebiak, 1985). Thus, not only do the extremes of the SO elicit large responses, but all stages of the SO are influential because of its varying effect on the mid-latitude response and SSTs, which are distinctly linked to the HM regime. Additionally, because of the mean winter atmospheric-circulation conditions that prevail in the Pacific Northwest when the SO is about average, the average state is also important.

A PNA index was calculated using the monthly 700-mb anomalies for the centers of Horel and Wallace (1981). This PNA has three centers—one south of the Aleutian Islands at 45°N,165°W, one in southwestern Canada at about 55°N,115°W, and one over the southeastern Unite States at 30°N,85°W (Horel and Wallace, 1981; Barnston and Livezey, 1987). The first two centers greatly influence atmospheric flow and the climatology of the Pacific Northwest (Yarnal and Diaz, 1986; Cayan and Peterson, 1989). The center south of the Aleutians consists of an area of anomalously low pressures—referred to as the Aleutian Low or the North Pacific Low. The importance of the Aleutian Low in mediating circulation over much of the continental United States has been recognized since the early 1900's (see discussion in Namias, 1976b). The center in southwestern Canada is an anomalously high-pressure region. These two centers generally are in phase, with a deepening of the Aleutian Low concurrent with a strengthening of the high-pressure ridge. This dipole is nearly reversed for a reverse-PNA pattern, with the Aleutian Low having anomalously high pressures that are translated slightly west and north and the high-pressure region having anomalously low-pressures that are translated slightly west and south.

An excellent representation of this pattern (not shown) can be obtained from the January composite of the 700-mb anomalies for water years 1950, 1956, and 1974—the years when both water-year and March-August streamflow for most of the Pacific Northwest were above the 80th percentile values (this co-occurrence is not common). The 700-mb composite anomalies for winters with the co-occurrence of below-normal coastal air temperatures and a cold event also display the reverse-PNA pattern (fig. 6 of Yarnal and Diaz, 1986). Because of the regional, in contrast to hemispheric, importance of this dipole, an index (PNW) was calculated using both the 700-mb heights and anomalies for these two Pacific Northwest centers of the PNA index.

The monthly 700-mb data were used in several ways, the first of which was to calculate the PNA and PNW indices. The PNA index was calculated similar to the method of Horel and Wallace (1981), by subtracting the average of the anomalies for the Aleutian Low and southeastern centers from the anomalies for the southwestern Canada center. For the PNW index, the southwestern center was dropped from the equation. Second, two indices or measures were calculated on the basis of differences in geopotential height at two pairs

of grid points to estimate the relative strength of the monthly westerly and northerly components of geostrophic flow (centered on eastern Vancouver Island, British Columbia); the pairs were 45°N-55°N, 125°W for the westerly component and 50°N, 120°W-130°W for the northerly component. Third, the geopotential height field of these two pairs of grid points was also analyzed using an index.

Last, a subset of the 700-mb data was analyzed; this subset was chosen to closely correspond to the spatial extent of the SST data set and to include the Pacific Northwest centers of the PNA index. This subset of 162 grid points includes the area between 15°-75°N, 110°W-130°E and thus extends over most of the North Pacific (see figure 1 for spatial domain). Generally, anomalous patterns of 700-mb heights and SSTs are well related (Namias, 1965), with this linkage being very strong in the area of the Aleutian Low. For the Aleutian Low and its negative phase, anomalously colder SSTs are associated with northerly atmospheric flow and anomalously warmer SSTs with southerly flow. Thus, there should be some consistency in the results of the analyses of the atmospheric information and the SST data.
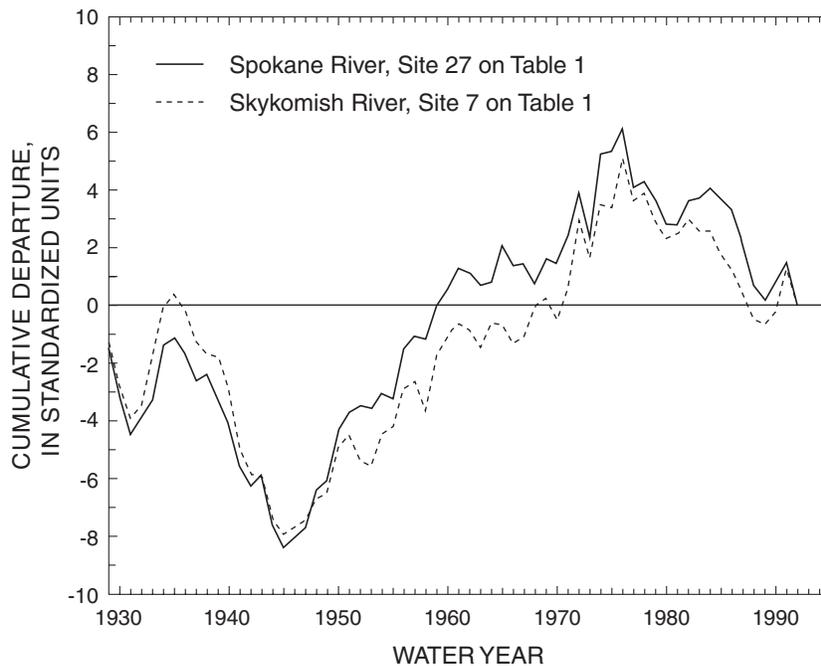
Figure 6. Cumulative departures of water-year streamflow for an eastern Washington stream (Spokane River) and a western Washington stream (Skykomish River).

A strong positive PNA index generally is associated with increased meridonal flows and weak westerlies, whereas a strong negative PNA index (reverse-PNA) generally is associated with strong zonal flow and strong westerlies. The northerly component is about 20 percent of the magnitude of the westerly component, mainly because, as a first approximation, the lines of equal geopotential generally parallel latitude lines over this region of the Pacific Northwest. Typically, the fall-to-early spring progression of flow near the Pacific Northwest coastline changes from the southwest to the northwest and then back to the southwest. Northerly flows are not that common, especially on a monthly-average basis, and are associated with dry, cold winter or dry, warm summer conditions; that is, dry continental air masses in contrast to maritime air masses. Additionally, on a monthly basis, the geopotential height field (defined as the average of the two pairs of grid points) is relatively stable, with its standard deviations being about 2 orders of magnitude smaller than its long-term means. Differences and changes in the westerly, northerly components and the average height field associated with them are reasonable measures of the Pacific Northwest atmospheric conditions and capture more of the regional atmospheric-circulation variability than do the PNA and PNW indices. As shown by Speers and Mass (1986), small changes in atmospheric-flow direction along coastal Washington can have large effects on downstream precipitation in western Washington; this is due to the net-moisture fluxes associated with different circulation patterns and the attendant orographic effects on the spatial distribution of precipitation. Other investigators have used circulation measures such as these, for example, in the analysis of precipitation in western Washington and British Columbia (Leytham, 1982), in the analysis of precipitation in part of the Pacific Northwest that was defined by a rotated factor analysis (Walsh and others, 1982), and in the study of estuary dynamics in the Pacific Northwest (Ebbesmeyer and others, 1989).

The atmospheric and SST information analyzed thus includes hemispheric measures (the SOI and the PNA index), North Pacific measures (a subset of the 700-mb data, the SST data, and the PNW index), and regional measures (westerly and northerly components, the average height field, and a coastal SST from the gridded North Pacific data series).

METHODS OF ANALYSIS

The analyses and techniques are based on averaging the data and measures over pre-defined successive periods of record and estimating if the data (monthly-seasonal-annual) within these periods have different characteristics, regardless of the overall intermonthly-to-interannual variability in those periods of records. This method is based on the concept that the observed data within a period indicate distinct regimes that reflect a persistent change in the mean, inhomogenieties near the boundaries or, in the case of the HM data, differences in climatic forcing between the interdecadal regimes. Although much of the data displays rather abrupt shifts, the data also show more complex relations, as will described later, and other shifts that are not captured by using defined periods of record. For this analysis, causes of potential changes in the HM regime are not explored; only potential linkages to the circulation features and SSTs are explored, generally using simple graphical analysis. The last part of the analysis explores the timing of regime shifts and their spatial coherency.

Periods of Interdecadal Regimes

The selected periods for averaging and analysis were (1) from the beginning of record through water year 1946, (2) water years 1931-46, (3) water years 1947-76, (4) water years 1977-88, and (5) water year 1977 to end of record. Periods 1, 2, 4, and 5 vary to take maximum advantage of the available data. Periods 1 and 2 generally correspond to a dry regime throughout the Pacific Northwest (a decrease in streamflow in the Pacific Northwest from the turn of the century to the late 1940's was noted early on by McDonald and Riggs (1948)); period 3 to a wet regime; and periods 4 and 5 to a dry regime. Herein, when results are discussed, periods 1-2 are referred to as PRE, period 3 as BASE, and periods 4-5 as POST.

The 1946-47 and 1976-77 boundaries of the interdecadal periods are clearly defined in much of the data; the 1976-77 boundary is well documented and is often referred to as the 1977 climate shift (Miller and others, 1994a,b). Additionally, using intervention analysis, Francis and others (1995) have shown distinct and sudden regime shifts at 1928, 1947, and 1977 for selected fish populations in the North Pacific and changes in oceanic circulation in the eastern North

Pacific, suggesting large-scale effects (and their persistence) because of changes in climatic regimes, including ocean currents, during these periods. Ebbesmeyer and others (1989) have shown shifts at 1925-26, 1946-47, and 1976-77 for an index developed for the Pacific Northwest that was used to analyze decadal variability of oceanic, atmospheric, and hydrologic parameters.

The cumulative departures for two streamflow sites in Washington, (one in western Washington—site 7 in table 1 and one in eastern Washington—site 27 in table 1), which are about 500 km apart, show generally above-average streamflow after about 1947 and below-average after about 1977 (fig. 6). Indeed for site 27 (table 1), 20 of the 30 annual values for the BASE period were larger than the long-term mean, and 8 of the 10 BASE-period values that were smaller than the mean were within one-half of a standard deviation of the mean. Cumulative departures and 9-year moving averages for precipitation at a western Washington site (Cedar Lake—considered to be a reference site for precipitation in the Cascade Range in western Washington) and streamflow at the eastern Washington site 27 not only show changes near these years (fig. 7) but also the information on figure 7 strongly suggests that there is large-scale spatial coherence between precipitation and streamflow for parts of the Pacific Northwest.

No single pre-1947 regime shift is well defined in the HM data series. Analysis of the precipitation and streamflow data using tests of means for various pieces of the pre-1947 record compared to the same length of the BASE-period record (having a minimum length of 10 years--that is, decadal-scale shifts) suggests several boundaries—1908-10, 1920-22, 1927-28, and 1934-35. Considering the dates of the earlier regime shifts identified by Francis and others (1995) and Ebbesmeyer and others (1989), these differences in years may result from spatial variations in the response of precipitation and streamflow to persistent anomalies in the direction of atmospheric flow along the Pacific Northwest coast and the evolutionary nature of these anomalies. These aspects are part of the more complex relations that will be described later. For example, the information on figure 7B shows precipitation and streamflow becoming closer into phase in the mid-1920's, which suggests not only a shift but also complex changes in the climatic forcing during that period.
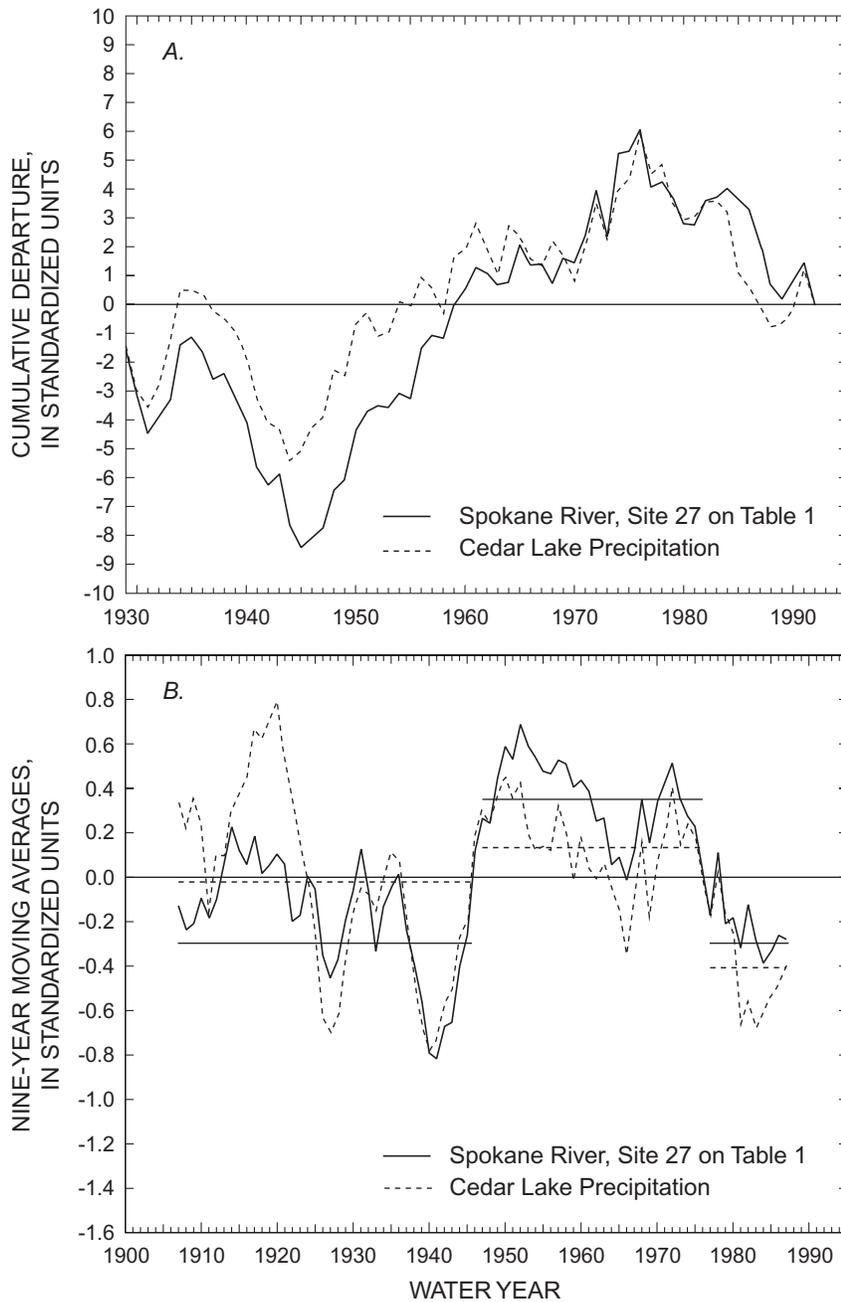
Figure 7. Cumulative departures and 9-year moving averages of water-year streamflow for an eastern Washington stream and of water-year precipitation at a western Washington precipitation site.

The precipitation site is located in the central part of the western Cascade Range at 475 meters in the transient-snow zone and was used as a reference site for precipitation in western Washington. Horizontal lines in (b) represent, from left to right, the averages for the PRE, BASE, and POST periods.

For the early (PRE) period of record, the streamflow data from period 1 were analyzed because the lengths of records for the 94 streamflow sites with data prior to water year 1947 are variable (however, only 8 sites have data prior to 1920); and the precipitation data from period 2 were analyzed because all 50 sites have records for water years 1931-46.

Because precipitation was well above average in water years 1933 and 1934 and may have had a large influence on the 16-year mean for period 2, precipitation data from period 1, starting at 1921 was analyzed to test the robustness of the results obtained using the data from period 2. Records for 34 of the 50 sites extend back to at least 1921, which was also identified as a year in which a regime shift occurred for many of these sites. For the middle (BASE) and late (POST) period of record, the precipitation data were analyzed with respect to periods 3 and 4, respectively; and the streamflow data with respect to periods 3 and 5 (records for 98 sites extend to water year 1992, see [table 1](#)). Atmospheric and SST information are analyzed for periods 3 and 5; the SOI is also analyzed for period 1 beginning in water year 1933.

The precipitation data for the climate divisions are analyzed on the basis of successive equal lengths of record bounded by the interdecadal boundaries. For comparing the PRE and BASE periods, 16 water years from each period are used (1931-46 and 1947-62, respectively). For the POST and BASE period comparison, 18 years of each record are used (1977-94 and 1959-76, respectively).

The principal emphasis of the study was to determine changes between regime periods within each data set using the longest record that was available over the course of this study. Analysis of subsets of the precipitation, streamflow, atmospheric, and SST data based on equal record lengths showed no significant differences from the results obtained using variable length records. Additionally, spatial correlation structures between the HM data and 700-mb and SST data and the coherency of response of the HM regime within regions of the Pacific Northwest (based on principal component analysis) indicate that using different lengths of records for defining the PRE and POST periods would produce similar results. For example, the ratios of mean (monthly and annual) precipitation for period 4 to the mean streamflow for periods 4 and 5 are nearly identical; in practical terms, there was no interdecadal regime shift between 1988 and 1993. Thus, not only do the analyses using the periods of record defined above meet the main objective, but also comparisons can be made between data sets, even though the analyses employed different periods of records.

Time Periods for Comparing the Interdecadal Means

The HM data are principally analyzed within the framework of differences in means (PRE or POST minus BASE period) and ratios of means (PRE/BASE or POST/BASE) for water year, winter season (October-February), and runoff season (March-August). In addition, streamflow values were analyzed for the baseflow season (August-September) because of the importance of low-flow values for meeting fisheries, water-supply, hydroelectric, and recreational needs. Based on analysis of 7- to 90-day low-flow values for many of the streamflow series, the August-September period appears to capture the low-flow characteristics of most of the 112 streams (see [fig. 5](#), days 305 to 365). Streamflow during this period mainly reflects, in order of importance, ground-water discharge, snowmelt, and glacier melt, all of which contain memory of prior precipitation and temperature regimes. Results are referenced to the BASE period, except when differences between PRE and POST are being explicitly described.

In addition to the discussions concerning the averaging seasons, much of the discussion of the atmospheric-circulation measures also focuses on the months of December through March (individually and in aggregate), when circulation patterns have the greatest effect on the HM regime with respect to the net moisture input and when most of the 700-mb data exhibit the largest mean differences between the BASE and POST periods. As will be described later, it appears that characteristics of the atmospheric-circulation data for the December-March season (and also the January-March season) are more coherent to the HM regime than the characteristics for the October-February winter season during the winter season. This is probably due to the fact that during the October-November fall-transition season the atmospheric circulation is highly variable and evolving.

The subset of the 700-mb data are analyzed on a monthly basis because of the natural seasonal progression of circulation patterns and their intermonthly variations. For the discussion of the 700-mb data, the dominant circulation modes of interannual variability in the Northern Hemisphere as described by Horel and Wallace (1981), Rogers (1981), and Barnston and Livezey (1987) are incorporated.

However, based on the results of a rotated principal components analysis of the subset of the 700-mb data, it is recognized that there are distinct differences between the dominant modes for the North Pacific region in comparison to the hemisphere, especially during the important winter season.

The SST data are analyzed on a monthly and water year basis because of the seasonality in the data caused by solar forcing. The monthly analyses include discussions of the spatial variations in the results.

Techniques

The values used to calculate the means are reported values (precipitation in centimeters, streamflow in cubic meter per second (m^3s^{-1}), 700-mb data in meters, SSTs in degrees Fahrenheit), anomalies (deviations from the mean over some base period), normalized values (precipitation), unit discharge values (streamflow), or standardized values (mean of zero, standard deviation of one). Monthly precipitation values are normalized by subtracting the smallest value and then dividing by the largest remaining value, yielding a time series of values for each month that ranges from 0 to 1. Unit values are obtained by dividing the streamflow values by the drainage area, yielding discharge per unit area in units of cubic meters per second per square kilometer ($m^3s^{-1}km^{-2}$). Most of the figures presented display standardized values, generally as simple x-y plots or as cumulative departure plots; cumulative departures are used because they readily display persistent periods or episodes of above- or below-average values. Although cumulative departures are well suited for showing changes or shifts (the persistent periods of below or above average values), differences in interannual variations between series and initiation of trends in the series generally cannot be discerned. However, the persistence of anomalous periods is important for water resources because shifting means are linked to and translated through the system, whereas an initially downward or upward trend with above- or below-average values is generally linked to the same above- or below-average hydrologic conditions.

The data also are analyzed on a monthly-to-seasonal basis for both the successive and combined (aggregated) periods using Kendall's tau for detection of trends and by unrotated or rotated principal components analysis for estimating regions of similar response (precipitation data—water years 1931-88; streamflow data—water years 1948-89 and 1932-89;

subset of 700-mb data—water years 1947-91). The results of the principal components analysis are not discussed in detail, but were used to provide additional information for interpreting results.

A correlation analysis also was performed using the HM data (individual site series and the first three modes of their principal component series) and the atmospheric-circulation data (indices and 700-mb subset) and SST information by lag correlating the HM data to monthly and moving-season information. For the monthly analysis, correlations were calculated for each of the 12 months prior to and after the October of the water year of the HM data. For the moving-season analysis, a 3-month aggregate of the atmospheric and SST data, starting and centered on October, was used for calculating correlation coefficients. The 3-month period was moved forward and backward 1 month at a time for 12 months, and the correlation coefficients were calculated. As an example, for each of the averaging seasons, there would be 25 spatial-correlation fields between the 700-mb subset or the SST data and each of 162 HM series and 12 principal component series. Although this information is not presented, it provided valuable insight on potential linkages, including the space-time domain, between the HM data and the other data. As an example, when the first mode of the rotated principal components time series of the streamflow data for the runoff season is used a surrogate for the 112 sites, the correlation fields between this time series and the 700-mb subset in April and August prior to the runoff season (fig. 8) show distinct, well-defined patterns with centers that correspond to the largest correlations (and possibly to low or high geopotential heights). Correlation fields such as for April on figure 8 suggested patterns that were later identified in the monthly analysis of the 700-mb data and in the spatial distribution of the principal component loadings already calculated; these fields also indicated the locations of SSTs to be analyzed in more detail.

Last, the three long-term data series (two sea-level pressure indices and Arctic sea-ice cover) were analyzed independently of the other data series. This analysis was completed in order to test the realism of the results—use of defined periods, regime changes, and potential linkages—and to roughly estimate the spatial extent (Pacific Northwest in contrast to hemispheric) of the identified shifts. The analysis also examined whether changes in the atmospheric circulation and SSTs for the earlier period of record may reflect those of the HM regime.
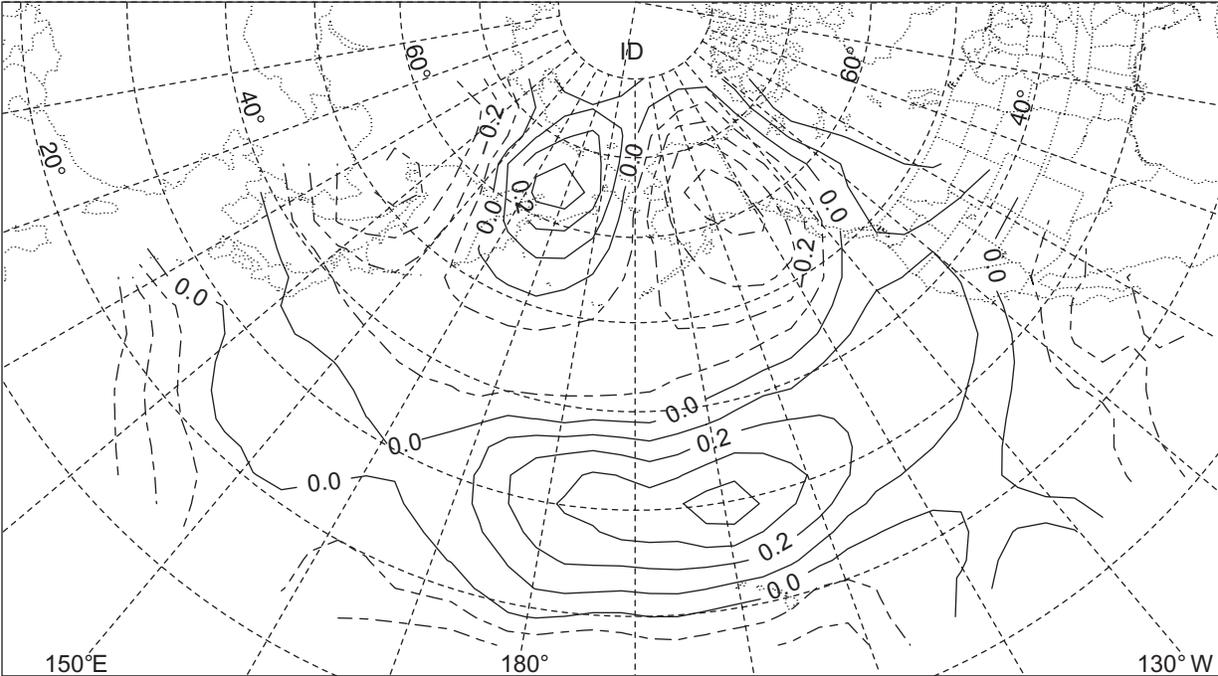
April
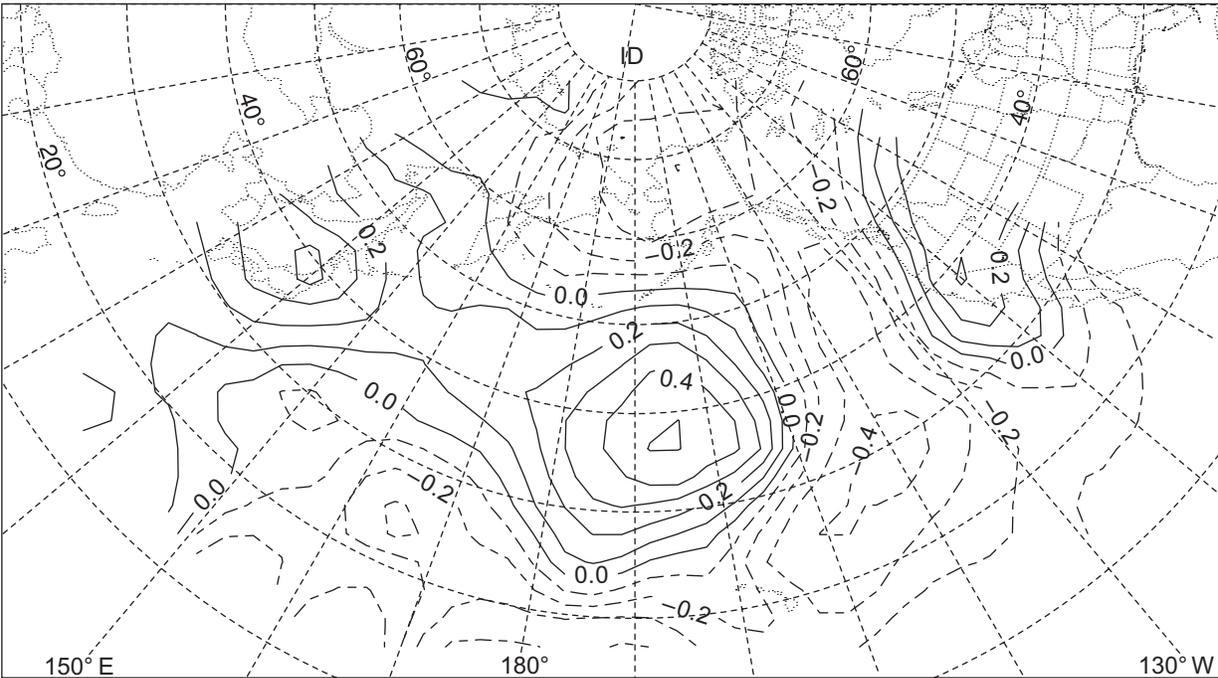
August

Figure 8. Spatial correlation field between the first mode of the rotated principal components of runoff-season streamflow and monthly 700-millibar heights prior to the runoff season for April and August.

Solid lines are positive correlations and dashed lines are negative correlations.

RESULTS

The results are described in the order of data categories: precipitation, streamflow, atmospheric information, and SSTs. The measure of precipitation (the net input) is described first in order to estimate potential regime shifts and their magnitude, which may be reflected in streamflow, and to help identify why streamflow characteristics may exhibit shifts. The results of the analyses of streamflow are then discussed; streamflow is the important planning parameter for water resources. The analysis of the atmospheric circulation and SST data is then described; these results are later used to estimate potential linkages to interdecadal-regime shifts in the HM data.

Precipitation

The results suggest that, referenced to BASE period, the precipitation regime in western Washington changed over the successive periods. Although these changes may be considered small, they can have a large effect on water-resource availability. Overall, mean water-year precipitation was less for both the PRE and POST periods (owing to their winter-season decreases in the mean) than for the BASE period. Runoff-season changes are not as well-defined statistically; however, when runoff-season changes are referenced to the water-year and winter changes and to runoff-season changes estimated using period 1 data, several facts stand out. (1) The runoff season for the PRE period was drier than the BASE period; (2) the runoff season during the POST period was wetter than the BASE period; (3) the above two facts suggest that different climatic regimes existed in the PRE and POST periods; and (4) increasing precipitation in the runoff season for the POST period may not be translated into increases in streamflow because it occurs during the season of large evaporative demand when only about 35 percent of the total water-year precipitation occurs. Thus, large changes in the atmospheric-circulation regime between the interdecadal periods are suggested not only by the marked changes in the important winter-precipitation season but also by the precipitation changes during the runoff season when atmospheric circulation features are more stable than those during the winter season.

Water Year and Winter Season

The normalized means of precipitation for the water-year and winter seasons for the PRE, POST, and BASE periods are shown on figures 9A and B. Means for the PRE and POST periods that are less than the BASE period mean fall below the diagonal line. All but 3 of the 200 water-year and winter means for the PRE and POST periods are smaller than the BASE-period means (figs 9A,B; table 2); two of the three increases are for the PRE period for one site, suggesting that there may be problems with the data for the early period of record for this site. About 75 percent of the water-year and winter-season means are significantly different from the BASE-period means at a 0.05 level.

The preponderance of ratios less than 1 indicates that the water year and winter seasons during both the PRE and POST periods were generally drier than during the BASE period. These differences correspond to reasonably large changes in the net moisture input, which can be measured by the cumulative difference in precipitation for all sites, which in turn is reflected by the average ratio. For example, the average winter-season PRE/BASE and POST/BASE ratios for all sites are 0.88 and 0.84, respectively, reflecting a 600- and 830-cm change from the BASE-period total of 5,170 cm; similarly, the average water-year ratios are 0.91 and 0.92, reflecting cumulative differences of 690 and 685 cm from the BASE-period total of 7,830 cm (table 2).

The 29 winter-season divisional means were smaller during the POST period than the means for the prior 18 years of the BASE period, and 9 of these POST period means were significantly different from the BASE-period means at a 0.05 level. Using the complete 30 years of record for the BASE period and comparing means also shows that all 29 divisions had smaller means, but for this analysis, 17 of the 29 means were significantly different from the BASE period means at the 0.05 level and 7 at the 0.01 level. For the PRE period, winter-season means were smaller than the means for the following 16 years of the BASE period for 23 divisions. Five of the climate divisions that had larger means during the PRE period were Idaho divisions, and the remaining one was the southeastern Oregon division, which abuts two of the Idaho divisions.
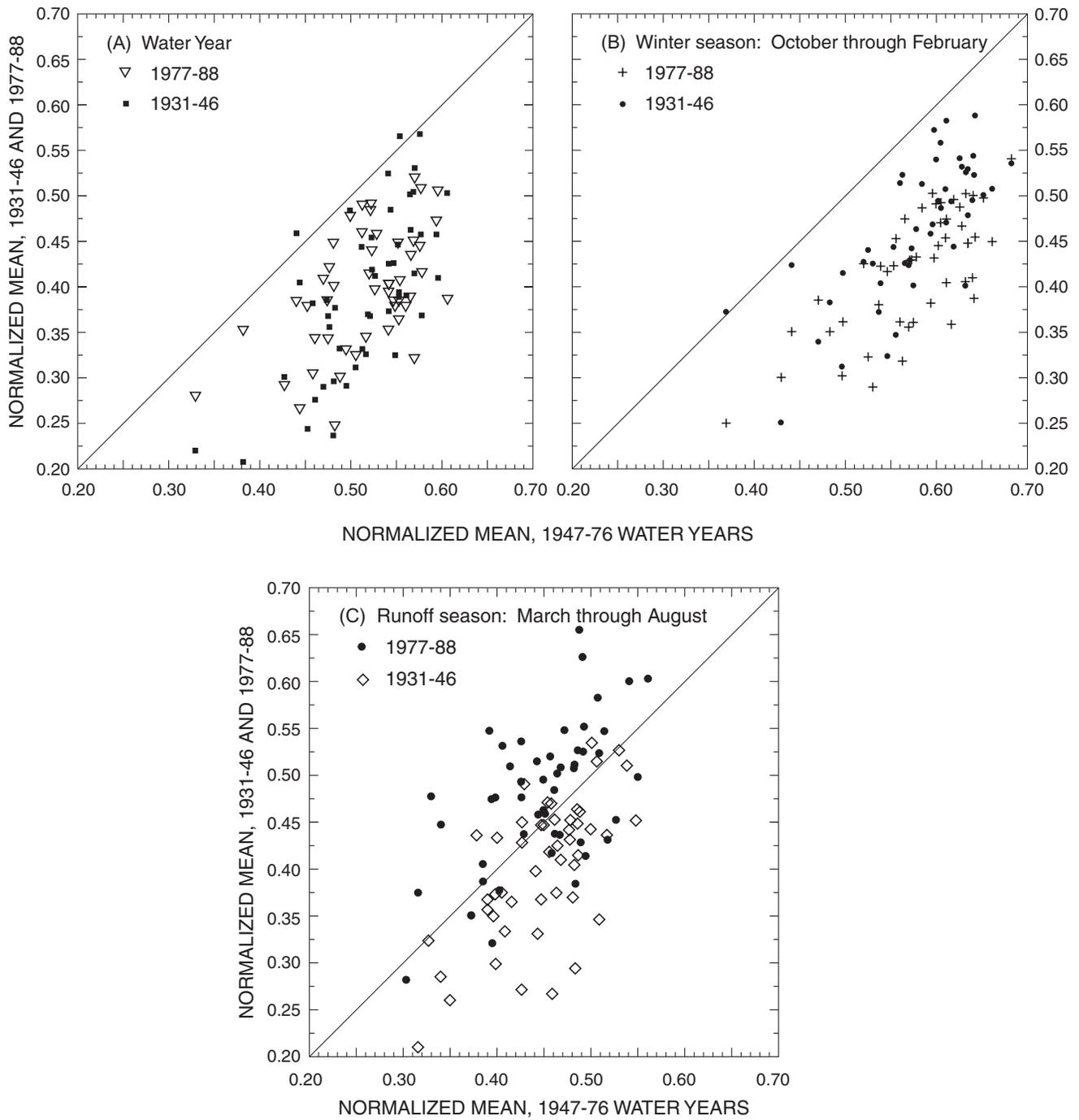
Figure 9. Normalized means of precipitation at 50 sites in western Washington for the water year, winter season, and runoff season.

Means for the PRE (1931-46) and POST (1977-88) periods are referenced to (plotted against) the mean for the BASE period (1947-76). Values plotted below the diagonal line have a smaller mean than the mean for the BASE period.

Table 2. Summary of results of analysis of the precipitation and the streamflow data

[**Ratio**: ratio of the means for Pre-1947 and Post-1976 values to 1947–1976 values; **Averaging periods**: periods are Pre-1947 water years, 1947–1976 water years, and Post-1976 water years. Results are based on comparing Pre-1947 and Post-1976 values to 1947–1976 values; **Ratio - Average**: average of all sites for defined averaging period; **Ratio - Number of values**: N = 50 for precipitation; N = 112 for streamflow for Post-1976; N = 90 for Pre-1947, based on sites with more than 5 years of record prior to 1947. **Ratio - Total change**: the sum of the differences between means; in centimeters for precipitation and in cubic meters per second per square kilometer for streamflow. **Abbreviations**: cm, centimeter; m^3s^{-1}, cubic meters per second; $m^3s^{-1}km^{-2}$, cubic meter per second per square kilometer]

Averaging period	Ratio						Total change	
	Average		Number of values less than 1		Number of values greater than 1			
	Pre-1947	Post-1976	Pre-1947	Post-1976	Pre-1947	Post-1976	Pre-1947	Post-1976
Precipitation								
Water year[1]	0.91	0.92	48	50	2	0	-690	-685
Winter season[1]	0.88	0.84	49	50	1	0	-600	-830
Runoff season[1]	0.96	1.04	40	13	10	37	-80	70
Streamflow								
Water year	0.83	0.86	93	97	1	15	-802	-780
Winter season	0.78	0.87	94	101	0	11	-895	-702
Runoff season	0.87	0.87	87	97	7	15	-822	-955
Baseflow season[1]	0.81	0.95	85	81	9	31	-330	-191

Averaging period	Differences in unit discharge ($m^3s^{-1}km^{-2}$)			
	Average		Total change	
	Pre-1947	Post-1976	Pre-1947	Post-1976
Streamflow				
Water year	-0.0063	-0.0055	-0.59	-0.62
Winter season	-0.0086	-0.0063	-0.81	-0.70
Runoff season	-0.0051	-0.0056	-0.48	-0.63
Baseflow season	-0.0029	-0.0015	-0.27	-0.16

[1]Water year is October through September ending in named year; winter season is October through February; runoff season is March through August, and baseflow season is August through September.

The analysis of the divisional data for the winter season showed that, for western Washington, there was about a 20-percent reduction in the POST-period means and about a 10-percent reduction in the PRE-period means. These reductions are consistent with the western Washington PRE/BASE and POST/BASE winter-season ratios described above; indeed, the mean ratios calculated using the western Washington divisional precipitation data were the same as those calculated using the site data. The largest decreases in the winter-season means for the POST period in western Washington were for the coastal and west slope of the Cascade Range divisions (the two wettest divisions), with reductions from the BASE-period means of 29.0 and 25.6 cm, respectively; these reductions are about double those of the PRE period.

Runoff Season

For the runoff season, there generally was less precipitation during the PRE period and more precipitation during the POST period, compared with the BASE period (fig. 9C and table 2). These results are consistent with the differences between the winter-season and water-year means and their PRE/BASE and POST/BASE ratios. Because only 11 sites had significantly different means for the runoff season, long-term monthly trends were analyzed by calculating Kendall's tau for all site data for the 1931-88 period. The results showed two important monthly trends: (1) a transition in the spring to predominantly positive Kendall's tau (increasing precipitation), with all sites having a positive tau in April and May, and (2) an abrupt transition to negative Kendall's tau (decreasing precipitation) in October, when all but two sites have negative taus. These two aspects support the results showing differences in the runoff-season means between the PRE and POST periods. Also note that the runoff-season ratios are closer to 1 (fig. 9C) than are either the winter-season or water-year ratios (figs. 9A,B) because the circulation patterns in the North Pacific during the runoff season are relatively stable. To elicit interdecadal changes in the mean runoff-season precipitation that are on the order of the winter-season changes, large, perhaps hemispheric, anomalous circulation patterns associated with the transport of water vapor would need to persist during the runoff season.

Precipitation for the PRE period, in comparison to the BASE period, was larger at 10 sites (table 2). Eight of these sites were low-lying coastal sites that are relatively unaffected by either orographic effects (Schermerhorn, 1967) or direction of atmospheric flow along the coast and are mainly influenced by net moisture fluxes to the region. The remaining two sites were clustered. To further determine if there was a consistent change at most sites and if the PRE period was drier during the runoff season, two additional analyses were completed. First, extending the runoff season to include September in the runoff-season mean (because of the transition to negative Kendall tau in October) showed that mean precipitation during the PRE period, in comparison to the BASE period, was larger at two more sites—a coastal site and a site located near the two clustered sites. Next, the data were averaged over period 1 beginning in 1921 because of the potential "conservative" influence of the wet spell during water years 1933-34 on the results. The PRE/BASE ratio changed from 0.959 to 0.922 and the number of sites with ratios greater than 1 was reduced to one, suggesting the robustness of results based on period 2 data.

Mean precipitation for the POST period during the runoff season was less than for the BASE period for only 13 sites. These sites generally grouped within two areas, which lie along a northwest-trending band. With the increase in the runoff-season length to include September, the number of sites that had smaller means during the POST period was reduced to seven, all of which lie on this band, which reflects the influence of northerly atmospheric flow during this season.

Last, because the April-May period displayed positive a Kendall tau at all sites and it accounts for about 40 percent of the total precipitation during the runoff season, it was analyzed separately to further check differences between the PRE and POST periods. This analysis showed that all 29 divisions had larger POST-period means in comparison to the BASE period, and 13 of the divisional means were significantly different at the 0.05 level. In contrast, for April and May, all but one division had smaller means during the PRE period; this division, located in south-central Idaho, had one of the smallest mean April-May precipitation values (4.7 cm) of the 29 divisions.

These differences for April and May are consistent with the Kendall tau values and suggest variations between the PRE, BASE, and POST periods in atmospheric circulation during this summer-transition season, which, in turn, affects the total water input during the runoff season. Aspects of changes in the circulation during this season will be described in the subsequent section 'The April-June Summer-Transition Season'.

Streamflow

Results of the streamflow-data analysis described below show that mean water-year streamflow during both the PRE and POST periods was much less than during the BASE period. Only in one well-defined region, and mainly for the POST period, was there more streamflow than during the BASE period. Winter- season streamflow also was much less than the BASE period. All but 11 of the 112 sites had smaller mean winter-season streamflow, and the larger means occurred during the POST period. The sites that experienced increased streamflow either are consistent with the sites that had larger means during the water year during the POST period or suggest the effects of increasing air temperature on snowpack accumulation and ablation. The mean streamflow during the PRE period also was much less than during the POST period for the winter season. Streamflow during the runoff season generally was less than the BASE period during both the PRE and POST periods, and the few sites that had larger means were generally clustered in one region. Unlike streamflow in the other seasons, mean baseflow-season streamflow indicated that many more streams experienced increased runoff, mainly during the POST period in several well-defined regions, but otherwise, mean streamflow during the PRE and POST periods was less than during the BASE period everywhere else.

Water Year

Water-year changes in the interdecadal regimes identified in the streamflow data are more pronounced than those identified in precipitation data. For both the PRE and POST periods, the mean water-year

streamflow was less than for the BASE period for all but 15 of the 112 sites (table 2), and all but 21 of the means were significantly different from the BASE period means at a 0.05 level. Of the 15 sites displaying larger means, 1 is a small glacier-driven stream (site 1, table 1) located in northwest Washington and the other 14 are clustered within a single area (southeastern Oregon and southern Idaho, herein referred to as "Idaho-Oregon") and were part of the group of 21 that did not have significantly different means. Fourteen of the 15 sites had larger means only for the POST period. Computing Kendall's tau of water-year values for the combined BASE-POST period (ending at 1991) shows negative taus for all but 14 sites (12 of which also were common to the group of 15 with larger means). The consistency of results showing decreased streamflow for the PRE and POST periods for all but 15 of the sites (which had increased streamflow during the POST period) suggests that differences in the HM regimes between PRE and POST periods are perhaps related to variations and changes in the atmospheric flow regime.

The Idaho-Oregon region apparently responds to different atmospheric flow conditions than does the rest of the study area. This region includes some streams that display temporal variations in their hydrographs distinctly different from those of most of the other stream hydrographs, and the region also includes a large part of the study area where mean annual runoff is less than 13 centimeters per year (cm yr^{-1}). This region appears to be transitional between the northern and central parts of the Western United States with respect to the influence of large-scale circulation features on precipitation (Redmond and Koch, 1991); it defines an area which had larger variations in the spatial extent of extended wet-dry periods compared to the surrounding area (Graumlich, 1985); and it is clearly defined in several figures presented in McDonald and Riggs (1948). The average cumulative departures of the standardized water-year values for the 15 sites (the Idaho-Oregon sites plus the northwest Washington site) with POST/BASE ratios of the mean greater than 1 (dashed line, fig. 10) and the remaining sites with ratios less than 1 (solid line, fig. 10) clearly show that the streams in the Idaho-Oregon region responded to different climate forcing than the other streams from 1947 through 1992.
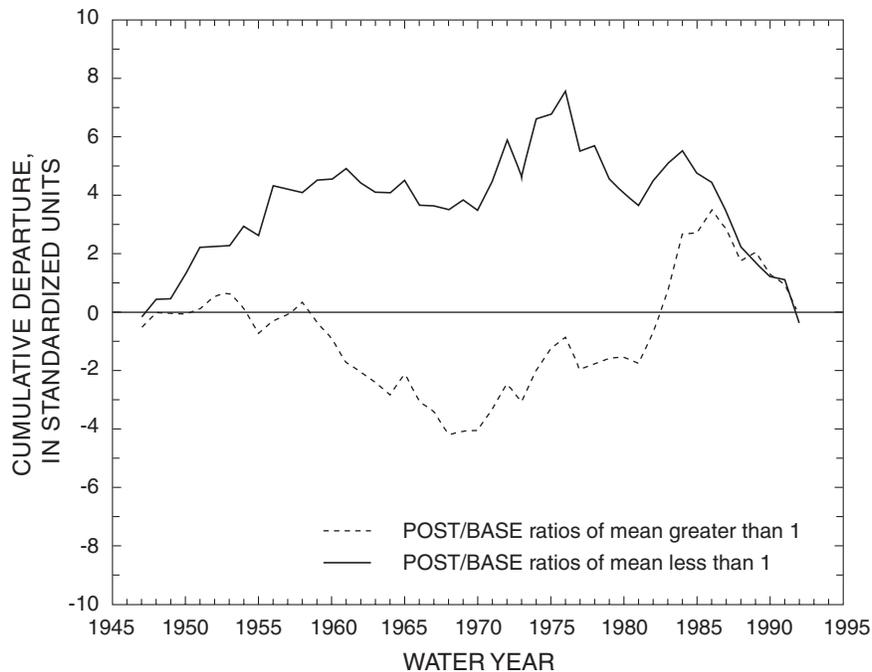
Figure 10. Cumulative departures of water-year streamflow values for all sites with ratios of POST/BASE greater than and less than 1.

Streamflow values for each ratio are the average of the standardized values for all sites with data for the identified water year.

The PRE/BASE and POST/BASE ratios of the means for the water year ranged from 0.43 to 1.2 and averaged 0.83 and 0.86 (table 2), respectively. Note the closer correspondence to the precipitation ratios for the winter season (versus water year) because of the importance of this season in defining the total water input. A ratio of 0.86 reflects a total cumulative difference of -780 m^3s^{-1} compared to the BASE period value of 4,891 m^3s^{-1}; the 780 m^3s^{-1} value is equivalent to the mean annual flow of the four largest streams (table 1) and reflects an average loss of about 6 m^3s^{-1}. The differences between the water-year unit discharge (fig 11A, table 2) indicate the large regime change identified by the average ratios. The water-year unit discharge ranged from 0.001 to 0.12 $m^3s^{-1}km^{-2}$ (table 1), and the changes ranged from -0.019 to 0.0015 $m^3s^{-1}km^{-2}$ (fig. 11A); the PRE- and POST-period differences from the BASE period averaged -0.006 and -0.005 $m^3s^{-1}km^{-2}$, respectively, reflecting total cumulative changes of -0.59 and -0.62 $m^3s^{-1}km^{-2}$ (table 2).

Winter Season

Streamflow during the winter season also was less during the PRE and POST periods compared to the BASE period. Differences in unit discharge between the BASE period and the PRE and POST periods were negative for all but 11 sites (fig. 11B, table 2). Additionally, the total cumulative changes from the BASE period for the PRE and POST periods were -895 and -702 m^3s^{-1} (or -0.81 and -0.70 $m^3s^{-1}km^{-2}$). Thus, significantly less streamflow occurred during the PRE and POST periods for all but these 11 sites. These 11 sites are of interest because all had larger means only during the POST period, when winter-season precipitation in western Washington was smaller than the BASE period, and all 29 climate divisions had smaller winter-season precipitation means for the POST period.
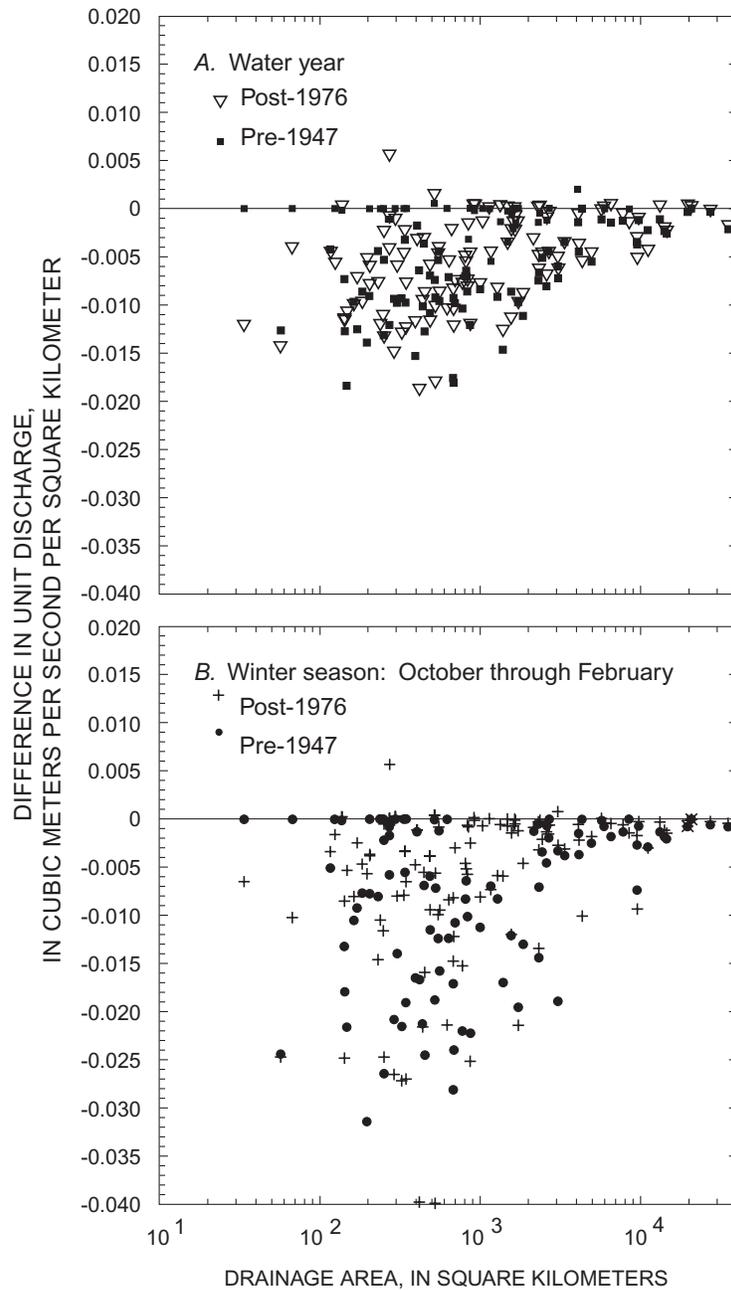
Figure 11. Differences in unit discharge for the water year, winter season, runoff season, and baseflow season.

Negative values indicate that mean unit discharge is less than the mean unit discharge during the BASE period. Streamflow information for the sites is listed in table 1.
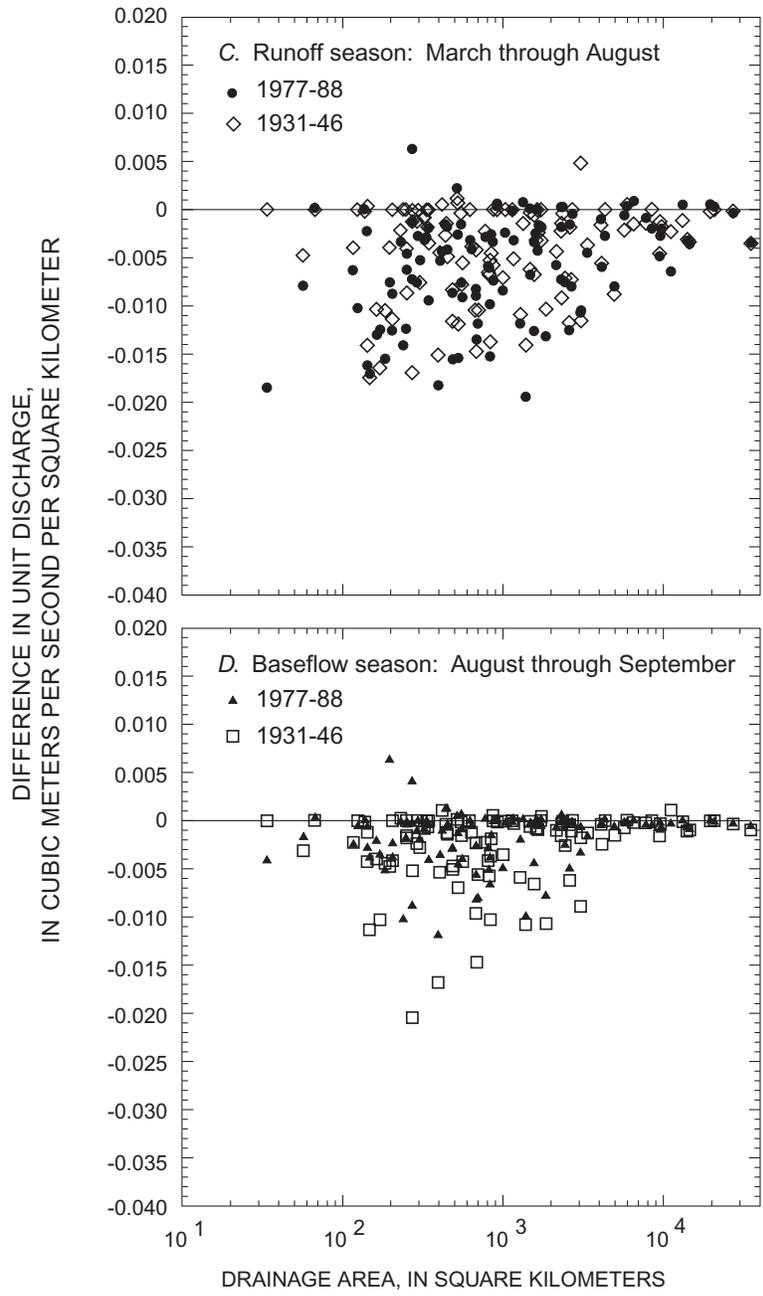
Figure 11. —*Continued.*

Five of the 11 sites are located in the Idaho-Oregon region and 2 on its boundary, again suggesting that this region was climatically different from the remaining area during the POST period. The eighth site is the only snowmelt-driven stream analyzed in this study that is representative of a region in northcentral Washington; although other data were not examined in this study, this region appears to be part of a larger one that extends into the interior of British Columbia and that may also experience different climatic conditions, as determined by figures presented in McDonald and Riggs (1948).

The remaining 3 of the 11 sites with larger POST-period means (sites 1, 2, and 5, table 1) cluster in northwestern Washington (two glacier, one snowmelt driven), where winter-season precipitation was significantly less (on the order of 20 percent) than that during the BASE period; this suggests a change in the runoff regime with more runoff concentrated during the winter season, perhaps related to increasing air temperatures. If air temperatures have affected the runoff regime, there may be distinct differences in winter-season streamflow between the PRE and POST periods. This aspect is explored below.

The average of the PRE/BASE-period ratios of the mean streamflow for the winter season was almost 10 percent smaller than the average of the POST/BASE ratios; this difference applied even to the ratios for sites in western Washington where the winter-season precipitation during the PRE period was larger than the POST period. Mean winter-season streamflow during the PRE period was more than 20 percent smaller than the BASE period for 54 sites (39 of which had ratios greater than 0.80 for the POST period), and 12 of the 54 sites had ratios of less than 0.70--7 of these are located in central Oregon. Thus, although streamflow throughout the Pacific Northwest for the winter season was less for both the PRE and POST periods than for the BASE period, winter-season streamflow during the PRE period generally was much less than during the POST period. Variations to this overall pattern exist. For example, 26 sites had POST/BASE ratios of less than 0.80; 25 of these sites lie in two well-defined areas: (1) western Oregon and southwestern Washington—18 sites, and (2) northeastern Washington and northern Idaho—7 sites. The climate divisions with the most significant changes (decreases)

in mean monthly precipitation from the BASE to the POST period coincide with these areas. The differences described above suggest a changing runoff regime over the interdecadal periods that is related to shifts in both precipitation and air temperature.

Air Temperature and Snowpack Effects On Winter-Season Streamflow

In an analysis of changes in the timing of west coast streamflow, Aguado and others (1992) present results with respect to both streamflow values and temperature for the period 1948-86 that suggest a change in the runoff regime and increasing air temperatures in parts of the Pacific Northwest; Wahl (1991) also presents results that suggest changes in runoff regimes. Dettinger and Cayan (1995) show that trends in early snowmelt runoff are related to recent changes in atmospheric forcing. In an analysis of temperature and precipitation at Wolverine Glacier in maritime southern Alaska, Mayo and March (1990) describe a trend of increasing temperature and precipitation being initiated at the beginning of water year 1977. A trend in this region is consistent with the previously described changes in the precipitation regime in the Pacific Northwest and would also indicate increasing air temperatures in the Northwest (Yarnal and Diaz, 1986). Jones and others (1986) present surface air temperature departures from a base period of 1951-70 for the Northern Hemisphere showing the annual departures for 1977-84 were positive and that 14 of the 16 annual departures for 1931-46 were positive. Together, the above information suggests a warmer regime existed during the PRE and POST periods that did not affect winter-season streamflow during these periods in the same manner; this fact is based on the differences in streamflow for the winter season between the PRE and POST periods.

Differences from the mean monthly daily-minimum temperatures of the BASE period for the PRE and POST periods for five sites with good-quality records in the Pacific Northwest are presented in table 3. The sites vary from a low-altitude inland-coastal site (Olga 2 SE) to one of the highest altitude sites in the Pacific Northwest (Crater Lake NPS HQ).

Table 3. Differences in mean monthly daily-minimum temperature at five weather stations in the Pacific Northwest. Differences are from the 1947–76 BASE period

[**Identification No**. is National Weather Service Station Index Number; **POST-minus-BASE**: BASE period of record for Baker FAA AP is 1948–76, all other sites are 1947–76. POST period of record is 1977–94.]

Site	Identification No.	Altitude (meters)	Differences in mean monthly temperature (in degrees Fahrenheit)					
			January	February	March	April	May	June
POST-minus-BASE								
Olga 2 SE	6096, Wash.	24	2.8	1.5	2.6	2.6	2.2	1.5
Cedar Lake	1233, Wash.	475	2.5	0.7	1.8	1.4	0.9	0.3
Stampede Pass WSCMO	8009, Wash.	1,206	2.3	0.1	3.0	1.8	0.4	0.3
Baker FAA SP	0412, Oreg.	1,026	0.2	-0.4	1.8	2.1	0.7	0.8
Crater Lake NPS HQ	1946, Oreg.	1,974	1.1	0.3	2.2	1.6	-1.1	-0.5
			July	August	September	October	November	December
Olga 2 SE			1.9	1.9	1.1	1.6	-0.2	-0.5
Cedar Lake			0.7	1.3	0.1	-0.4	-1.1	-1.3
Stampede Pass WSCMO			-0.6	1.3	-0.8	1.4	-1.5	-1.9
Baker FAA SP			0.7	2.4	1.5	1.4	-0.8	-2.1
Crater Lake NPS HQ[2]			-1.9	-0.1	-1.2	0.5	-2.8	-0.9
PRE-minus-BASE								
			January	February	March	April	May	June
Olga 2 SE[1]	6096, Wash.	24	1.7	0.1	1.3	1.5	1.1	0.7
Olga 2 SE[2]	6096, Wash.	24	2.1	-0.2	1.3	1.6	0.9	0.1
Cedar Lake[2]	1233, Wash.	475	2.8	0.2	2.0	2.5	1.7	1.0
Crater Lake NPS HQ[2]	1946, Oreg.	1,974	1.5	0.2	3.6	3.2	1.2	1.7
			July	August	September	October	November	December
Olga 2 SE[1]			0.4	0.5	0.2	0.9	0.5	0.3
Olga 2 SE[2]			0.1	0.1	0.4	0.8	0.3	0.8
Cedar Lake[2]			1.7	1.9	1.8	2.6	1.4	2.0
Crater Lake NPS HQ			1.3	1.8	0.1	1.5	0.6	1.9

[1]PRE-period of record is 1921–46.
[2]PRE-period of record is 1931–46.

Mean monthly daily-minimum temperatures are presented because, except for Stampede Pass, all mean monthly daily-maximum temperatures were above freezing, and thus the major control, on a monthly basis, to snowpack accumulation is the minimum temperature. For Stampede Pass, mean monthly daily-maximum temperatures during December-January were below freezing during the BASE period. Consistent with the previously cited work, the differences in means (table 3) suggest an overall warming during the PRE and POST periods compared to the BASE period that could have affected streamflow—warming in the lowlands with an attendant increase in evapotranspiration, warming in the uplands with an attendant decrease in snowpack. For example, the mean daily minimum for February at Cedar Lake changed from less than freezing during the BASE period to greater than freezing during the POST period. In addition, the differences suggest a cooling during November and December during the POST period and a warming during the PRE period (table 3). That is, there were distinct differences between the PRE and POST periods in air temperature for the winter season, and that these differences may account for the differences in the winter season streamflow.

A comparison of the mean monthly temperatures during the PRE, BASE, and POST periods for the 29 climate divisions for the October-December and the January-February parts of the winter season indicates several aspects on the differences between PRE and POST air temperatures. For the October-December period, all 29 divisions had smaller POST-period means than BASE-period means; 18 of the divisional means changed from greater than freezing during the BASE period to less than freezing during the POST period. In contrast, 27 of the divisions had larger PRE-period means than those of the BASE period. These differences between the PRE and POST period for the months of October-December further suggest overall climatological differences between these two periods during this important winter season.

For the January-February period, 25 of the divisions had larger means during the POST period than during the BASE period, with the most significant increases in the mean occurring in the divisions representing the coast and west slope of the Cascade Range in Washington. The latter increases may affect snowpack and streamflow, in that, although winter-season precipitation in western Washington during the POST period was less than during the PRE period, the

higher air temperatures may account for less snowpack and more water delivery, thus moderating what could have been a larger decline in mean streamflow during the POST period for the winter season. Additionally, three of the four divisions that had smaller POST-period means for this January-February period are located in the Idaho-Oregon region, where possibly greater snowpack sustained nearly average streamflow in this region during the POST period.

During January and February of the PRE period, 7 divisions had larger means and 22 had smaller means than during January and February of the BASE period. For the 22 divisions with smaller means, snowpack was probably larger than would have occurred with average BASE-period temperatures, resulting in less winter-season streamflow in comparison to both the BASE and POST periods. Five of the 7 divisions with higher mean air temperatures include all of western Washington; the other 2 divisions are located in Oregon and include the low-lying Willamette Lowland in western Oregon and the Crater Lake NPS HQ site (table 3). The analysis of the divisional climate data for air-temperature suggests not only that air temperature had changed from the BASE period but also that the PRE and POST periods were climatically different during the winter season, accounting for some of the differences in streamflow.

A final assessment of the potential effects of air temperature on an earlier runoff regime was to compare simulated monthly values of snow accumulation and snowmelt for the three interdecadal periods for a site in the transient-snow zone in western Washington. Monthly values were calculated using the snow accumulation and ablation part of the model of Bauer and Vaccaro (1986). The model was operated under open-forest conditions using daily precipitation and daily minimum and maximum air temperatures at Cedar Lake (see table 3) for the period 1932-94. The comparison was completed for a site in the transient-snow zone because the effects of air temperature are largest in this zone (van Heeswijk and others, 1996), and this zone (between altitudes of about 300 to 900 m in western Washington) encompasses a large area in western Washington. In the simulations, snowmelt extended into April only three times—two during the BASE period and one during the PRE period. For two nearby snow-course sites (period of record 1961-95) at altitudes of 365 and 550 m, the lower-altitude site had no April 1 snowpack.

The higher-altitude site had an April 1 snowpack for 6 of the years (all prior to 1977), and the two largest values occurred in the 2 years that melt was estimated to occur at the Cedar Lake site (altitude of 475 m); also, there was no April 15 snowpack over the period of record for this site. In addition, the January 1 snowpack at the low-altitude site closely matched the simulated January 1 snowpack. These results indicate that the simulated values are reasonable and can provide information for comparing differences between the three interdecadal periods.

The simulated mean snowpack for the PRE period was 21 percent smaller than the mean for the BASE period, and the POST-period mean was 35 percent smaller than the BASE period mean. About 10 percent of the total melt occurred in March during the BASE period, whereas only about 4 and 3 percent occurred in March during the PRE and POST periods, respectively. During the POST period, only 6 percent of the simulated melt occurred in October and November, mainly due to the fact that snow accumulation was small and temperatures were lower during these months. By contrast, 14 and 13 percent of the simulated melt occurred during these months in the BASE and PRE periods, respectively. About 76 percent of the total melt occurred during the months of December-February in the BASE period, and 91 percent of the melt occurred during these months in the POST period. In addition, the model was operated using the precipitation data from the POST-period but using various combinations of years of the air temperature record from the BASE period. For all simulations, the 18-year mean snowpack was greater than the POST-period mean calculated using the POST-period data. Together, these results further indicate the combined effect of increasing air temperatures and decreasing precipitation on snowpack, which would result in an earlier occurrence of runoff for parts of the Pacific Northwest and, thus, would affect the total winter-season and water-year streamflow.

Runoff Season

In comparison to the BASE period, significant decreases in mean streamflow occurred during the runoff season (table 2), with the total cumulative change for the POST and PRE periods being about -822 and -955 m^3s^{-1}, respectively. For the ranked mean runoff-season streamflow of the 112 sites, these changes represent about a 90-percentile runoff-season streamflow value—equivalent to 'shutting-off' the flow at the gages of the two streams with the largest mean streamflow during the runoff season (table 1). The differences in unit discharge (fig. 11C) clearly show that regional changes occurred in the runoff season throughout the Pacific Northwest, with total cumulative changes from the BASE period being -0.48 and -0.63 $m^3s^{-1}km^{-2}$ (table 2) for the PRE and POST periods, respectively. For the POST period, the average ratio of the means and the change in unit discharge from the BASE period for western Washington were 0.86 and -0.017 $m^3s^{-1}km^{-2}$, respectively, indicating that increased precipitation during the runoff season was largely evapotranspired (or, in the case of two streams to be discussed in the next section, translated into the increased streamflow during the baseflow season). The Idaho-Oregon region had the same trend of larger mean streamflow during the POST period— 16 of the 22 ratios of the means greater than 1 were for this region, and 13 of the 16 were for the POST period (table 2), indicating consistency of results with those from the other averaging seasons.

Baseflow Season

Although streamflow during the baseflow season accounts for only a small part of the water-year total (table 1), the signature of climatic extremes and shifts is perhaps best displayed by streamflow during this season. The changes in unit discharge (fig. 11D) were small compared to the other seasons (compare fig. 11D with figs. 11A,B,C), but they are significant because they reflect a time of low flow when in-stream flows for fisheries and water-quality standards are highly dependent on flow quantities.

Compared to the other seasons, more sites had larger baseflow-season means during the PRE and POST periods than during the BASE-period. In particular, 31 of the 40 ratios greater than 1 were for the POST period (table 2). The sites with larger POST-period means are located in three regions: (1) the Idaho-Oregon region and surrounding area, (2) western Oregon, and (3) western Washington. The larger means in the Idaho-Oregon region correspond to sites having larger water-year and runoff-season means during the POST period, again implying that this region experienced a climatic regime during the POST period that was different than that during the PRE period.

The larger means for streams in western Oregon are for the rainfall-runoff-driven streams of the Coast Range—no glacier- or snowmelt- driven streams of the Cascade Range in western Oregon had larger baseflow-season means than the BASE period.

Although the larger means during the baseflow season for glacier-driven streams in western Washington region may perhaps be accounted for by higher air temperatures, the larger means for the two ground-water-driven streams are more difficult to understand, especially considering that the baseflow-season POST/BASE ratios of the means for the remaining western Washington streams are quite small. During the baseflow season, these two streams are highly correlated to the western Oregon streams that also had POST/BASE ratios greater than 1. Essentially, these two streams lie along gaps in the coastal mountains, which act as barriers to approaching storm systems, and would generally experience the same atmospheric-flow conditions as the Oregon streams, given that the storm tracks intersect the shoreline south of the gaps. These results suggest enhanced coastal precipitation (discussed later) and streamflow during the baseflow season for the POST period from south of the Olympic Mountains in Washington to southwestern Oregon (but west of the Cascade Range). This area is clearly defined in several modes of the principal components analysis. Last, a comparison of POST- and BASE-period mean monthly air temperature for the baseflow season for the 29 climate divisions shows that all mountainous regions in western Washington that contain glaciers were significantly warmer during the POST period. The hydrograph for a glacier-driven stream (see fig. 5) shows enhanced baseflow-season streamflow because of glacial meltwater in comparison to the two other streams, and, thus, higher air temperatures during the POST period would account for the larger baseflow-season streamflow for glacier-driven streams in western Washington. Note that the climate division in western Oregon that contains glaciers had a smaller mean monthly temperature during the POST period than during the BASE period, thus accounting for the POST-period differences during the baseflow season between western Washington and Oregon glacier-driven streamflow.

In comparison to the BASE period, there were significant decreases in the PRE-period means during the baseflow season. Of the 24 sites with ratios less than 0.70, all but 2 were for the PRE period. Of the 24 sites, 4 are located in central Oregon (all of which had winter-season PRE/BASE ratios of less than 0.60—more than a 40-percent reduction in the mean compared to the BASE period), and 19 are located in Washington. Thus, there also appear to have been distinct differences in the HM regime between the PRE and POST periods during the baseflow season.

Southern Oscillation Index

Water year

The water-year values for the SOI for 1933-94, calculated as the sum of the monthly standardized values to reflect persistence, generally show that both the annual values and the mean annual value for the POST period were less than means for the BASE period (fig. 12A, means for the three periods plotted as horizontal lines). For the PRE period, the mean annual value is smaller due to the extraordinary persistence of the El Niño events during water years 1940-41 (the SOI was negative during all 24 months). As noted previously, negative values are generally associated with warmer and drier conditions in the Pacific Northwest. The change in mean between the BASE period and the PRE and POST periods was -2.8 and -7.2 standard units, respectively, and the means were significantly different from the BASE-period mean.

The persistence of negative values after 1976 (15 of 18 values for the 1977-94 period) corresponds to the average climatic regime in the equatorial region during the POST period being different not only from the BASE period but also from the PRE period. This persistence of negative values after 1976 is not observed in other parts of the instrumental record, has been described by Quin and Neal (1984), and indicates the occurrence of a pronounced shift. Other periods that may have exhibited persistently negative values have been described by Quinn and others (1987) using historical literature.
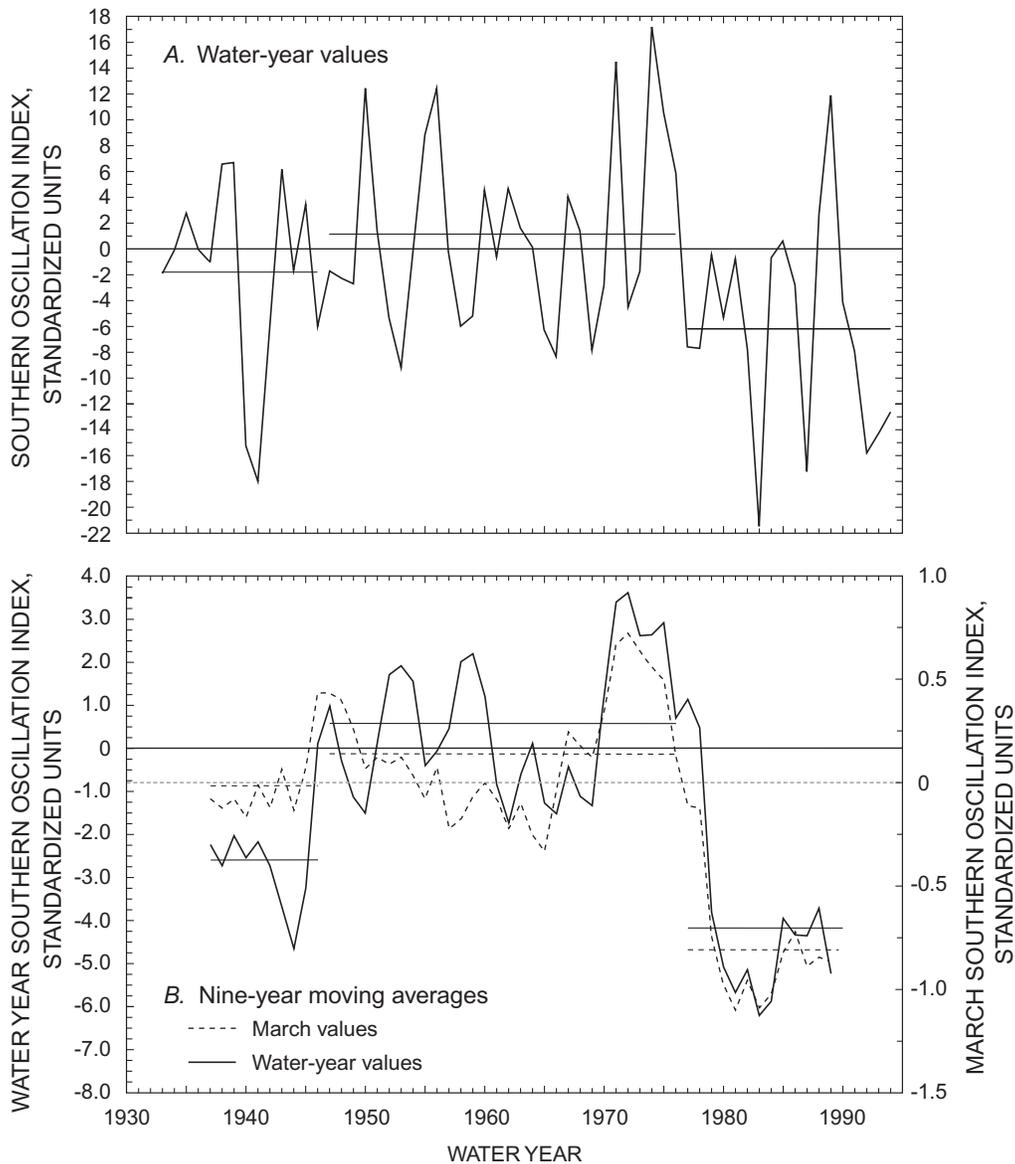
Figure 12. Water-year values and 9-year moving averages of water-year and March values for the Southern Oscillation Index, 1933-94.

Water-year values are the sum of the monthly standardized values. Horizontal lines represent the averages, from left to right, for the PRE, BASE, and POST periods.

Although the PRE values also suggest a shift, none of its means for the three averaging seasons were significantly different from the BASE-period means. Nine-year moving averages (fig. 12*B*, horizontal lines correspond to the means for each period) not only show the POST shift more clearly but also suggest that the PRE period may contain a decadal-scale component in the SOI (fig. 12*B*); the 9-year averages essentially filter out the principal high-frequency modes contained in the SOI (Cane and Zebiak, 1985; Cane, 1986; Quinn and others, 1987; Rasmusson and others, 1990). Although Quinn and others (1987) show that the period 1925-32 was one of "unusual activity" that they defined (similar to their description of the POST period) as representing long-term climatic change, they did not describe any subsets of this study's 1933-46 PRE period as such.

Mean monthly values of the SOI for the POST period (all negative) also showed large differences compared to the BASE period—the largest change was -1.3 standard units for March (9-year moving averages are shown on fig. 12*B*, March is dashed line). However, over the combined 1933-94 period, only March had a significant trend.

When the monthly values are averaged over the three averaging seasons, the ratios of the means to the BASE period are very large.

	Winter	Runoff	Baseflow
PRE/BASE ratio	-1.66	-1.48	-3.10
POST/BASE ratio	-5.83	-5.32	-5.61

These large negative seasonal ratios, especially those of the POST period, are consistent with the seasonal ratios for the HM data; that is, negative values of the SOI are related to dry conditions. Also note that whereas the POST-period ratios are nearly equivalent, the PRE-period baseflow ratio was different than the other seasons, indicating changes in the evolution of warm events. The other atmospheric-circulation measures and SST information should contain changes in their monthly-to-seasonal regimes of a similar magnitude because of the strong linkage of the SO to mid-latitude circulation and to SSTs in the North Pacific.

Pacific/North America Pattern

The PNA pattern is a dominant mode of interannual variability in the northern hemisphere during the period September through April and has a profound influence on the HM regime in the Pacific Northwest. An index of the PNA pattern was calculated for the 1947-91 period using the 700-mb anomalies for the three centers of Horel and Wallace (1981), and the PNW index was calculated using the two Pacific Northwest centers of the PNA index. Because of the record length of the 700-mb data, only changes from the BASE to the POST period are discussed. For both indices, a positive value represents a strengthening of the PNA pattern that is generally associated with warmer and drier conditions throughout much of the study area, and a negative value represents a weakening of the PNA pattern (strengthening of the reverse-PNA pattern) that is generally associated with colder and wetter conditions. As with all large-scale, quasi-stationary atmospheric-circulation patterns, the actual locations of the centers or regions of anomalously low and high pressures of the PNA pattern vary on a monthly-to-seasonal basis; thus, the indices do not capture this variability, which can have large effects on the HM regime (Yarnal and Diaz, 1986; Walters and Meier, 1989).

Means for the water year, winter, runoff, and the baseflow seasons have all changed from negative to positive values from the BASE to the POST period. The largest significant change (POST/BASE ratio of -25.4) occurred for the winter season when the PNA pattern is a dominant mode of hemispheric circulation. The difference between the water-year values (calculated as the sum of the standardized monthly anomalies) between the POST and BASE periods is about 1.6 standardized units, much of which is accounted for by the change in the winter season and by strengthening of the pattern during March and April. About 60 percent of the change in the water-year mean from the BASE to the POST period is accounted by the larger means during the January-March aggregate season; Kendall's tau for an increasing trend was significant at the 0.01 level for this season for the period 1947-91. The January-March data (fig. 13*A,B*) suggest that both the trend and difference between the means are due to shifts in the persistence of the PNA pattern, one after 1956 and another after 1976. The change after 1956 corresponds to a strong El Niño event occurring during 1957-58, and the change after 1976 corresponds to a moderate event occurring in 1976 (Quinn and others, 1987). Whether there is a plausible physical mechanism for these tandem occurrences is unknown.

The water-year and winter-season means for the PNW index for the POST period were significantly different from the BASE-period means. For the runoff season, only the mean for the high-pressure center over Canada was significantly different; this strengthening of the high-pressure cell is perhaps linked to the increased precipitation in western Washington during the runoff season.
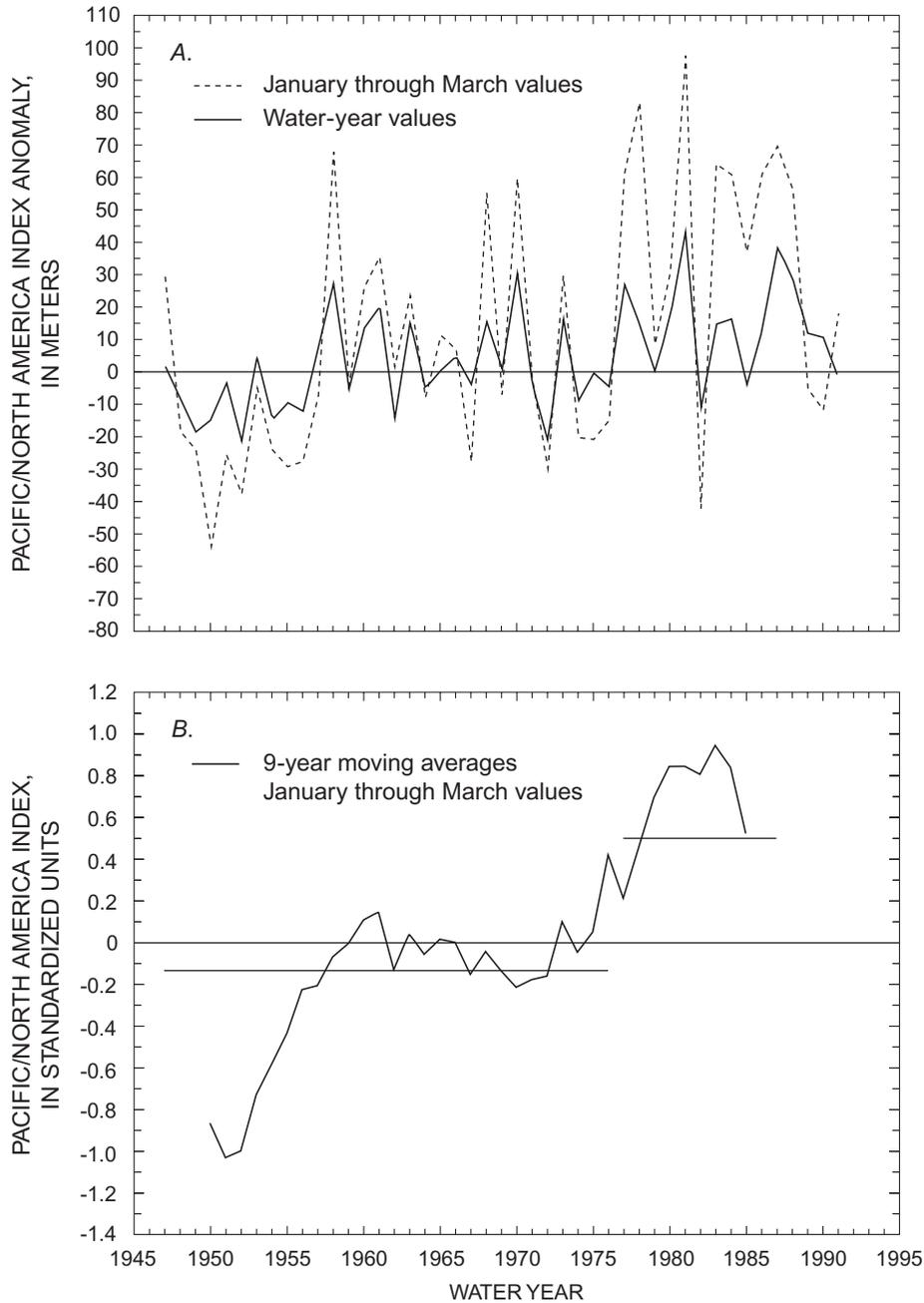
**Figure 13.** Annual aggregated January-March and water-year values and 9-year moving averages of the aggregated January-March values for the Pacific/North America index.

Values for the aggregated and water-year index are averages of the respective monthly values. Horizontal lines in (b) represent, from left to right, the averages for the BASE and POST periods.

The changes in the PNA index from the BASE to the POST period and its temporal variability have some connection to those of the SOI. The PNA index for the January-March season shows a reasonable relation—a correlation coefficient of 0. 42—to the water year SOI (fig. 14; the SOI has been reversed in sign for comparison). This relation between the PNA pattern and the SO, indicating a mid-latitude atmospheric response to the SO, has been described by Horel and Wallace (1981) and Cayan and Peterson (1989).
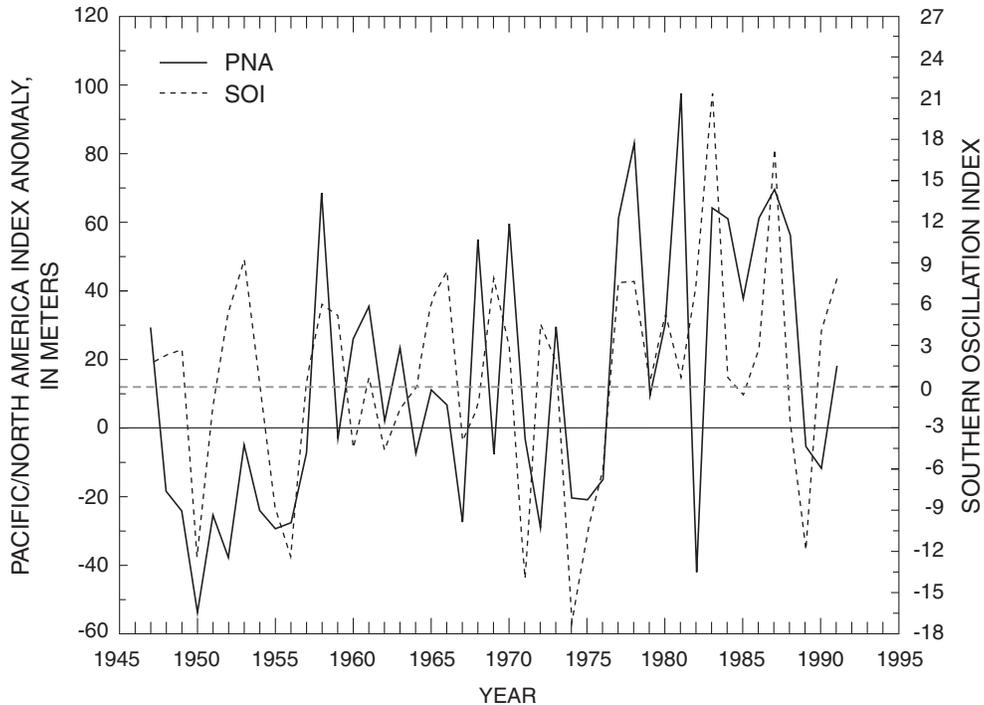
Figure 14. Relation between the January-March aggregated Pacific/North America (PNA) index and the Southern Oscillation Index (SOI).

The SOI has been reversed in sign for comparison purposes. The aggregated index is the average of the three monthly values, and the water-year values of the SOI are the sum of the monthly standardized values.

Monthly

Most of the monthly changes in the mean from BASE to POST were increases. The largest monthly changes, from 0.5 to more than 1 standard unit, were for December through April. Considering the important October-April period, when much of the precipitation falls, the weakening of the PNA pattern in November is different from its strengthening during these months. Recognizing the highly transitional nature of circulation over the North Pacific in November, a weakening of the pattern during the POST period is of interest because the persistence of a strong PNA pattern from October through November is related to periods of below-average streamflow for the runoff season for much of the Pacific Northwest. The occurrence of below-average streamflow during the runoff-season for the POST period was previously described. In addition, other November measures of atmospheric flow are strongly related to selected HM data. Thus, circulation features related to the PNA pattern in November are briefly analyzed below.

Differences between mean monthly values of the PNW index for the BASE and POST periods show the same overall pattern as that of the PNA except that the PNW index had a larger mean, a strengthening, for November during the POST period than during the BASE period. This strengthening not only reflects that of other winter months, but also suggests that the circulation patterns over the North Pacific-Pacific Northwest may have undergone changes that are not represented in the full PNA pattern, which includes the third center over the southeastern United States at 30°N, 85°W. This result is consistent with Barnston and Livezey (1987), who show that the dominant circulation mode in November is the West Pacific Oscillation, which contains features of the PNA—the spatial patterns of the two modes of circulation overlap. Using the atmospheric pressure centers of Horel and Wallace (1981) for the Western Pacific Oscillation and calculating a 700-mb index results in an index displaying a strengthening during the POST period for November with a concurrent decrease in variability.

Kendall's tau for the Western Pacific Oscillation index for the combined BASE-POST period also indicates a strengthening during November.

Cumulative departures and 2-year moving averages of anomalies for November for the three centers of the PNA index (fig. 15A,B, respectively) show that the southeastern center displays the lowest variability, is relatively stable with some change in 1967 and 1984, and its POST-period mean is larger than the BASE-period mean because of rising pressures after 1984. In contrast, the two Pacific Northwest centers display greater variability and are generally "in phase" (increases in high pressure are tandem with decreases in low pressure). The North Pacific Low center displays the largest variability that results from the effects of atmosphere-ocean coupling, and its negative mean anomaly for the POST period is consistent with the persistence of a strong Aleutian Low. Also note that none of the averaging-season means for the southeastern center for the POST period were significantly different from the BASE period. A factor that may explain these differences between the southeastern center and the Pacific Northwest centers is both a change in and a more direct linkage to the North Pacific SSTs.

Westerly and Northerly Components of Geostrophic Flow

Mean winter-season circulation for the BASE and POST periods is indicated by the composite anomalies of the 700-mb subset for each period (fig. 16A,B). The anomalies for the BASE period (fig. 16A) indicate strong zonal flow that is associated with strong westerlies. By contrast, the anomalies for the POST period (fig. 16B) indicate strong meridonal flow with weakened westerlies and also typify a strong dipole pattern that reflects the positive phase of the PNA pattern, with the high-pressure center translated westward.

The changes in the mean westerly component of geostrophic flow from the BASE to the POST period are decreases in the magnitude of the westerlies, which is consistent with the POST-period anomaly pattern (fig. 16B). The largest and most significant (0.01 level) change in the mean westerly component was for the

winter season (POST/BASE ratio of 0.89), which was translated into a significant change in the water-year mean. Anomalies for the aggregated January-March season (fig. 17A) generally parallel those of the PNA index (see fig. 13A). Differences between the January-March season and the winter season correspond to a fall-to-early-spring change in the monthly westerly component from the BASE to the POST period. For example, the months of December through March had the largest BASE-to-POST monthly changes, reflecting those of the PNA index.

There were large negative anomalies in the westerly component during water year 1983 (fig. 17A), when the strongest instrumented El Niño event occurred as of this study—1995 (see figs. 17A,B). Although there is typically a strong response in the Pacific Northwest to an El Niño event (the PNA index was positive during 1983, see fig. 13), the streamflow throughout much of the Pacific Northwest was above average, as was the precipitation in western Washington. This shows the importance of the locations of the two centers of the PNW index. That is, differences in the location of the dipole (the trough and ridge system of the PNA pattern) largely affects where winter frontal systems move into the Pacific Northwest (Yarnal and Diaz, 1986; Walters and Meir, 1989). These differences were not captured by either the westerly component (a regional measure) or the PNA index (a hemispheric measure).

The northerly component modifies the overall atmospheric flow conditions and measures the relative strength of zonal versus meridional flow. A smaller, absolute northerly component corresponds to lines of equal geopotential that are more colinear with latitude lines, indicating more zonal flow. Generally, strengthened northerly flow is associated with decreased precipitation, and strong southerly flow is associated with increased precipitation. A larger water-year mean of the northerly component during the POST period was due to the larger means for the runoff season and the January-March season, owing to the persistence of values of like sign (fig. 17B). The mean (absolute) for the runoff season was significantly larger (ratio 1.32) during the POST period, whereas the winter- and baseflow-season means were smaller, although not significantly, than those during the BASE period.
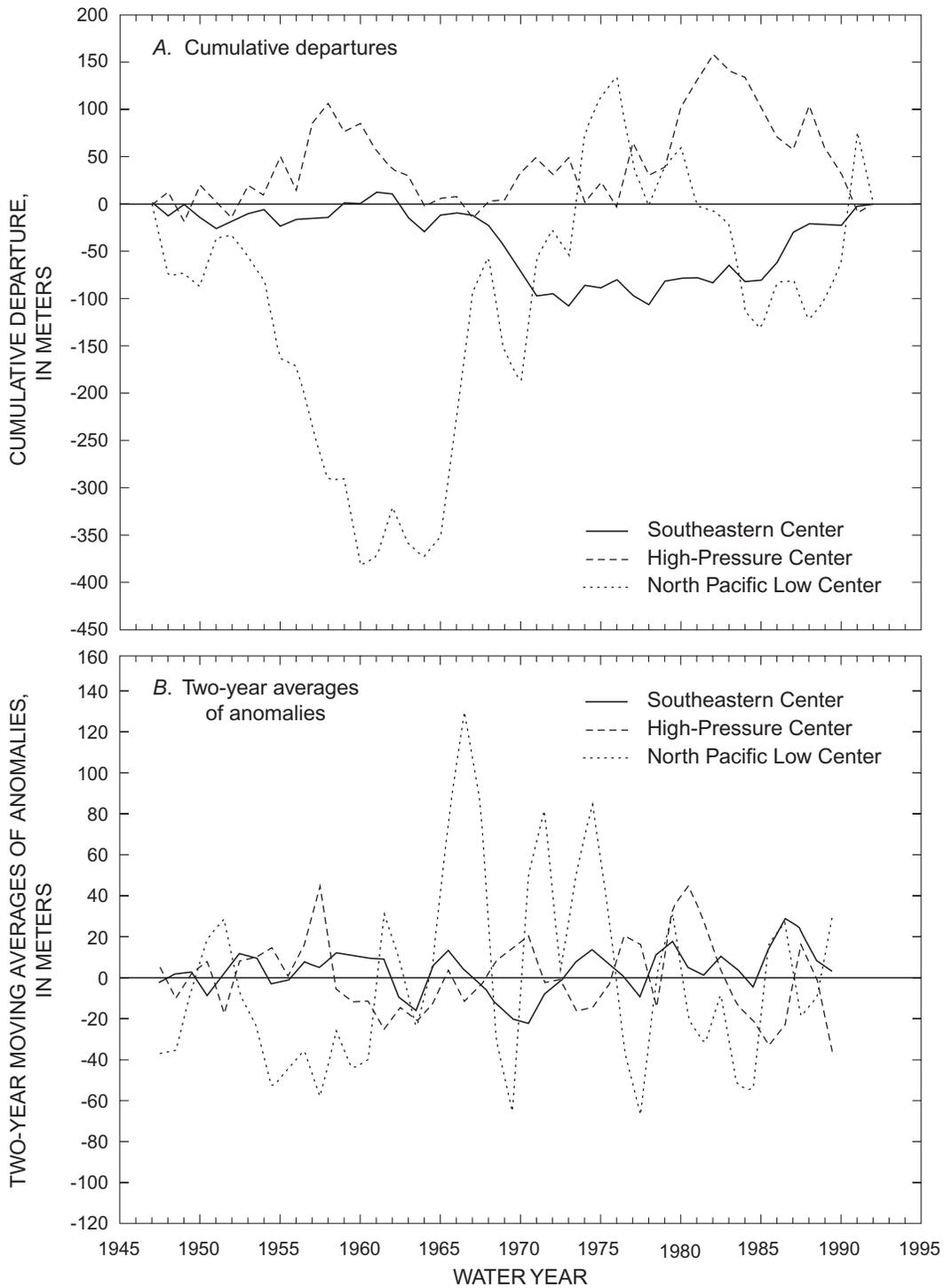
Figure 15. November values of cumulative departures and two-year averages of anomalies for the three centers used to calculate the Pacific/North America index.
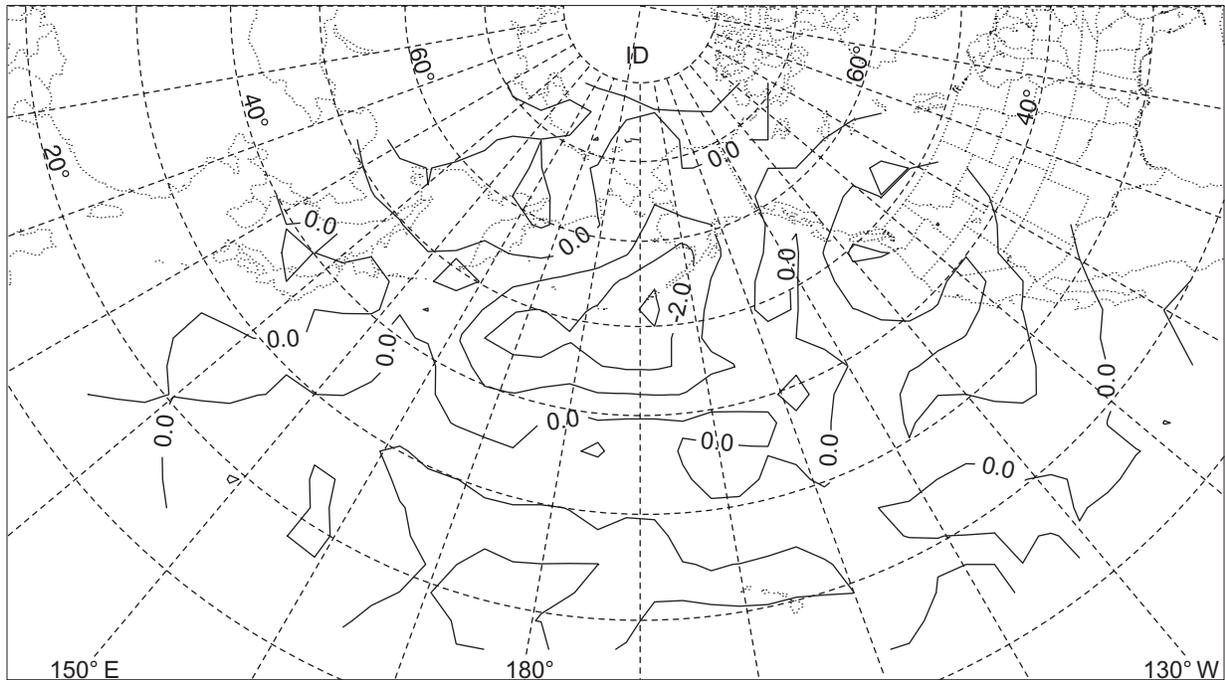
A. Base period
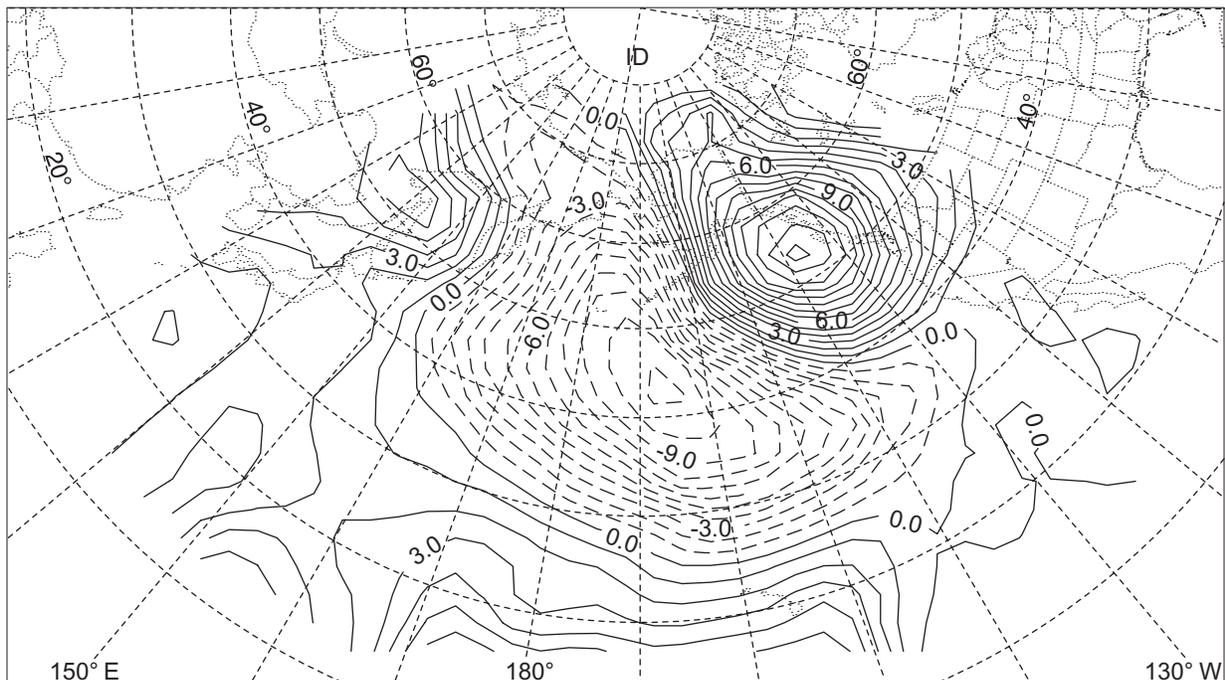
B. Post period

Figure 16. Composite anomalies of the 700-millibar data for the winter season during the BASE period and POST period.

Solid lines indicate positive anomalies and dashed lines negative anomalies. Anomalies calculated by Cayan (written commun., U.S. Geological Survey, 1993) using calendar years 1947-72 as a base period.
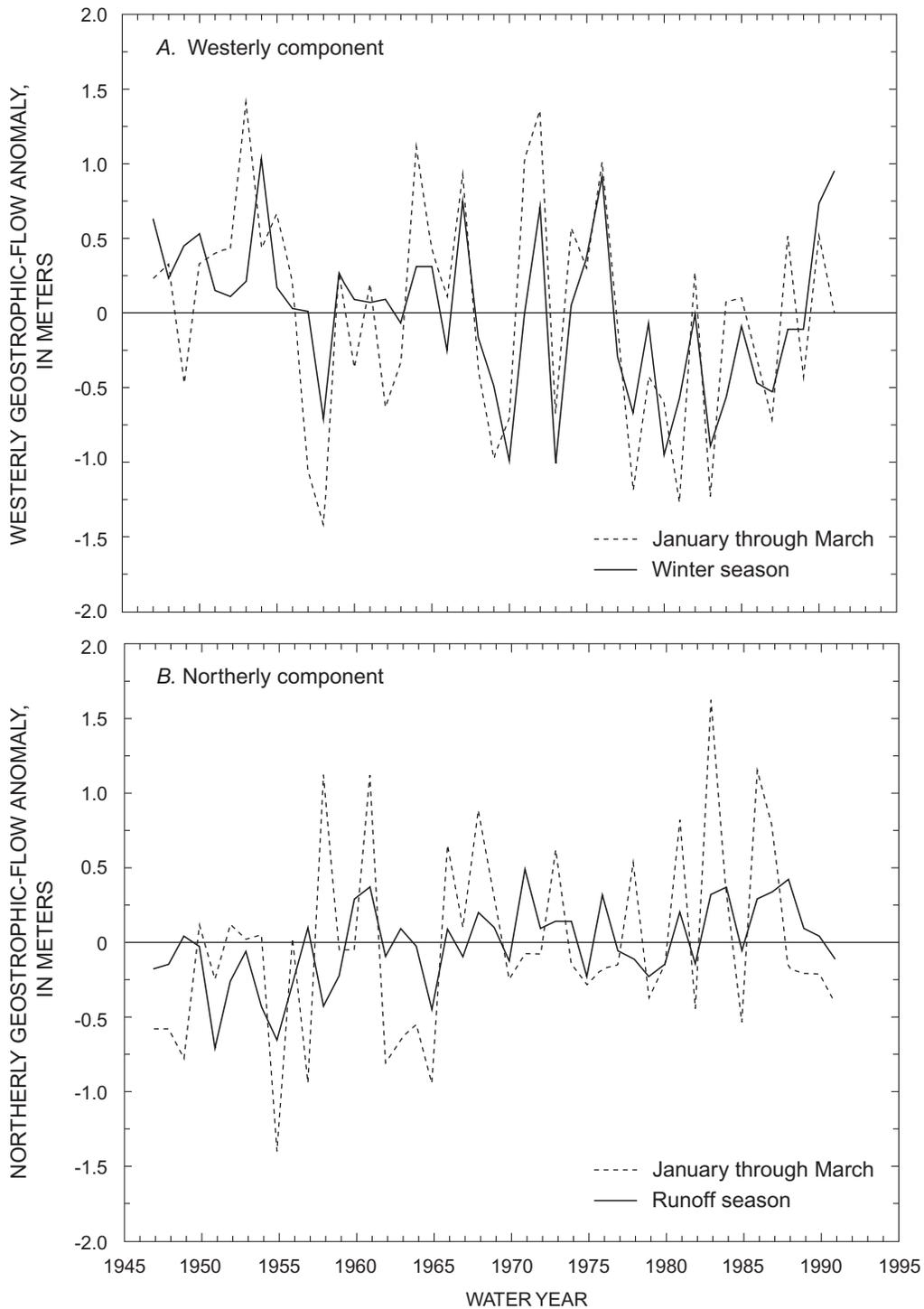
Figure 17. Measures of geostrophic flow components for the westerly component during the January-March period and winter season, and the northerly component during the January-March period and runoff season.

Values are anomalies, deviations from the mean.

Similar to the westerly component, the differences between the winter and January-March seasons result from changes in the monthly values, showing the importance of intermonthly variations in contrast to seasonal variations with respect to the analysis of the atmospheric data. However, the changes in seasonal means are important because they identify increased persistence of circulation features, which can have a profound effect on the HM regime.

The differences (POST minus BASE) between the monthly values of the northerly component indicated increasing zonal flow from October through December, increasing meridonal flow for January through June, and no change from July through September. The data illustrated on [figure 17*B*](#) suggest that the monthly changes are related to a distinct change after about 1965-67 that is not obvious in the westerly component. There appears to have been a weaker meridional flow component (identified by the northerly component) that was increasing from about 1965-67. Additionally, there were eight occurrences of a predominantly northerly flow for the January-March season during the BASE period (none after 1965) and no occurrences during the POST period. This further suggests that there has been a persistent shift in the geopotential height field. This shift may be linked to some of the shifts in the HM regime. For instance, the runoff season shift in the northerly component in the mid-1960's ([fig. 17*B*](#)) appears to correspond to the increasing runoff-season precipitation and increasing baseflow-season streamflow along the coast during the POST period.

Average Geopotential Height Field

The geopotential height field is calculated as the average of the values for four 700-mb grid points centered at 50°N,125°W. This area defines an important transitional area during both phases of the PNA pattern (Yarnal and Diaz, 1986) and, thus, should be distinctly linked to the HM regime. The analysis of the height field showed that it had a significantly larger mean during the POST period than during the BASE period for the water year, winter, and runoff seasons. The POST/BASE ratios of the means for these three seasons were 1.03, 1.02, and 1.01, respectively; the magnitude of the ratios reflects the small variability in the height field. There was a significant increasing trend for the water-year values over the 1947-91

period, most of which is accounted for by increasing trends in December through February. The change in the mean and ratios, and the trends for the height field, together indicate that part of the change in precipitation and streamflow from the BASE to the POST period was influenced by the increasingly persistent high pressures after 1976.

Increasing heights are generally related to an increasing PNA index because the grid data used to calculate the height field are located near the center that corresponds to the high-pressure center of the Pacific Northwest index dipole. However, whereas the PNA index measures the strength of a hemispheric circulation pattern, the height field is a regional measure that identifies the strength of high-pressure 'blocking' ridges off the coast and, to some extent, the PNA's (PNW's) high-pressure center. In turn, the magnitude of height field influences the HM regime because of its effect on regional circulation. For example, both the PNA index and the westerly component indicated meridional flow during the winter of 1983, whereas the height field during the January-March season was the fourth smallest of the 45 seasonal values (fifth smallest on a water-year basis), representing a greatly diminished high-pressure ridge in this area with an attendant southward shift of the mean storm track generally associated with a positive PNA index. The movement of the high-pressure cell and the storm-track shift is related to the movement, usually southeasterly, of the Aleutian Low.

North Pacific 700-Millibar Data

This discussion will briefly focus on monthly differences and their spatial patterns because other investigators have described distinct regime changes in water year and seasonal 700-mb data, including atmospheric-circulation patterns; for example, Douglas and others (1982), Namias and others (1988), and Dettinger and others (1993). The monthly differences are between the composites of the 700-mb data subset (162 grid points for the area between 15° and 75°N, 110°W and 130°E) for the BASE and POST periods. For the analysis, the intermonthly changes in these differences and spatial patterns of Kendall's tau for each month for the period 1947-91 are discussed, generally by grouping of months. The patterns of Kendall's tau typically parallel the difference in composites patterns.

However, some features are produced with more fidelity by one or the other pattern; for example, an area that underwent a shift in 1965 for some particular month may be reproduced by the difference pattern with less fidelity than by its tau pattern because the BASE-period composite would contain 12 years of the change in mean. Thus, variations between the two different spatial patterns also indicate that there may have been a regime shift prior to or after 1976-77.

Both the difference and the Kendall's tau pattern show a distinct PNA pattern for December through March; that is, there has been a tendency for a strong, deep Aleutian Low phase of the PNA pattern during the POST period relative to the BASE period. This result is consistent with the analysis of the PNA index and also relates to the fact that these months are when the PNA is an important mode of interannual variability. Kendall's tau for water-year values for the 1947-91 period and differences in water-year composites between the BASE and POST periods display patterns that are similar to these monthly patterns, especially with respect to a large, well-defined Aleutian Low, and is consistent with the results of Dettinger and others (1993). The differences in composites for January (fig. 18*A*) show some of the general features found in the December through March patterns.

December shows increasing atmospheric pressures in the southern and western part of the region and a distinct high-pressure area centered offshore around 55°N,135°W. The December high-pressure cell is the most pronounced of the 4 months, and its center is also translated north and west from both the December PNA center of Barnston and Livezey (1987) and the center of the PNA index. Anomalously low pressures extend along a northwest-southeast band in the central North Pacific (centered around 40°N,165°W). The increasing pressures to the south and the deepening of the Aleutian Low correspond to a dipole that is sometimes called the North Pacific Oscillation. Overall, the December pattern reflects the winter-season anomalies for the POST period (see fig. 16*B*).

Both January and February display a well-defined PNA-type pattern with a large spatial extent (see fig. 18*A* for January composite differences). However, there are important differences between these 2 months: the February pattern has a more extensive low-pressure region (although with less significant values of Kendall's tau and smaller anomalies) and a poorly defined high-pressure center. Additionally, some features partially contained in the January tau pattern are clearly defined in both February patterns, particularly increasing atmospheric pressures centered around 25°N,135°E and 55°N,155°E—a strengthening of the North Pacific Oscillation.

The PNA pattern of the March composite differences has a much smaller spatial extent than the February pattern, with increasing pressures in the southern, southwestern, and northwestern regions. These areas with positive trends (increasing heights) expanded from April through June, when only 26 of the 162 grid points of the 700-mb subset had negative differences. The pattern also contains features of the Western Pacific Oscillation of Wallace and Gutzler (1981) and Barnston and Livezey (1987), which was starting to develop in March with the increasing pressures at 55°N,155°E.

The April patterns still retain the features of the PNA, corresponding to the PNA index having a significant positive (increasing) trend in April for the 1947-91 period. However, compared to the prior 4 months, the strength of the anomalies and Kendall's tau for the PNW dipole are much smaller. The largest taus (positive) occur in the south-central and western regions and in an area centered at about 60°N,145°E. May patterns show increasing heights over most of the analysis region except western North America and two small areas (40°N,150°E and 65°N,175°E). The dominant features in May include the increasing heights below about 40°N and the decreasing heights centered between about 45°-50°N,125°W, which reflect the Pacific Transition pattern of Barnston and Livezey (1987).

June has two distinct patterns (figs. 19*A,B*), the pattern of Kendall's tau (fig. 19*A*) which reflects the Pacific Transition pattern, and the composite-difference pattern (fig. 19*B*), a North Pacific pattern that has been described by Barnston and Livezey (1987) and Rogers (1981). Both patterns indicate not only a changing circulation regime in the region, but also that the regime was changing in June prior to 1977. The patterns defined by the composite differences and Kendall's tau for July are consistent with and seasonally transitional from both of the June patterns.
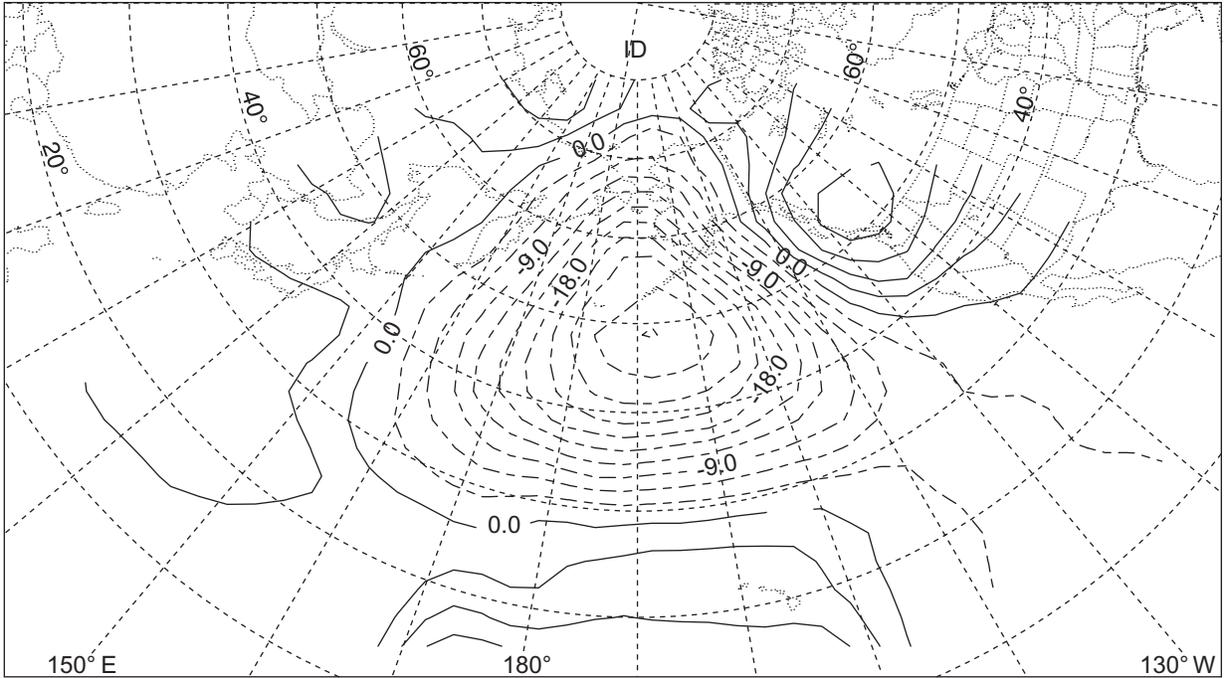
A. Composites
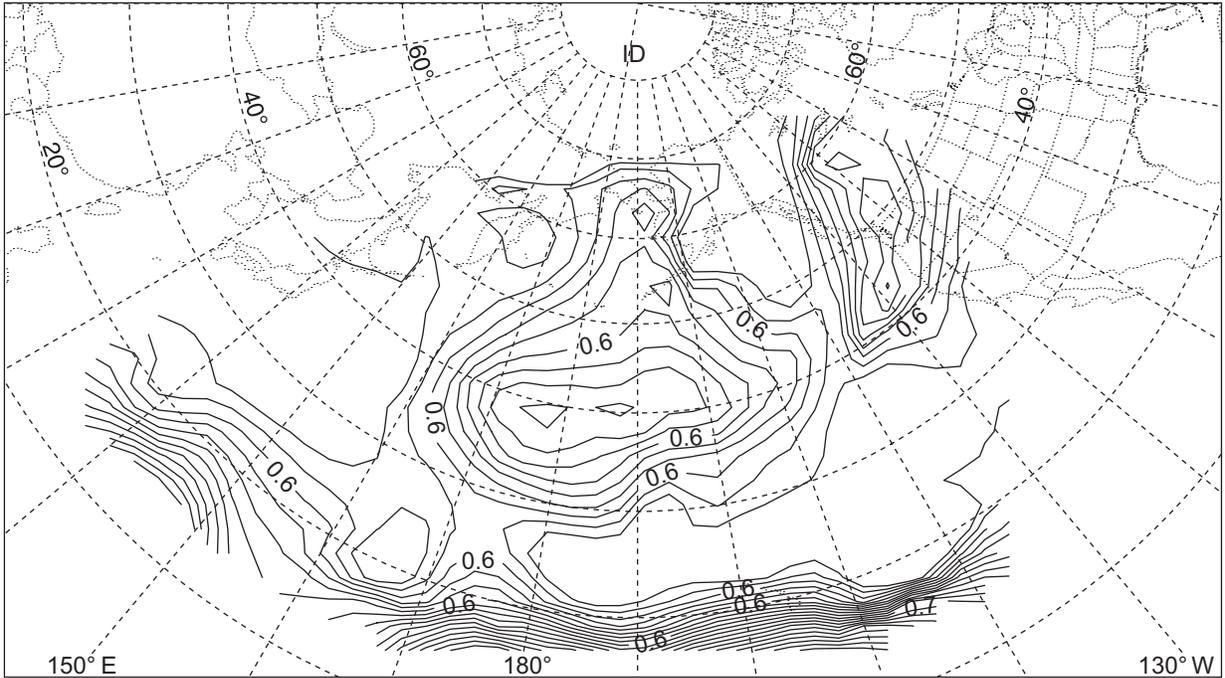
B. Hurst coefficients

Figure 18. Differences in composites (POST minus BASE) and Hurst coefficients for the 700-millibar geopotential heights.

Only contours of the Hurst coefficients greater than 0.55 are shown. For the composites, solid lines indicate positive values and dashed lines negative values.
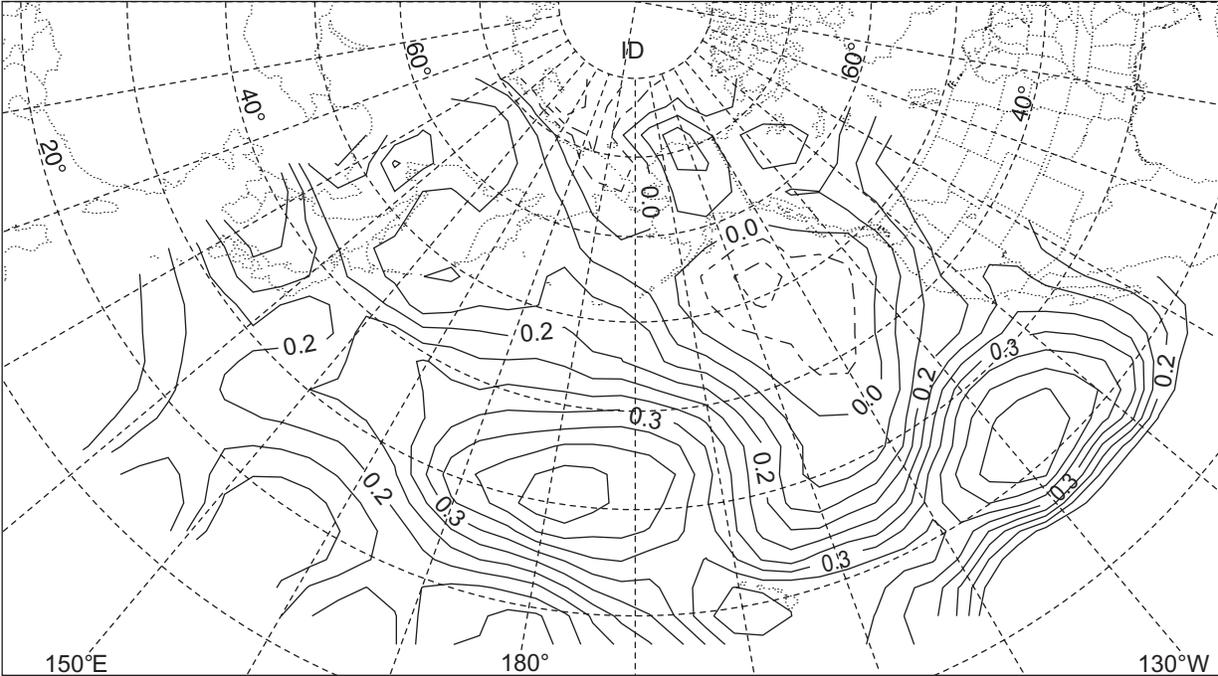
A. Kendall's tau (1947-91)
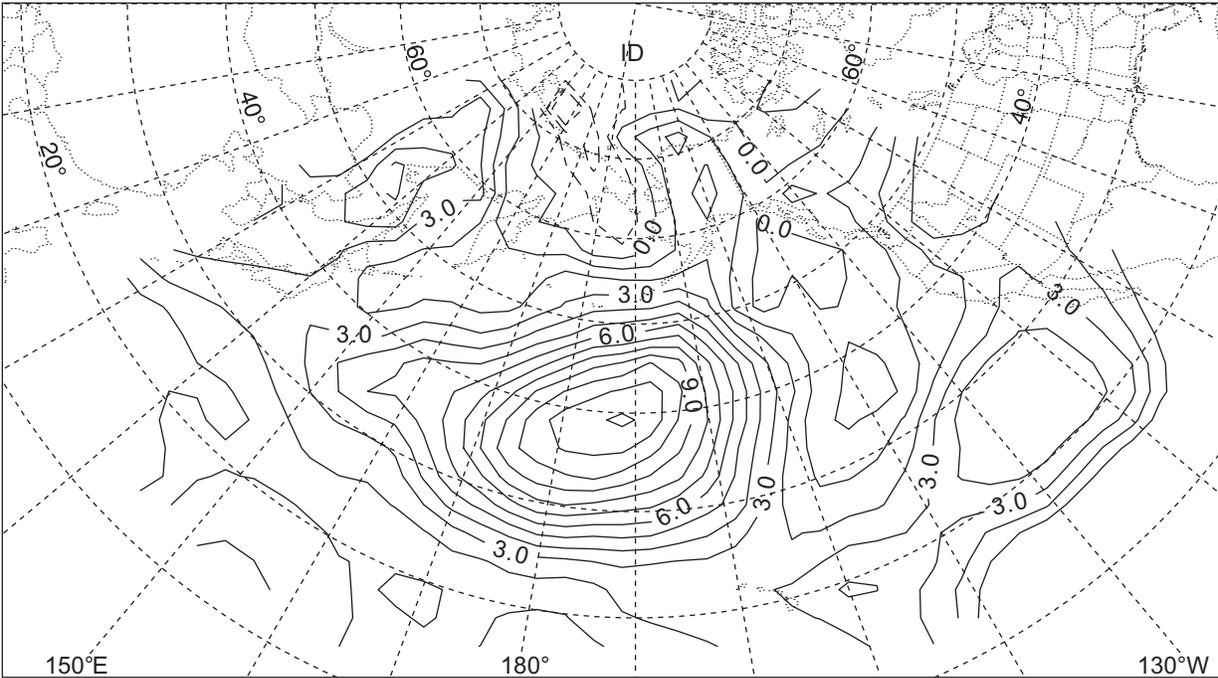
B. Differences in composites (POST minus BASE)

Figure 19. Kendall's tau and differences in composites for June 700-millibar geopotential heights.
Solid lines indicate positive values and dashed lines negative values.

For July, a broad band of increasing heights is displayed from about 55°-75°N, 145°W-130°E, and another area of increasing values is centered around 25°N-130°W; a band of decreasing heights is centered about 40°N,165°W-130°E. The spatial distribution of the increasing and decreasing heights in July reflects the Subtropical Zonal pattern of Barnston and Livezey (1987). By August, the northern east-west band of increasing values has dissipated in strength, and the other area of increasing values that was present in both the July and June patterns has increased in strength (especially between 15°-25°N,115°-170°W, see fig. 19A). There is also a corresponding development of a central North Pacific low (40°N,155°W) and an increase in heights over western Canada, which was developing in July. These two features reflect a PNA-type pattern.

Differences in composites between the BASE and POST periods for September are mainly reflected in a band of increasing heights, extending from 15°-35°N between 110°W-130°E. Both the difference and the Kendall's tau patterns show decreasing heights centered on California and increasing heights in the central North Pacific, where heights were decreasing in August. The latter changes in the central North Pacific suggest the highly transitional nature of circulation in this region during the summer.

With the onset of fall, significantly increasing heights are displayed in October (fig. 20A) for all but two areas—an area of decreasing heights centered at 50°N,140°E and another with essentially no differences between the BASE and POST periods in the south-central North Pacific (30°N,135°W-175°E). There are three centers with maximum anomalies and Kendall's tau—(20°N,125°W), (25°N,150°E), and (55°N,160°W). Although the October patterns are well defined, they do not reflect any single northern hemispheric pattern, but contain features of several patterns. For example, Barnston and Livezey (1987) show that the dominant mode of interannual variability in atmospheric circulation for October is represented in a pattern they define as the Northern Asian pattern, and another dominant mode is the PNA pattern. Parts of these two patterns are contained in the composite-difference pattern for October. These results suggest that for October the dominant patterns have not particularly strengthened or weakened during the POST period, but that other features appear to be

evolving. Last, the transition from October to November appears to be consistent. Both the Kendall's tau and composite-difference patterns for November retain some similarity to October in the western and southeastern regions—the principal differences from October are decreasing values over most of western North America and the dissipation of the high-pressure region centered at 55°N,160°W.

The 700-mb data thus display distinct monthly differences between the BASE and POST periods. The differences represent areas of increasing or decreasing heights that change on a monthly basis. These monthly changes are both transitional and non-transitional (small or no similarity between the patterns of adjacent months). The patterns generally contain parts of the major atmospheric-circulation patterns, such as the PNA pattern, and thus the monthly changes appear to correspond to monthly-to-seasonal changes and strengthening in some of the dominant modes of atmospheric circulation in the North Pacific region and, in some months, in the Northern Hemisphere. In turn, the correspondence between atmospheric-circulation patterns and the two calculated patterns suggests increasing persistence of selected hemispheric circulation features, especially during the November-March wet season when the largest anomalies and Kendall's tau occur, which also reproduce recognizable patterns. For example, the January differences between composites for POST and BASE (see fig. 18A) clearly reproduce a well-defined PNA pattern, and the Hurst coefficients, which measure relative persistence, for January (see fig. 18B, only values greater than 0.55 contoured) show the same overall pattern and indicate the persistence of this pattern. This increased persistence is undoubtedly related to changes in the HM regime.

The relation between the changes in both the HM regime and the monthly patterns is further suggested by comparison of several patterns for October. The October composite difference pattern (fig. 20A) shows the areas of increasing and decreasing heights that were described above, and these areas also are clearly defined in the October composites for water years 1963, 1973, and 1977 (fig. 20B), which were three of the driest years in the combined BASE-POST period. The pattern shown on figure 20B also reproduces with good fidelity the Northern Asian pattern in October.
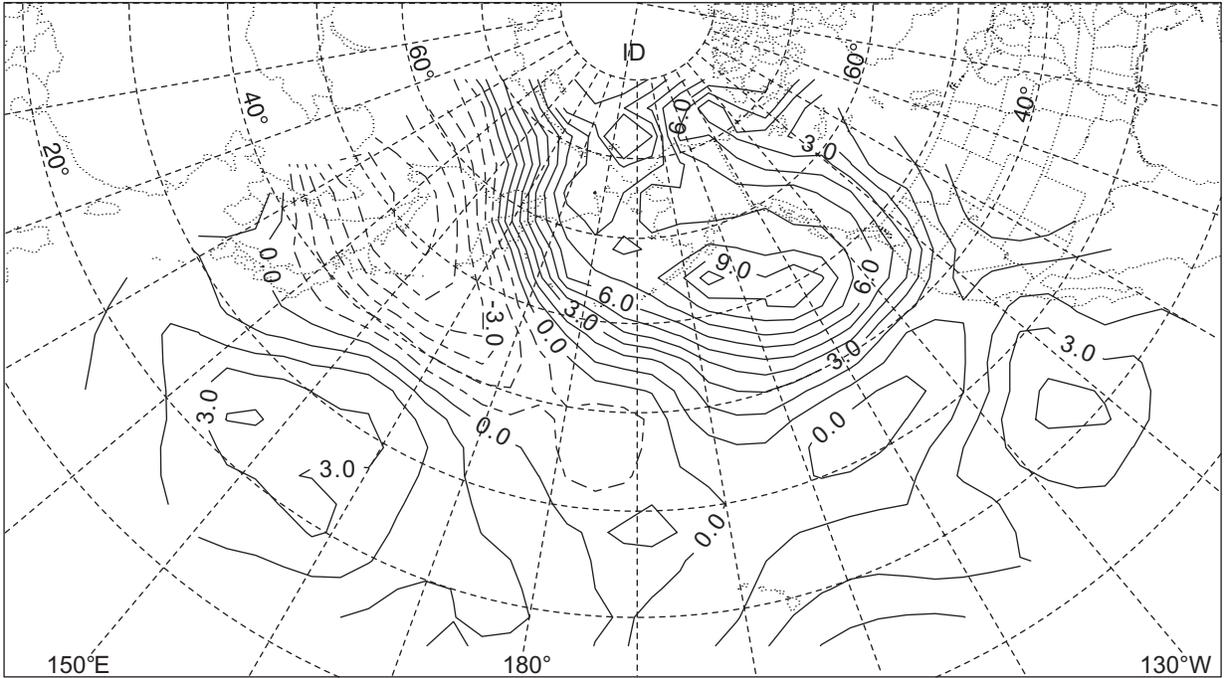
A. Difference in composite heights
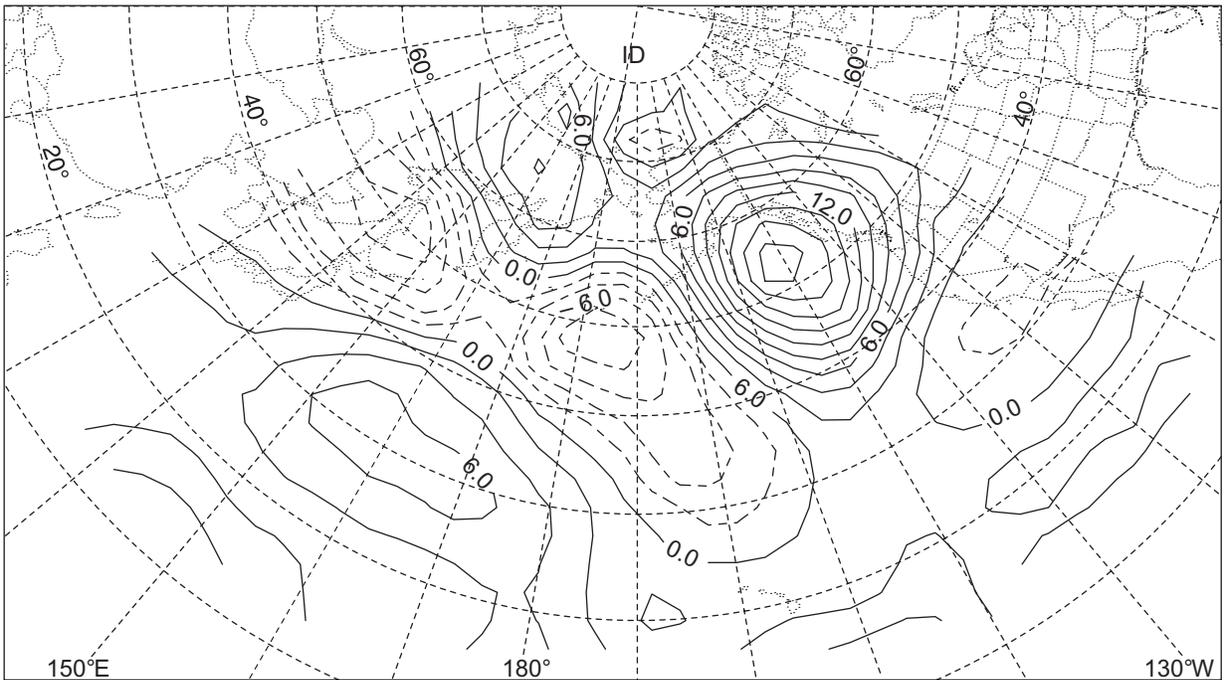
B. Composite anomalies for 1963, 1973, and 1977

Figure 20. Differences in composite heights (POST minus BASE), composite anomalies for 1963, 1973, and 1977, and composite anomalies for all water years when at least one of the 112 streamflow sites had a runoff-season streamflow value less than its 20th-percentile value, for October.

Calculations of 20th-percentile values were based on 1947-91 period and not the full period of record. Solid lines indicate positive values and dashed lines negative values.
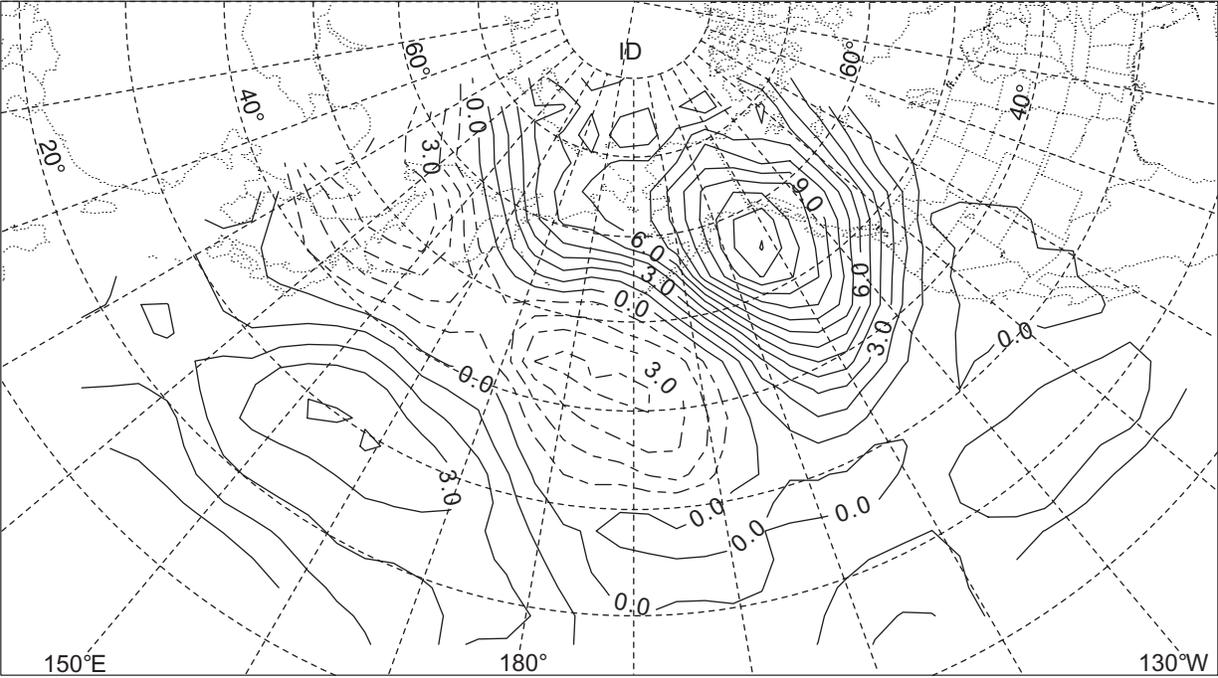
C. Composite anomalies for all water years

Figure 20. —*Continued.*

Additionally, October composite anomalies (fig. 20*C*) for all water years when any of the 112 streamflow sites had 20th-percentile or less runoff-season streamflow (calculated based on the post-1946 period of record) also show the same overall spatial pattern as the composite difference and 3-year anomaly patterns (figs. 20*A,B*). This not only suggests that the October difference pattern is related to and foreshadows decreases in streamflow and precipitation from the long-term mean, but also may account for the trend of decreasing October precipitation in western Washington.

North Pacific Sea-Surface Temperatures

Similar to the analysis of the interdecadal regime changes in the 700-mb data, the following analysis focuses on monthly changes from the BASE to the POST period. The analysis employs differences between the BASE and POST periods of the mean monthly values of the SSTs, composite anomalies for the POST period, and monthly values of Kendall's tau calculated from the complete period of record. As described previously, the SST data set consists of 5°-gridded monthly means and anomalies for the area 20°-60°N, 110°W-130°E for water years 1947-92.

Changes from the BASE to the POST period in the monthly means (calculated using all data regardless of the sample size for a grid) were all negative and ranged from -1.35°F in September to -1.71°F in October. As a result, the water-year mean changed by -1.36°F, indicating a large, spatially consistent difference between the BASE and POST periods. These results are consistent with those of Dettinger and others (1993), who showed that there was a significant decreasing trend for January-March SSTs for the period 1947-93 for a large area of the North Pacific (centered near the North Pacific low-pressure center of the PNA pattern) and that the years with the most anomalously low temperatures generally occurred after 1976. Monthly differences between composite means for the two periods (calculated only when the sample size for a grid point was at least one-half of the total number of years for each period) showed about a 2-to-1 ratio of number of grid points with lower temperature to the number of grid points with higher temperature. Except for April and May, the grid points with lower

mean monthly SSTs during the POST period generally include water that is warmer than the grid points with larger mean monthly SSTs. Thus, although the pattern of the changes and their persistence in the monthly SSTs are the principal items of interest, the overall changes described above indicate that a relatively large cooling has occurred in the North Pacific SSTs during the POST period and that this cooling should be reflected in persistent patterns. Additionally, the variations for the April-May summer-transition season appear to be important and will be discussed later in the section 'The April-June Summer-Transition Season'.

Values of Kendall's tau for January through September for the 1947-92 period show decreasing SSTs in an area covering most of the western and central North Pacific that steadily expands eastward (reaching the northeastern coast in about July) and contracts northward. However, the southeastern North Pacific, from about 20°-35°N, 110°-140°W (encompassing part of the band with increasing geopotential heights in September), shows a consistent increasing temperature trend from January through September, with a decline in its overall spatial coherency from about October through December; a similar trend is displayed in part of the northeastern North Pacific from January to June. From October through December, there is a westward contraction of the area with negative values of Kendall's tau, although by December, it still covers more than 50 percent of the North Pacific. In conjunction with the westward contraction, a pool of water with negative tau in the northeastern North Pacific (40°-55°N, 125°-135°W) is isolated from the broad expanse of the North Pacific that is also negative; this pool displaced the pool with positive Kendall's tau. Ebbesmeyer and others (1989) have shown the relation between coastal SSTs in a small area of this northeastern region and part of the HM regime in western Washington.

The monthly SST anomalies for the POST period show the same overall pattern as the trend analysis, except that the area of maximum anomalies is smaller, nearly diminishes by November, and covers only a small part of the western North Pacific by December. The December to January change in the extent of the pool of water with large negative anomalies is very large—changing from about 11 grid points to 35 grid points (changing from a maximum eastern extent of about 175°E to about 155°W).

This extension to the eastern Pacific from December to January most likely is related to the increased persistence and extent of the Aleutian Low in January in comparison to December and is also probably related to the stronger change in atmospheric circulation for the January-March season in comparison to the December-March season (Namias, 1976b).

The changes in the SSTs are consistent with changes in the HM regime from the BASE to the POST period: cooler SSTs indicate less ability of the overlying atmosphere to store moisture and decreased evaporation, and thus, decreased net vapor transport into the Pacific Northwest (Namias, 1969). In turn, cooler SSTs and the persistence of the PNA pattern are probably intricately linked and mutually reinforcing, especially from about January through March (and perhaps April) when the composite monthly anomalies

for the POST period show a distinct central North Pacific pool of cooler SSTs near the North Pacific low-pressure center (45°N, 165°W); that is, the predominant westerlies are associated with the pool of lower-temperature water. The relation between a March SST (grid point 40°N,170°W) and the water-year PNA index (fig. 21; PNA has been multiplied by -1.0 for comparison) suggests this probable link. The trend in both data series over their complete record length also is significant, with standardized series for both having about one standard unit (a standard deviation) change in the mean from BASE to POST.

Another SST grid point with a large POST-period anomaly for March is 30°N, 155°W, which is at the southern extent of the North Pacific pool with negative anomalies. The southern extent also defines a boundary where SST correlations to the water-year PNA index are large to the north and small to the south.
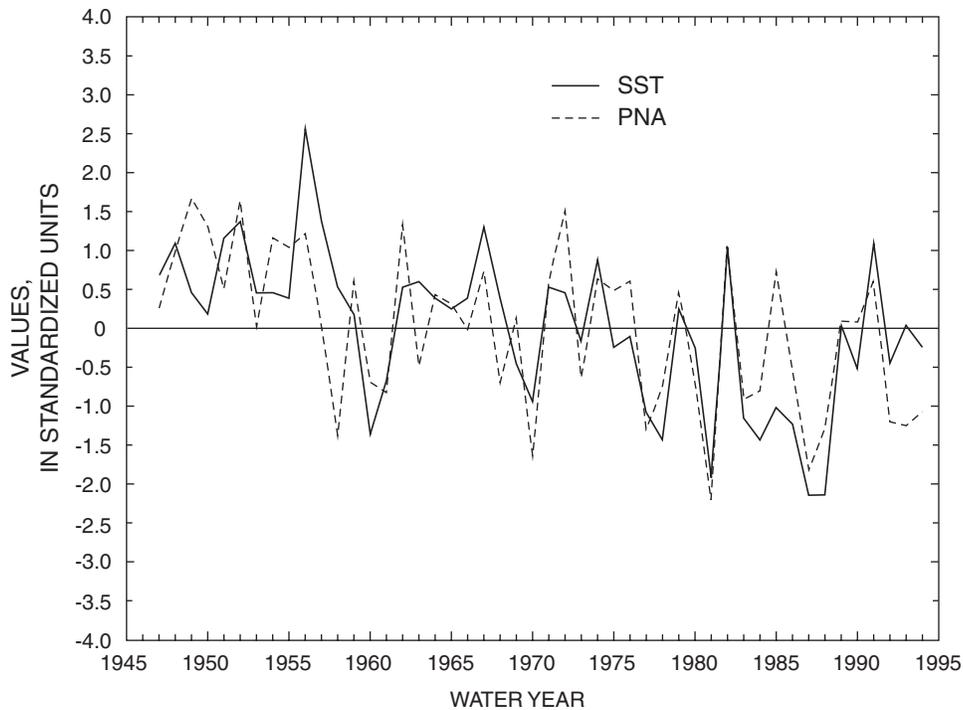

Figure 21. Relation between the March sea-surface temperature (SST) at 40°N,170°W and the water-year Pacific/North America (PNA) index.

Values for the PNA index have been reversed in sign for comparison.

The March spatial-correlation structure closely matches the PNA pattern and is related to the fact that this grid point (30°N, 155°W) is just south of the PNA pattern's oceanic low-pressure center in March (Barnston and Livezey, 1987). The cumulative departures for the March SST for this grid and for water-year values of a eastern Washington streamflow site (site 27, table 1, shown previously on figs. 6-7) clearly indicate above-average SST and streamflow for the BASE period and below-average for the POST period (fig. 22A), while the relation between those two variables and values for the low-pressure center for January-March (fig. 22B) not only suggests a good correspondence, but also an overall downward trend.

The monthly spatial patterns for the SST data and the 700-mb subset have many similarities, especially during the winter months, and indicate a rather coherent response in the North Pacific region, which has been described as early as 1959 (Namias, 1959). As described previously, the PNA index (a hemispheric measure of atmospheric circulation) includes a center over the southeastern United States that did not appear to be as related to interannual variations of the North Pacific low-pressure center as did the PNA index's other center, which is located over southwestern Canada, and it was hypothesized that this was due to the more direct linkage to North Pacific SSTs. Water-year cumulative departures for the SST at 35°N,165°W and the heights for the southeastern center and the North Pacific low-pressure center were calculated to roughly estimate (1) if the coherent response of atmospheric circulation in the North Pacific and SSTs also occurs in other regions (explicitly the region defined by the location of southeastern center because of the importance of the PNA pattern in affecting atmospheric flow over the North Pacific and the Pacific Northwest), and (2) if the differences in the variations between the three PNA index centers are related to the North Pacific SSTs. These departures (fig. 23) show a close relation between the North Pacific low and SST (correlation coefficient 0.71)—note the period of generally below-average values after 1977 and a smaller correspondence between the southeastern center and the SST. Additionally, the distinct change in the southeastern center after 1957 is not displayed by the other data series or the PNW index, but is displayed by the PNA index (see fig. 13).

The SSTs thus display significant differences between the BASE and POST periods on a monthly-to-annual basis. The SSTs at selected grid points, which are representative of major centers of action, are closely related to both 700-mb measures and streamflow. Depending on the month and the grid point, the SSTs show regime shifts at several boundaries; however, on an annual basis, influential SSTs (as determined by correlation analysis) generally show above-average temperatures from 1947-76 and below-average temperatures from 1977-92.

The relation between the interdecadal regime shift in the SSTs and the PNA pattern is indicated by the correlation structure from October through March SSTs and the aggregated January-March season PNA index. This structure closely resembles a type of PNA pattern (with the high-pressure center now corresponding to most of the northeastern North Pacific), which covers most of the North Pacific, and further indicates the prior and contemporaneous relation between winter SSTs and atmospheric-circulation features. In addition, a correlation structure between the aggregated January-March season PNA index and the monthly fields of SSTs is still well defined in April and May, indicating the memory contained in the upper ocean heat reservoir; the structure for June and July also displays large, spatially consistent fields of negative correlation and the movement of the positive correlation area from the northeastern to the southeastern North Pacific. These monthly correlation fields are generally consistent with the fields of Kendall's tau for the monthly SSTs for the 1947-92 period.
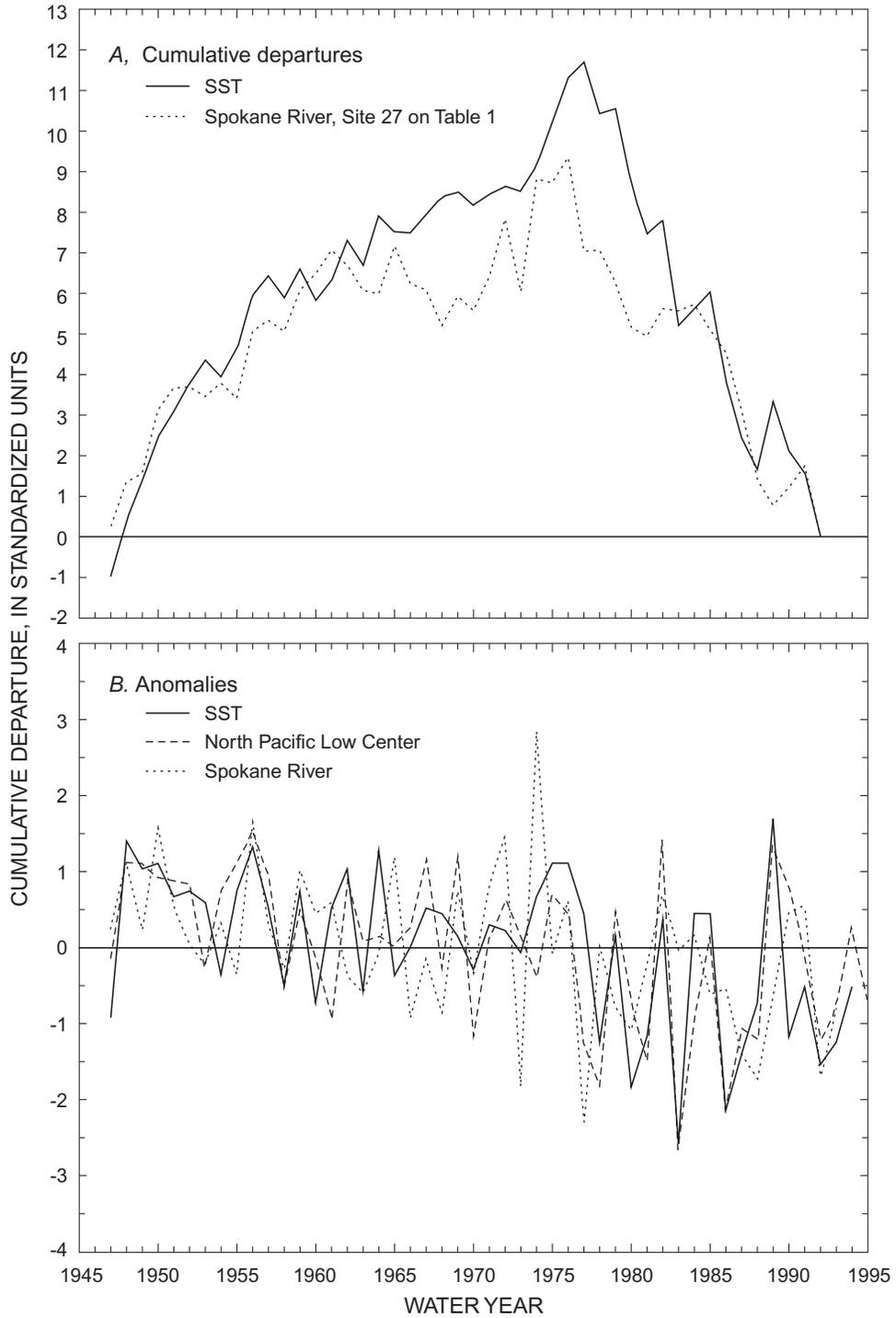
Figure 22. Cumulative departures of the March sea-surface temperature (SST) at 30°N,155°W and water-year streamflow for a site in eastern Washington, and anomalies of those variables and the January-March (average) North Pacific low-pressure center of the Pacific/North America index.
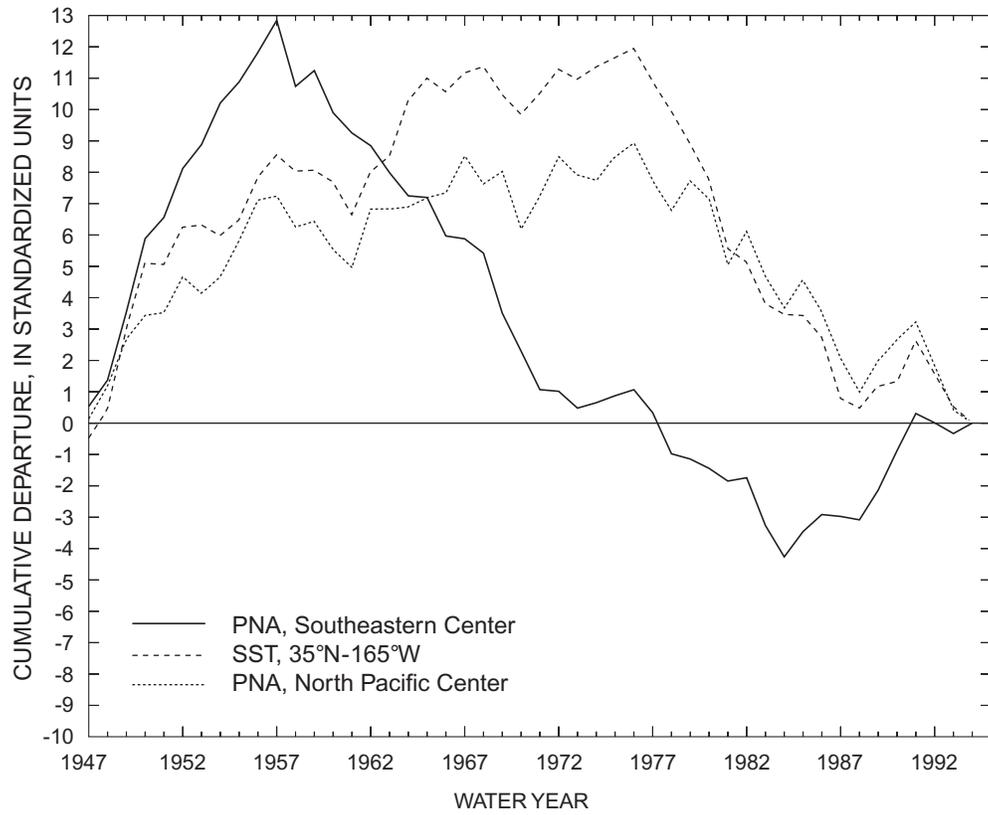
Figure 23. Cumulative departures of water-year values of the sea-surface temperature (SST) at 35°N,165°W and the two low-pressure centers of the Pacific/North America (PNA) index.

DISCUSSION

The following discussions are separated into three general categories: (1) a summary of the major HM findings, spatial-temporal variations in these findings, and potential impacts related to water resources; (2) potential linkages between changes in the HM regime and atmospheric/SST information; and (3) an analysis of additional information consisting of three long-term data series to assess consistency of results, with an emphasis on the occurrences of regime changes. That is, the presence or absence of shifts in selected long-term series is estimated in order to obtain some concept of the potential spatial extent of these interdecadal shifts, as represented in other geophysical data—principally to show the practical importance of regime shifts and, secondarily, to further independently check the results, including the existence and timing of shifts.

Findings

There have been significant changes in the HM regime in the Pacific Northwest over the three interdecadal periods. The differences between PRE- and POST-period precipitation and streamflow information also indicate that the HM regime was different during these two periods; this was especially reflected in the differences in the winter-season streamflow. While both periods were generally drier, with less streamflow than the BASE period, the HM regime during the POST period also appears to have been warmer in some ill-defined manner. The changes in the mean winter-season precipitation and streamflow and in the snow-water content (swc) series all suggest an attendant warming. Namias (1980) presents a composite North Pacific SST field for periods of warm winter temperature, and this field is dominated by cool SSTs centered in the region of the Aleutian Low. The previous analysis of the monthly SST data indicated the persistence of the cold-water pool and is consistent with warmer temperatures. Additionally, Yarnal and Diaz (1986) show that warmer temperatures are generally associated with a strong PNA pattern and that below-normal precipitation is also generally associated with a strong PNA pattern. The strengthening of the PNA pattern during the POST period is consistent with decreased precipitation, streamflow, and swc and higher air temperatures.

The larger mean streamflow in the Idaho-Oregon region and changes in both precipitation and streamflow along the coast indicate that the overall circulation regime has changed, probably related to a translation (with concurrent strengthening) of the mean position of the centers with anomalously high and low pressures. This latter aspect is briefly described in the section 'Variations During 1980 through 1985'.

Precipitation

The analysis of the precipitation data showed that, on a water-year basis, both the PRE and POST periods were drier than the BASE period. In comparison to the BASE period means, the largest change in the mean was during the winter season (a 16-percent decrease for the POST period), and the smallest change in the mean occurred for the runoff season (a smaller mean for PRE and a larger mean for POST). Thus, changes in the mean for the water year are principally accounted for by the changes during the winter season, when most of precipitation occurs. The larger mean precipitation during the runoff season for the POST period, in comparison to a smaller mean during the PRE period, also indicates that the climatic regime was different during the PRE and POST periods.

Statistical tests of means and simple graphical analysis show that interdecadal regime shifts at the 1946-47 and 1976-77 boundaries are well defined, especially for the water-year and winter-season precipitation values. The runoff-season values also were reasonably defined by these bounds, with some variations. However, there were spatial differences in the timing of the regime shifts for selected months. For example, mean precipitation for August through November has a well-defined shift at about 1967 in the southern part of western Washington, with precipitation having a larger mean than the BASE-period mean for some sites after 1967. This larger mean probably corresponds to the larger mean streamflow during the baseflow season for coastal-type sites south of the Olympic Mountains, Washington.

To estimate how these changes in the precipitation regime for the POST period would translate over the region, a simple analysis is presented. Long-term average annual precipitation in western Washington (area of about 63,600 km^2) was estimated to be about 210 cm or 4,190 m^{3}s^{-1} based on gridded values of average annual precipitation.

Thus, as a first approximation, the average POST/BASE ratio suggests a decrease in the net water-year input to western Washington that is on the order of 29 cm or 576 m^3s^{-1}. Because precipitation ultimately supports the water supply, the potential loss of this areally averaged, weighted value of 29 cm is significant.

It is of interest to estimate if snowcourse data show changes similar to the precipitation data because, outside of the mostly ground-water supplied regions (generally located in the arid-to-semiarid parts of the Pacific Northwest), much of the water supply in the Pacific Northwest is dependent on snowpack and snowmelt. The average April 1 swc for 69 sites in the Pacific Northwest has been calculated for the period 1948-87 using standardized April 1 values (fig. 24; M.D. Dettinger, written commun., U.S. Geological Survey, 1995). This swc series (mean 0.04, standard deviation 0.73) has a BASE to POST period decrease in the mean of -0.73 units, indicating a significant change (nearly 1 standard deviation); additionally, the series has a significant (0.02 level) negative trend for the 1947-87 period. Cumulative departures and anomalies of the swc series (fig. 24) show temporal variations similar to both the precipitation and streamflow data. The cumulative departures show a net cumulative decline after about 1976-77, whereas the anomalies show a more complicated regime with a rather abrupt change, representative of a shift, after 1974 (fig. 24).

Precipitation in western Washington should generally be aligned with the swc temporal variations because snowpack is determined by precipitation and there is spatial coherence between precipitation in western Washington and streamflow, largely driven by snowmelt, in parts of the Pacific Northwest.
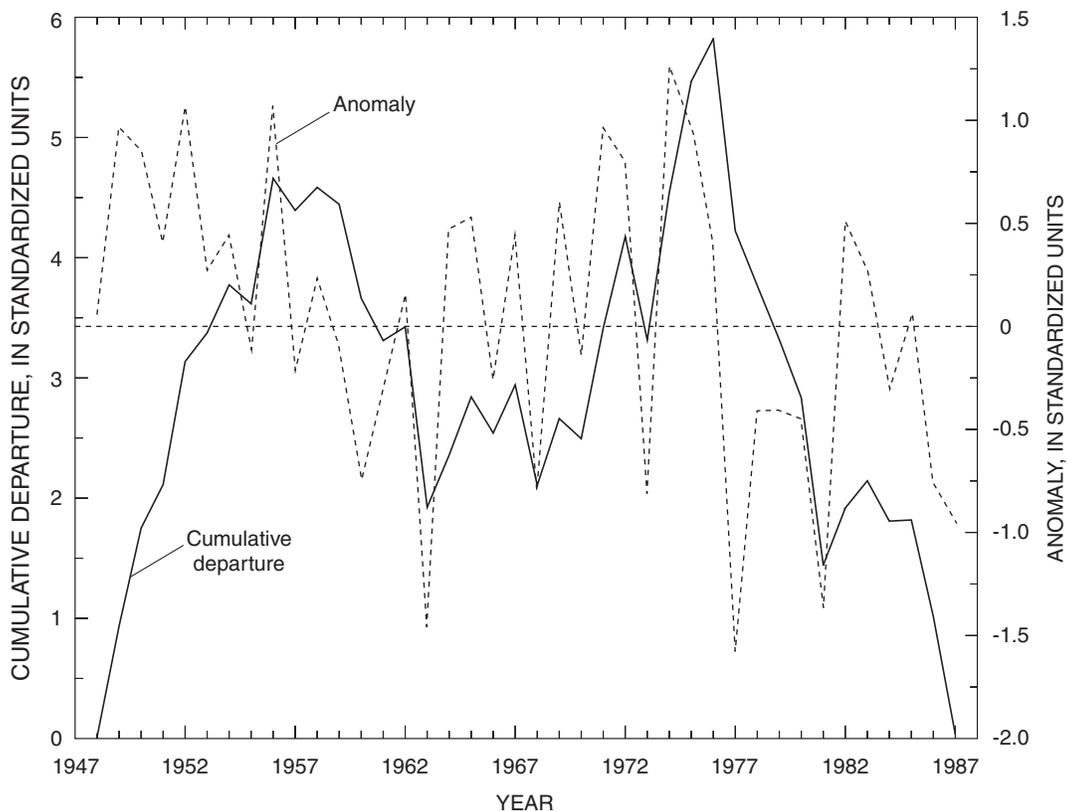
Figure 24. April 1 snow-water content for the period 1948-87.
Values are the average of the standardized values for 69 sites in the Pacific Northwest.

Using the average of the 50 standardized October-March values (1948-87 water years) of total precipitation as a surrogate series for precipitation in the Pacific Northwest and comparing this series to the swc series (fig. 25) shows that the precipitation series is similar to the swc series. There are some inconsistencies between the two curves in the earlier part of the record, with an apparent "phase-locking" beginning to be established in 1962, after which the differences generally relate to magnitude but not the sign of the anomaly. The larger and more significant negative trend in the swc series suggests the potential effects of increasing air temperature on swc. Nine-year moving averages of the mean monthly values of the daily maximum and minimum air-temperatures averaged over the months of January through April for Cedar Lake, Wash. (fig. 26) indicate an increase in air temperature and are consistent with the divisional climate data. The 9-year moving averages of

precipitation for this site (fig. 7B) show decreased precipitation for the POST period, which in conjunction with the increasing air temperatures would mutually contribute to decreased snowpack. This decrease in snowpack and earlier melting of the pack was described previously using simulations of snow accumulation and ablation at Cedar Lake.

Streamflow

The changes in the streamflow regimes from the BASE period were also significant, but were more complicated than those identified in the precipitation data owing to the larger spatial domain. For the PRE and POST periods, mean water-year streamflow was less than the BASE period for all but 15 of the 112 sites, with 14 of the sites experiencing larger means for only the POST period.
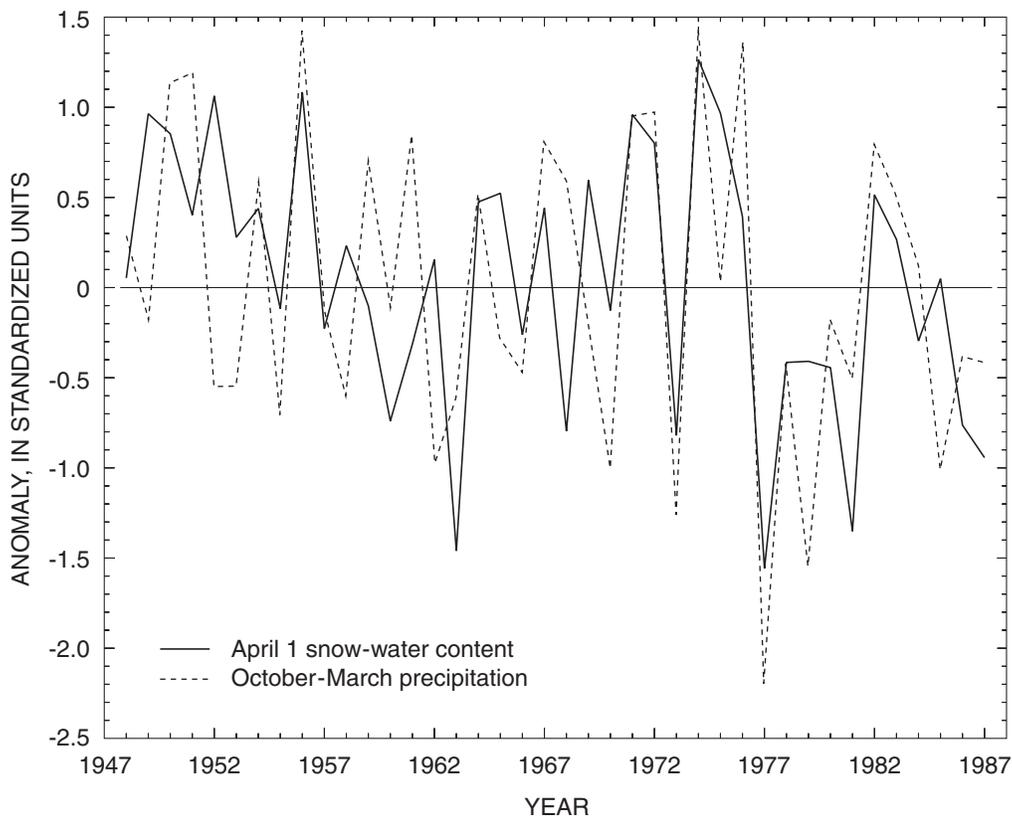

Figure 25. Anomalies of April 1 snow-water content for the Pacific Northwest sites and October-March precipitation in western Washington.
The anomalies are the average of 69 sites and precipitation is the average of 50 sites.
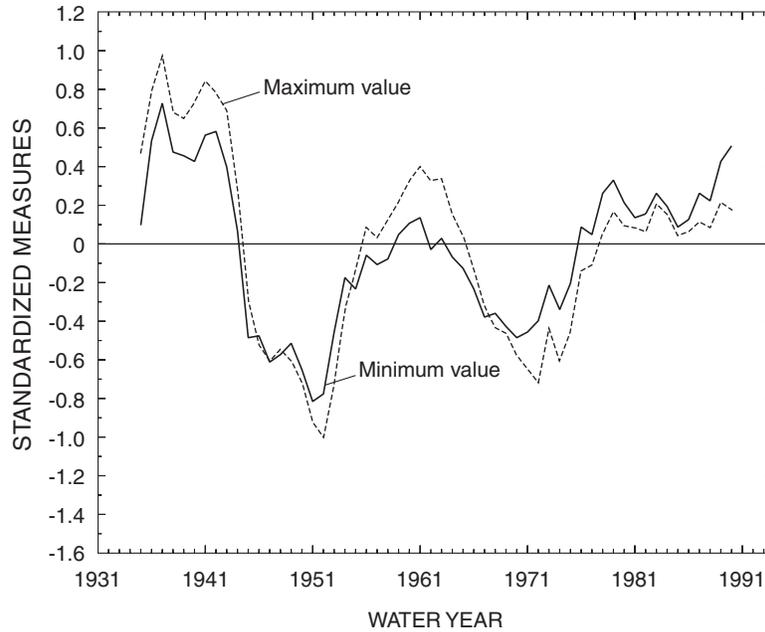
Figure 26. Nine-year moving averages of mean monthly values of daily maximum and minimum air temperature for the January-April period at Cedar Lake, Washington.

The sites with larger means aggregate in the Idaho-Oregon region. The average of the ratios of the means for the water year were 0.83 and 0.87 for the PRE and POST periods, respectively. On a cumulative basis, the ratios represent a decrease in streamflow equivalent to shutting off the four streams with the largest water-year discharges that were analyzed in this study. The consistency of the results suggest that, in comparison to the BASE period, the net decrease in outflow from the region during the PRE and POST periods, as represented by all streams in the Pacific Northwest, was very large. As an example, the BASE-to-POST cumulative decrease in mean water-year streamflow for the 24 western Washington streamflow sites was 136 m^{3}s^{-1}, whereas the total climatological water-year streamflow in western Washington is about 3,256m^{3}s^{-1}, suggesting a net decrease on the order of 390 m^{3}s^{-1} if the 0.87 ratio applies overall. This latter quantity is about three time more than the largest water-year streamflow value analyzed in this study for western Washington streams (sites 1-24, table 1) and approaches the mean annual value (470 m^{3}s^{-1}) of the largest stream in western Washington, which in turn is a major control on the hydrodynamics of the Puget Sound estuary (Ebbesmeyer and others, 1989).

Mean winter-season streamflow for both the PRE and POST periods was less than for the BASE period for all but 11 sites, which had larger means only for the POST period. Five of the 11 are located in the Idaho-Oregon region, and information from the other 6 sites suggests an earlier runoff regime. Hydrographs of the average ratios of the monthly mean/annual mean values for the BASE and POST periods for streams driven by (1) rainfall-runoff and ground-water, (2) rainfall-runoff and snowmelt, (3) snowmelt, (4) snowmelt, and (5) ground-water and snowmelt (fig. 27) clearly show changes in the timing of runoff, with runoff occurring earlier. Also consistent with the changes shown on figure 27 is the fact that all 29 climate divisions had significantly higher air temperatures during the POST period for the months of March and April (means for all but one division were significantly different at the 0.01 level); nine of the divisions (all mountainous) had mean March-April temperatures that were more than 3°F warmer than the BASE period means. The PRE/BASE ratios of the means for the winter season were also much smaller than the POST/BASE ratios. Of the 54 ratios that were less than 0.80, 39 only occurred during the PRE period, and 12 of these 39 sites had PRE or BASE ratios of less than 0.70.
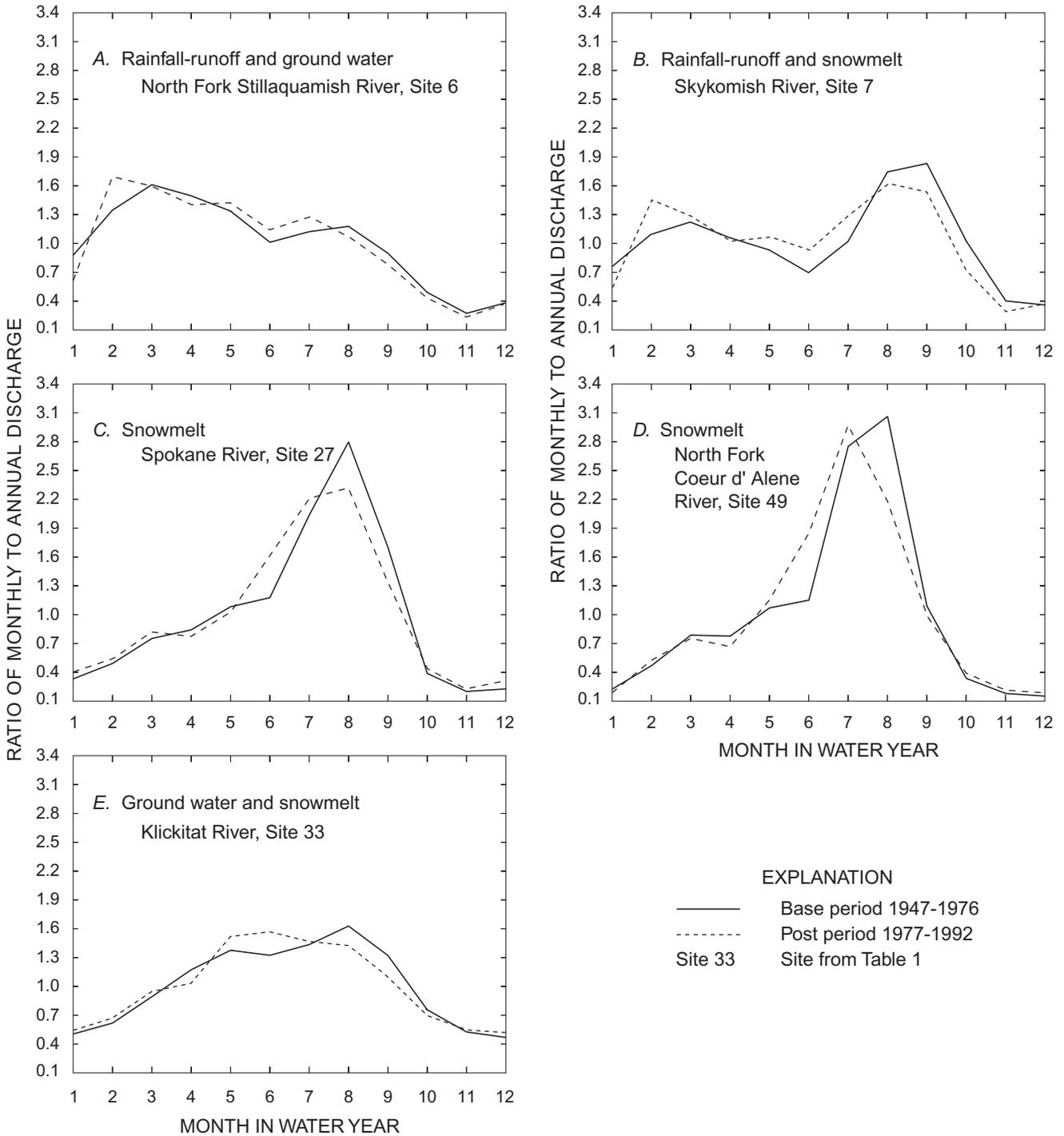
**Figure 27.** Hydrographs, for the BASE period and the POST period, of the ratio of mean monthly to mean annual streamflow of streams driven by rainfall-runoff and ground water, rainfall-runoff and snowmelt, snowmelt, and ground water and snowmelt.

There were also significant decreases in the mean runoff-season streamflow during the PRE and POST periods in comparison to the BASE period. Only 22 sites had larger mean streamflow, 16 of which lie in the Idaho-Oregon region, and 13 of these 16 had increases for only the POST period. The decreases in runoff-season streamflow in areas outside of the Idaho-Oregon region have large implications for water-supply management in the Pacific Northwest. In particular, hydropower and irrigation water use can be largely affected because the total outflow has been reduced by about 13 percent. Although this percentage does not apply to every stream, its order of magnitude indicates that, in total, it is equivalent to several large streams having no flow or many small streams having no flow. The consistency of results for the numerous streamflow series analyzed in this large area with its attendant

diversity in climatological and physiographic regimes indicates that the overall findings for the runoff season are reasonable.

Mean streamflow for the baseflow season at 40 sites was larger during the PRE and POST periods than during the BASE period; 31 of these larger means occurred only during the POST period, mainly in the Idaho-Oregon region and western Washington and Oregon. The increases in western Washington and Oregon are consistent with larger mean precipitation in coastal areas during this period. September streamflow for two streams with vastly different drainage-basin characteristics (fig. 28; sites 14 and 61, table 1) clearly shows increasing baseflow-streamflow, which accounted for a regime shift in 1967.
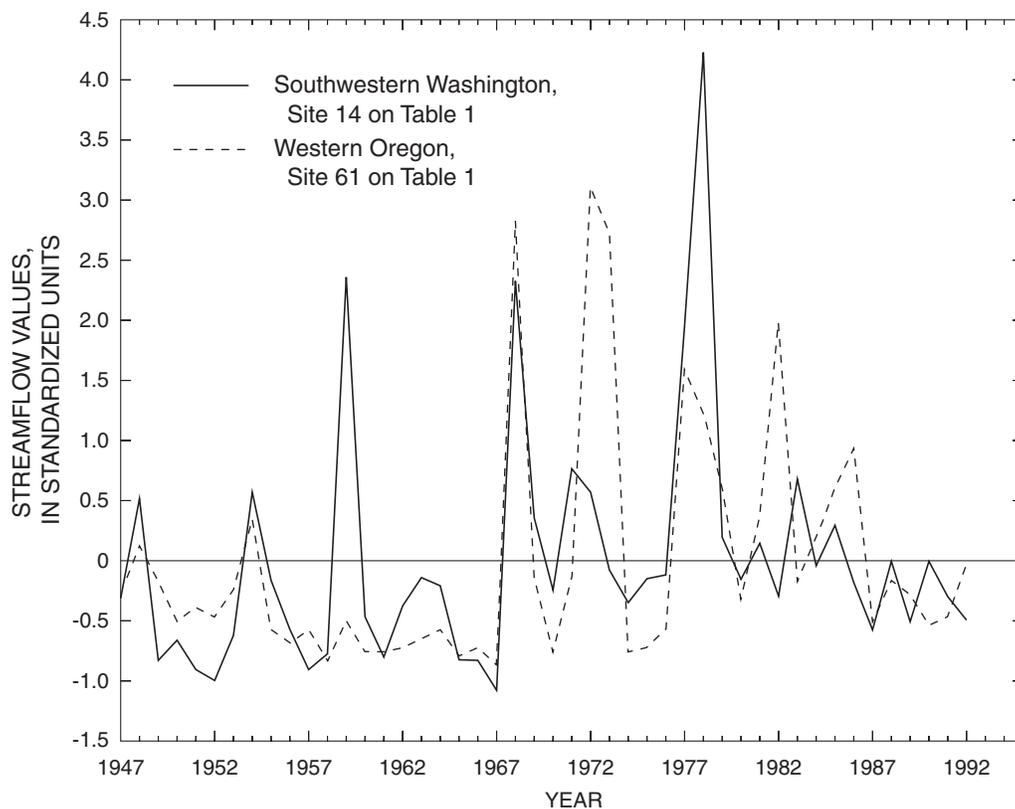
Figure 28. September streamflow for a site in southwestern Washington and a site in western Oregon. See table 1 for information on the streamflow sites.

Potential Linkages

The overall linkage of the HM regime in the Pacific Northwest to atmospheric circulation and to SSTs has been documented. For example, the linkages between atmospheric circulation and the HM regime have been described, both dynamically and statistically, by other investigators (as previously discussed). The relation between SSTs and the HM regime in this mid-latitude region, which has not received as much attention as the circulation-HM linkage, has also been described by previous work (for example, Torranin, 1972; Markham, 1979; Angell and Korshover, 1981; Christensen and Eilbert, 1985; Dettinger and others, 1993) and is further suggested by the information shown on figure 22. Although the SST relations may plausibly occur through the circulation linkage forcing, this aspect was not addressed in this study.

The overall climate linkage is perhaps best displayed in the similarities between the occurrences of the BASE-to-POST interdecadal regimes shifts in the HM data and the climatic data, and the PRE-to-BASE shifts in the HM data and the SOI. This section will thus first briefly present information, concentrating on the wet October-March period, related to this overall linkage between the shifts in the HM regime and the regional-to-hemispheric measures for the BASE-to-POST period and how these relations might translate to the PRE period. Regional and North Pacific measures for different periods will then be compared and their linkage to selected site-specific HM data will be analyzed. The remaining parts of this section will focus on the occurrence and linkage of other shifts that may be important for water resources in the Pacific Northwest. These other shifts were not directly analyzed because of the use of predefined interdecadal boundaries.

For several of the analyses, an index for the Subtropical Zonal pattern, a warm season east-west-banded pattern that indexes zonal-flow conditions between 25°-35°N, was calculated using the 700-mb data based on the centers for its July prototype (Barnston and Livezey, 1987). The Subtropical Zonal pattern is employed because on a monthly and 3-month basis it is the dominant North Pacific summer pattern (Barnston and Livezey, 1987). Also, this pattern should be generally consistent with the PNW (PNA) index because one of its July centers is essentially equivalent to the North Pacific oceanic center of the PNA in September. This consistency is probably related to the fact that the rotated principal components analysis used by Barnston and Livezey (1987) tends to spread, or partition, the variance over several modes, which would result in similar features being retained in the modes for coherent regions. Their rotated principal components analysis was explicitly chosen for this fact; that is, circulation modes are generally not spatially orthogonal. Thus, employing an index for this pattern allows for an analysis of the summer months and also captures the North Pacific fall transition in September reflected in the PNA pattern.

General Linkages

The overall linkage is strongly suggested by 9-year moving averages of October-March (1) for precipitation at Cedar Lake, the index for the Subtropical Zonal pattern, and the PNA index (fig. 29A) and (2) for precipitation at Cedar Lake, the SOI, and a SST at 40°N,170°W (fig. 29B). The 1977 climate shift is clearly defined in each data set (figs. 29A,B). Additionally, comparison of figure 29A with figure 29B indicates the coherency between the SST and the PNA and Subtropical Zonal index; especially note the 1947-57 period. The coherency to the Subtropical Zonal pattern suggests large-scale response because it is the only circulation pattern that extends longitudinally throughout much of the hemisphere.
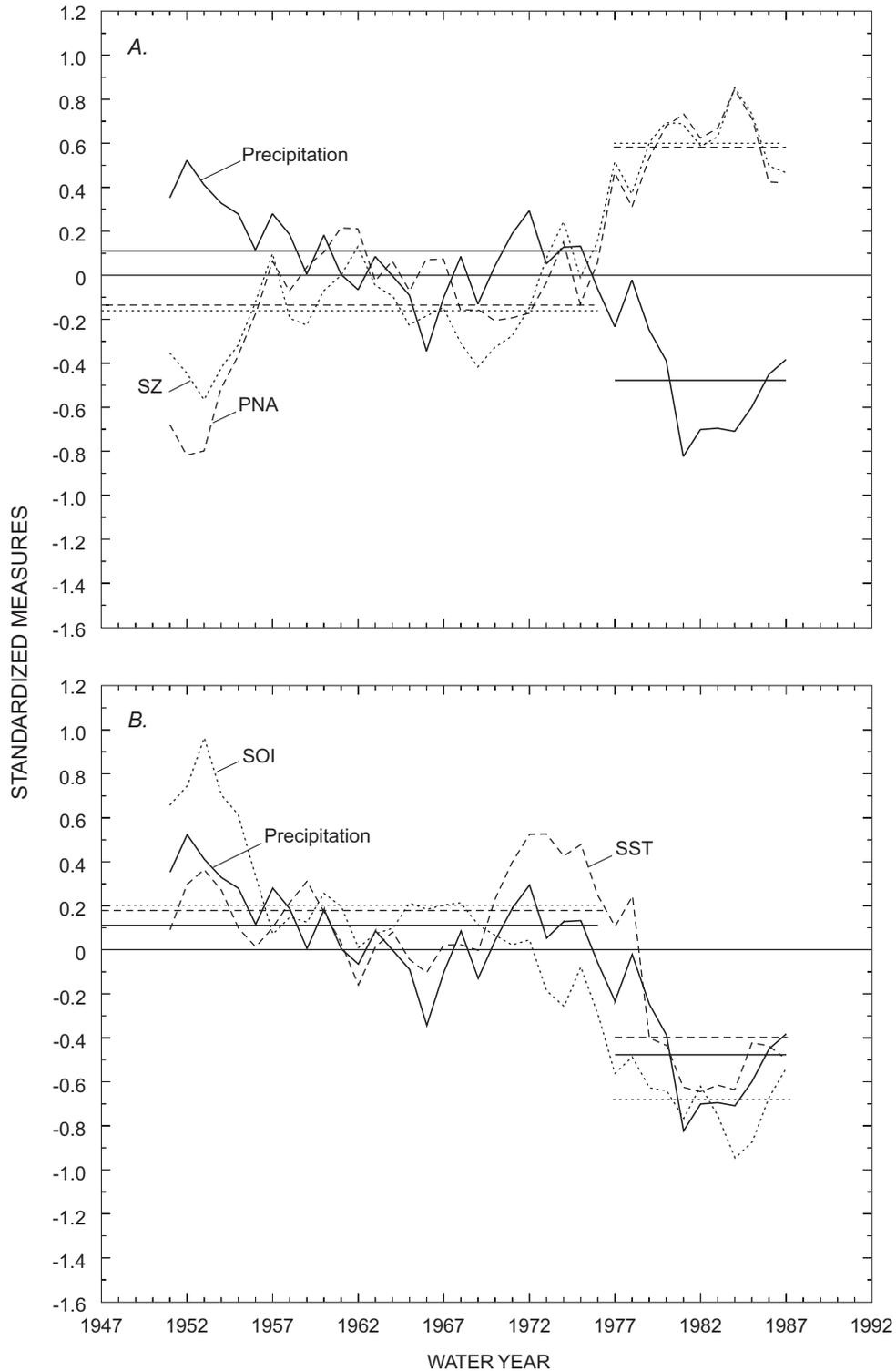
Figure 29. Comparison of the 9-year moving averages of the October-March values for precipitation at Cedar Lake, Washington, with those of the Pacific/North America (PNA) index and the Subtropical Zonal (SZ) index and with those of the Southern Oscillation Index (SOI) and the sea-surface temperature (SST) at 40°N,170°W.

Horizontal lines are, from left to right, means, calculated using the 9-year moving averages, for the BASE, and POST periods.

Considering the strong relation between precipitation at Cedar Lake and streamflow in eastern Washington for site 27, the Spokane River (see fig. 7B), it is plausible to estimate if the linkage identified on figures 29A,B exists for the PRE-to-BASE period shift by using the SOI as a PRE surrogate for the measures shown on figures 29A,B. Comparing 9-year moving averages of the water-year values of the Spokane River and the SOI (fig. 30) shows that the change in the mean at the 1946-47 and 1976-77 boundaries is prominently displayed, further suggesting that shifts in the North Pacific circulation patterns and SSTs were not only linked to the HM regime during the PRE period but were also linked to the interdecadal PRE-to-BASE period HM-regime shift.

Water-year values of (1) the westerly component—a regional measure, (2) a January-March season SST at 25°N,175°E—considered by the author to be a reference location of subtropical SSTs near the international dateline and thus a subtropical measure that is linked to the hemispheric SOI measure, and (3) the October-March PNA index—a hemispheric-to-North Pacific measure (fig. 31, a-anomalies and b-cumulative departures) suggest regional-to-hemispheric relations between the climatic measures, especially with respect to the coherency of periods with above-below average values and the 1977 shift. The seasons selected for each of the above measures were chosen to reflect their time of probable influence on the HM regime.
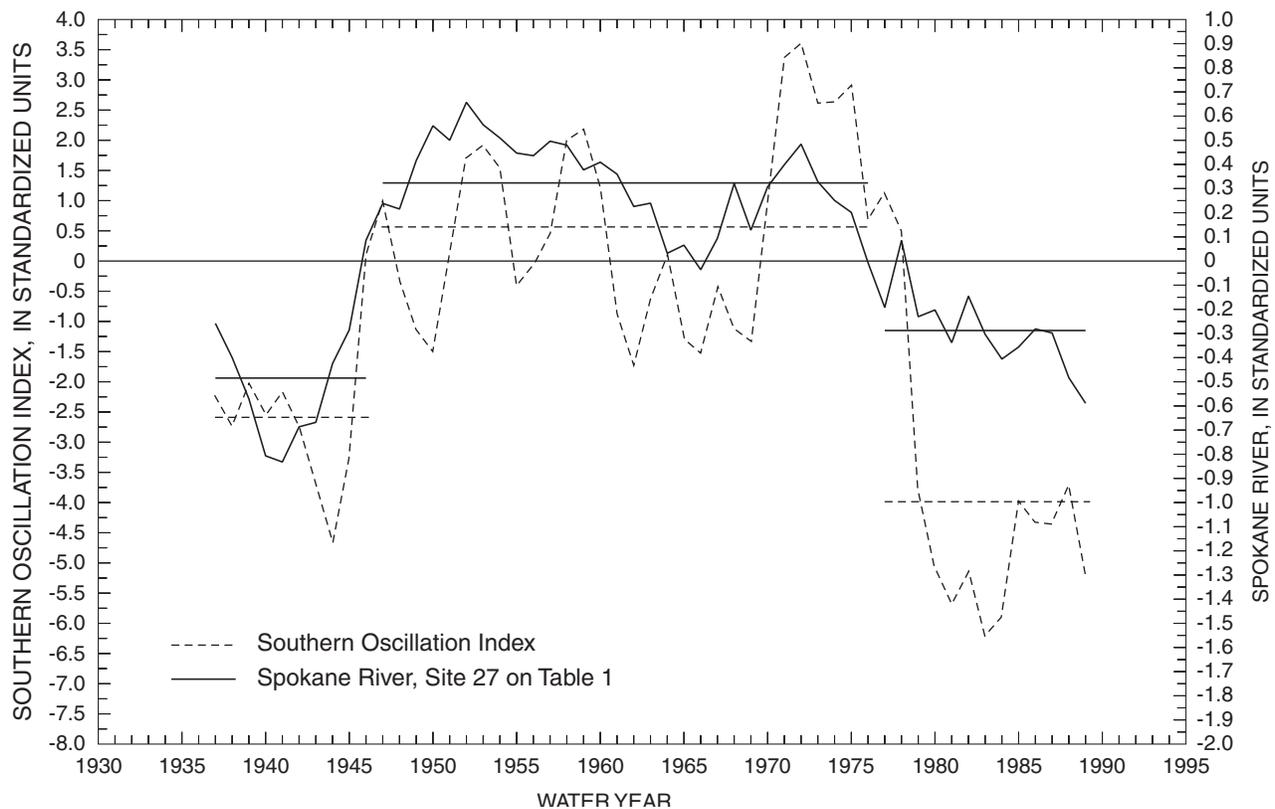
Figure 30. Nine-year moving averages of water-year values of the Spokane River and the Southern Oscillation Index (SOI).
Horizontal lines are, from left to right, means, calculated using the 9-year moving averages, for the PRE, BASE, and POST periods. See table 1 for information on the streamflow sites.
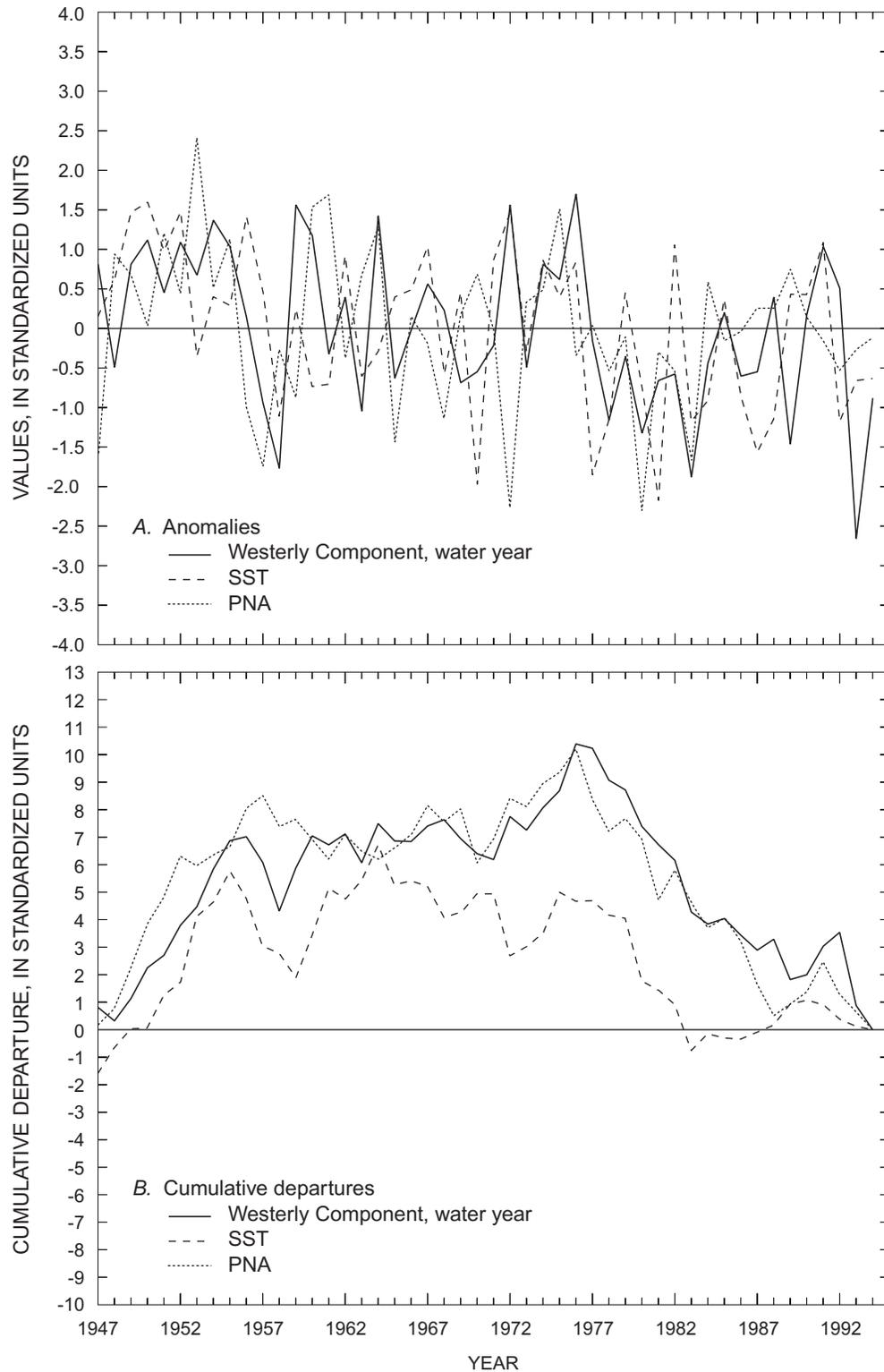
Figure 31. Anomalies and cumulative departures of water-year values of the westerly component, the January-March sea-surface temperature (SST) at 25°N,175°E, and the October-to-March Pacific/North America (PNA) index.

Values for the Pacific/North America index have been reversed in sign for comparison.

Water-year values of the westerly component, the October-March SOI, and October-March precipitation at Cedar Lake, Wash., (fig. 32) also indicate the regional-to-hemispheric relations and linkages to the HM regime. As would be expected, the regional correspondence between precipitation and the westerly component appears to be stronger than the correspondence of precipitation to SOI, although the 1977 shift is clearly displayed by each data set (fig. 32).

These potential linkages are also seen in October-March cumulative departures of the westerly component, a SST at 40°N,170°W, and precipitation at Palmer, Wash. (fig. 33). The Palmer site is located downslope from the Cedar Lake site and is not as influenced by orographic large-scale effects. The local variations in precipitation (and spatial variations in general) between Palmer and Cedar Lake appear to be influenced by atmospheric flow and SSTs, with the former influence being documented by Speers and Mass (1986).

Together, the information shown on figures 31, 32 and 33 indicates (1) a reasonably coherent response in the North Pacific region, (2) linkages of the measures of this response to the HM regime and its interdecadal shifts, and (3) the more direct link of regional and North Pacific data to the HM regime than hemispheric data, as measured by the SOI. To further address number 3 above, the results of Walsh and others (1982) are explored below.
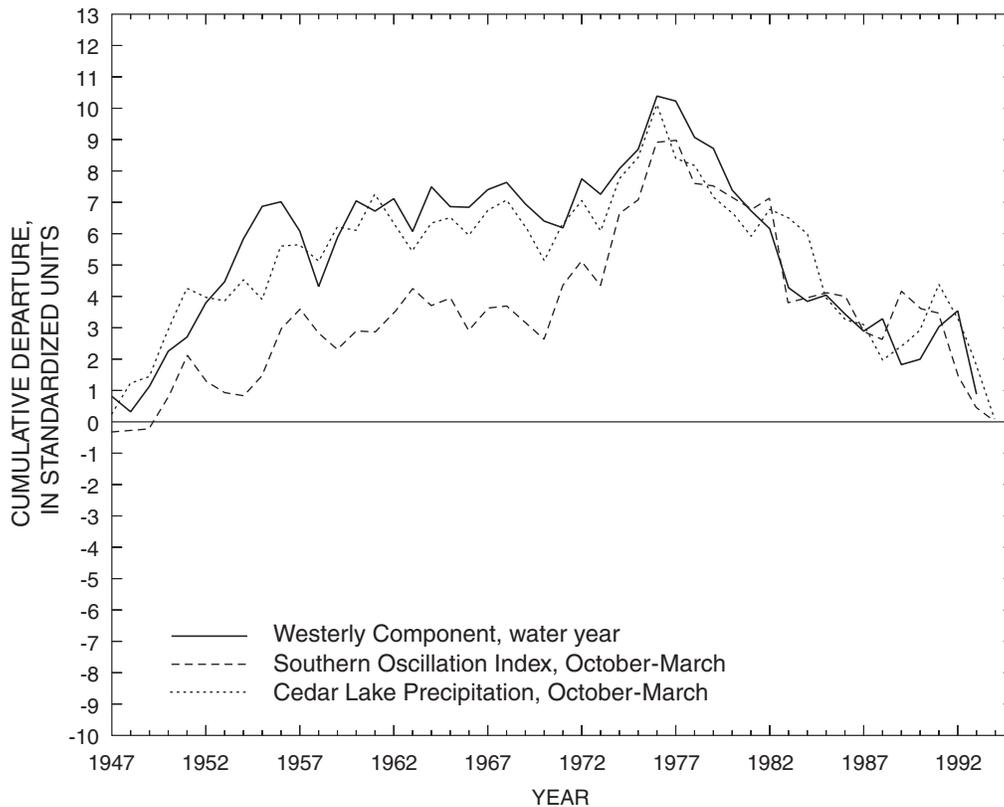
Figure 32. Cumulative departures of water-year values of the westerly component, October-March values of the Southern Oscillation Index (SOI), and October-March precipitation at Cedar Lake, Washington.
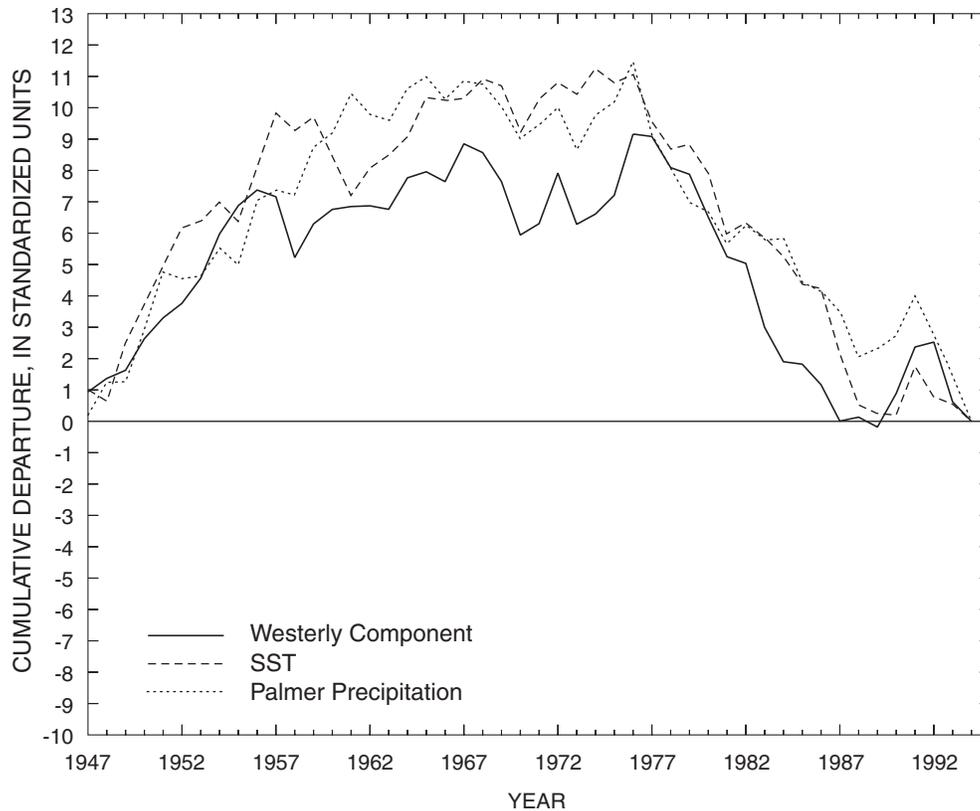
Figure 33. Cumulative departures of October-March values of the westerly component, the sea-surface temperature (SST) at 40°N,170°W, and the precipitation at Palmer, Washington.

This site, at 280 meters, is located "downslope" from the Cedar Lake precipitation site.

Walsh and others (1982) showed that winter precipitation in part of the Pacific Northwest correlated most with geopotential height (centered in their defined region) for the months of October-December, and with a northerly component of geostrophic flow for January-March. They also showed a strong relation between winter precipitation in the Pacific Northwest and the winter- and spring-season sea-level pressure centered at 50°N-125°W (located between the grid points used to calculate the measure for the average geopotential height field). Based on these results, total precipitation for the October-March period for a site near Spokane, Wash., which was used in the analysis of Walsh and others (1982), was correlated with the monthly 700-mb data subset, starting at January of the previous water year and extending to the end of the current water year; the precipitation and 700-mb data sets were for 1947-

88. These 21 spatial correlation fields showed that the largest correlations to the October-March precipitation totals were to the 700-mb data for November and the largest values were located at the center 50°N-125°W of the four grid points used to calculate the average geopotential height field of this study. Precipitation totals for each month of November through February (the months with the most precipitation) were then correlated in the same lagged manner to the measure of the average geopotential height field and to the geopotential height of the PNW index high-pressure center. The largest correlation coefficients (-0.56 and -0.55, respectively) for each month of precipitation were for the measures in November, further indicating the influence of the height field (a regional measure), especially in November, on the subsequent response of the HM regime.

The 1967 Baseflow-Season Shift

The POST-period increase in mean streamflow for the baseflow season along the coast (see fig. 28) is of interest because (1) linkages during this season have not received as much attention as those of the water year and runoff season, (2) the apparent shift at about 1967 was not explicitly analyzed in this study and is not clearly defined in the "wetter" seasons, and (3) it is a local phenomenon—most other regions in the Pacific Northwest experienced large decreases in the mean compared to the BASE period. The linkages may not be represented in the large-scale data analyzed in this study because of the generally decreased variability and strength of circulation during this season in comparison to the other seasons. For the following analysis, regional atmospheric measures (standardized values of westerly component, northerly component, and the average height field) are employed first, and then a coastal SST, the PNW index, and the index for the Subtropical Zonal pattern are analyzed.

For August, the mean value of the standardized westerly component changed from easterly flow (1947-67) to westerly flow (1968-91), with a concurrent reduction in its standard deviation of 0.4 standard unit. The mean for the northerly component also changed, from northerly (associated with decreased precipitation) to southerly (associated with increased precipitation). Concurrently, the mean of height field changed from a negative to a positive, with a reduction in its standard deviation, and it had an increasing trend for both periods. The height field was correlated to northerly component for the pre-1968 period and to the westerly component for the post-1967 period. For September, the only major change in the measure was for an increasing trend in the height field. However, averaging the three measures for August and September and comparing differences between the two periods showed that the averages retain the characteristics of August. Together, these suggest a changing geopotential height field centered at 50°N-125°W for the baseflow season, which was related to more northerly flows prior to 1968 and to increasingly westerly flows after 1967. The observed spatial variations of increases and decreases in the mean precipitation and streamflow for the POST period in comparison to the BASE period also suggest a possible translation of the location of the high-pressure center (this cannot be verified at the scale of the gridded data used in this analysis). The changes in the measures

correspond to the difference in composite heights of the 700-mb subset for the baseflow season for post-1968 and pre-1967. The difference field shows that all areas (except the continental United States below about 48°N) had increasing heights with two centers—one over the Bering Sea and the other at 25°N,130°W (refer to previous discussion of difference in composites for August based on the 1976-77 BASE-POST boundary on page 68). Although the differences in heights are not large, this pattern is still consistent with a strengthening of the mean westerlies that intersect the coast in southern Washington.

For the August-September baseflow season, the coastal SST (45°N,125°W; located near the center of the height-field measure) had a change in mean (standardized values) from 0.52 to -0.46 from pre-to-post-1967. The cooler offshore temperatures and the increased westerly flow should be linked to the increased baseflow-season streamflow in the coastal areas, probably because of increased precipitation. Indeed, analysis of the divisional precipitation data for the 29 divisions shows that all 29 divisions had larger means during August-September for the 1967-94 period in comparison to the 1947-66 period means, with significant increases in the Oregon coastal and Willamette Lowland divisions. The PNW index had only a small change in mean but a significant trend; the trend and mean value are consistent with the composite-difference field described above. The Subtropical Zonal index for this season had a change in mean of 0.22 standardized unit, with a concurrent decrease in its standard deviation of 0.41, and it displayed a significant increasing trend for the pre-1968 period. Two-year moving averages of these three measures for the baseflow season (fig. 34) suggest a rather distinct change after 1967, which is consistent with increasing coastal streamflow. The consistency between the Subtropical Zonal index and the PNW described previously is well represented (fig. 34) and further suggests that the interdecadal shift in 1967 would also likely be reflected in September atmospheric-circulation data.

The baseflow-season analysis highlights two points. The first is, although the regional and North Pacific/hemispheric climatic measures are well related, there are distinct differences. In addition, limited exploratory analysis indicates that none of the other atmospheric measures or SSTs analyzed display a prominent baseflow-season shift at about 1967.
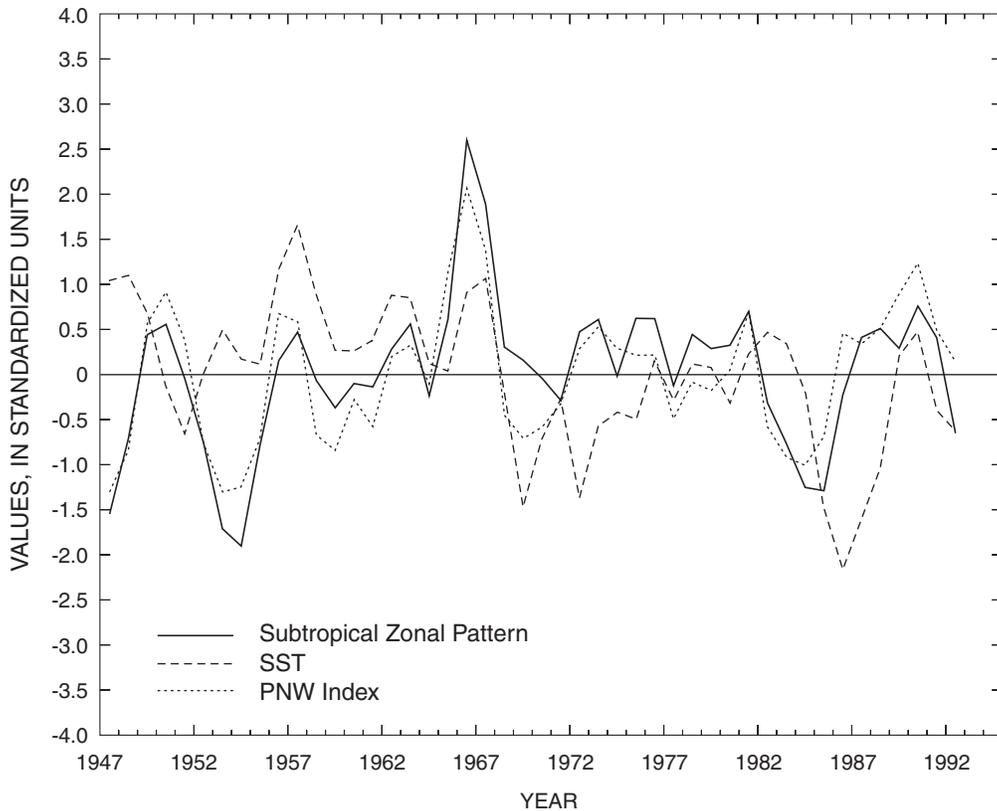
Figure 34. Two-year moving averages of the August-September values for an index representing the July prototype of the Subtropical Zonal pattern, the sea-surface temperature (SST) at 45°N,125°W, and the Pacific Northwest center of the Pacific/North America index.

The two centers form the PNW index. The atmospheric indices are calculated using 700-millibar data.

The second relates to the more complex relations displayed by the data which are not captured using the pre-defined interdecadal PRE-BASE-POST periods. This complexity was also demonstrated in the previous discussion of the differences in composites for August using 1967 and 1976 as the POST boundary, with the former reflecting a type of Subtropical Zonal pattern and the latter a PNA pattern.

The April-June Summer-Transition Season

The potential linkages of atmospheric circulation to HM changes in the April-June summer-transition season may be reflected in the hemispheric North Pacific pattern because during this season it is the dominant North Pacific circulation pattern (Barnston and Livezey, 1987). An index for the North Pacific pattern was calculated using the 700-mb data based on the centers for April when it is the first mode of hemispheric interannual variability (Barnston and Livezey, 1987). Two-year moving averages of the anomalies for the North Pacific pattern index, the North Pacific low-pressure center of the PNA index, and precipitation at Coupeville, Wash., for this period are shown on figure 35; coastal-inland sites with large, significant Kendall's tau for increasing precipitation during April and May for the 1931-88 period are clustered near Coupeville. The information shown on figure 35 suggests some coherency between the three data series with decreasing similarities after 1976 (although all three series have a larger POST mean than the BASE-period mean). However, values for the North Pacific pattern index and the low-pressure center are correlated, whereas neither is significantly correlated to precipitation.
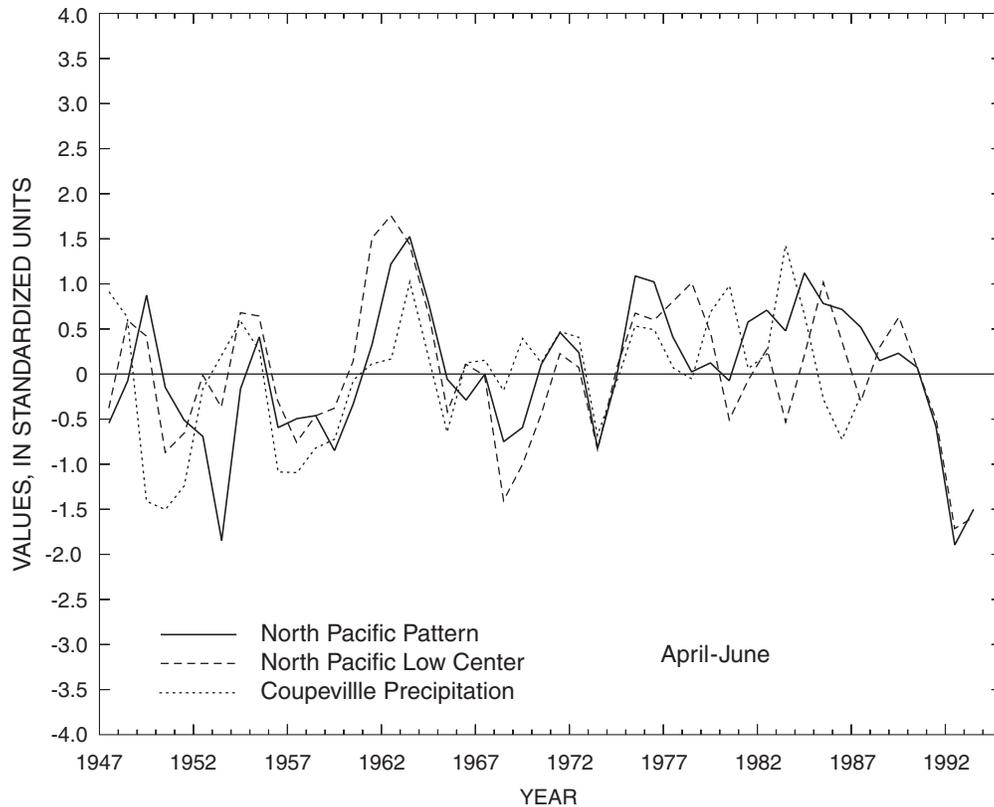
Figure 35. Two-year moving averages for April-June values of an index for the North Pacific pattern, the North Pacific low-pressure center of the Pacific/North America index, and the precipitation at Coupeville, Washington.

The North Pacific pattern is the dominant North Pacific circulation pattern for April-to-June, and the index was created using the first-mode pattern of Barnston and Livezey (1987). Precipitation at Coupeville is representative of coastal-inland areas in the north-central part of western Washington, which displayed some of the largest significant positive values of Kendall's tau for April and May.

These two measures are also not correlated to the other regional measures, such as the westerly component, which do not contain significant periods of above-below average values during this season. Additionally, the SST at 40°N,170°W is not correlated to either the North Pacific pattern index or the low-pressure values. The location of the SST grid point is just southwest of the grid location for the low-pressure values and is the same location for grid point used to calculate the North Pacific pattern index.

Thus for the summer-transition season, the North Pacific appears to be responding somewhat coherently with respect to atmospheric flow (at least until about 1977), but it is unknown how this coherency is linked to both the persistent periods of below-above average precipitation and to the trend for increasing precipitation during this summer-transition season. There also appears to be a summer-transition season "decoupling" between SSTs (35-45°N,160-170°W) and the analyzed atmospheric-flow measures. This decoupling may simply be related to a lag effect because the summer SSTs in the above area are highly related to fall circulation patterns in the North Pacific (Namias, 1976b). However, Barnett and Preisendorfer (1978) show that, for the Northern Hemisphere, contemporaneous relations (individual patterns of climate variability that occur at the same time) for SSTs and 700-mb heights and thickness for winter are different from those for summer; especially notable is the lack of contemporaneous relations for SSTs in the summer pattern of climate variability.

The SSTs over the central North Pacific display a significant downward trend during this season over the complete period of record, principally because of a shift in 1967 and secondarily to one in 1957. The timing of the SST shift was not seen in the SST data for most of the other seasons analyzed (for example, winter season), and it thus suggests that the baseflow-season change in streamflow described above is linked back to circulation changes during this season. In addition, the simulated January-March snowpack at Cedar Lake displays a strong shift in 1957, and the air temperatures for the western Cascade climate division indicate shifts in 1957 and 1967 during this season. As described previously, April and May were the only 2 months when the SST grid points with lower mean temperatures during the POST period included water that was colder than the grid points with higher mean temperatures. The difference in composite heights for April-May (fig. 36) (the months when Kendall's tau for the precipitation data for the 1931-88 period for all sites in western Washington was positive and when all climatic divisions had larger mean precipitation and higher air temperatures for the POST period) retain some of the features of the difference in composites for May, contain features of several circulation patterns, and are consistent with more vigorous flow into the region. This simple analysis suggests an evolving atmospheric-circulation/SST regime in the North Pacific during this season.

Variations During 1980 through 1985

Some temporal and spatial variations were not explicitly addressed by using the pre-defined interdecadal regimes that made up the successive periods of record for analysis. Although some temporal variations, such as the baseflow-season shift in 1967 and the shift in the southeastern center of the PNA index in 1957 (see fig. 23), have been described, additional variations related to a continually evolving climatic regime have not been discussed. The principal components analysis showed that for the POST period the first mode of both the unrotated and the rotated series for water-year values does not contain such a pronounced change in mean as did many of the individual streamflow series.
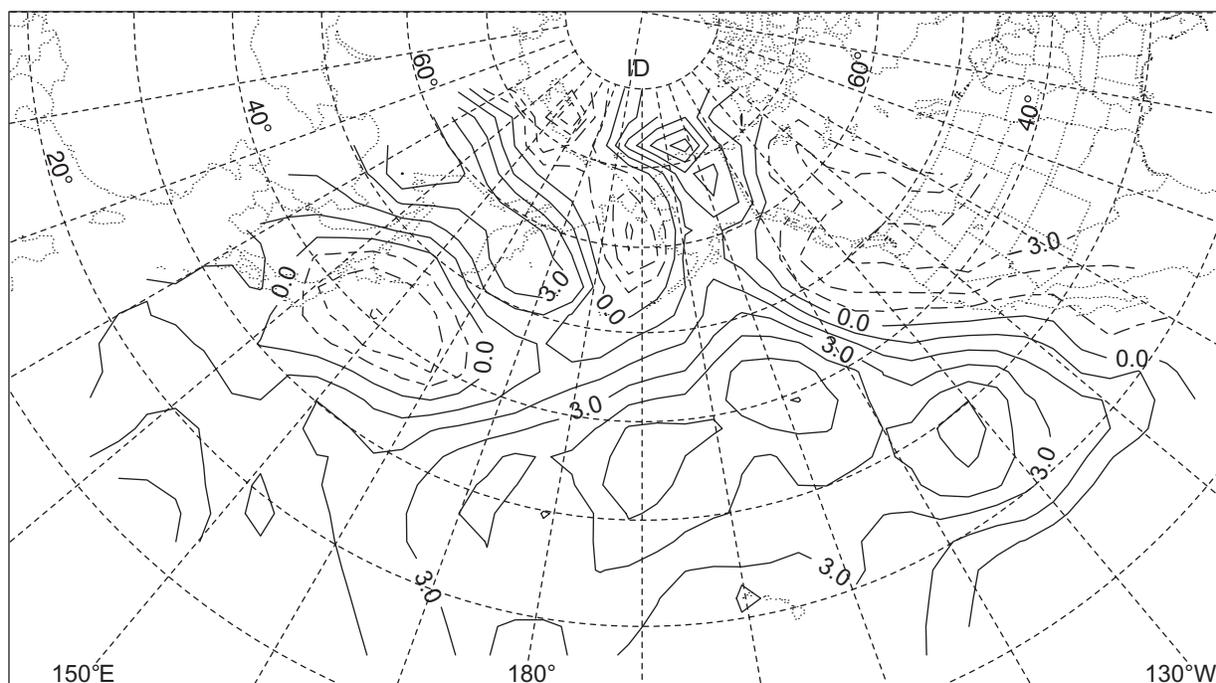

Figure 36. Difference in composite heights (POST minus BASE) for the April-May summer transition season.

The smaller change in the mean of the principal components series for all streamflow sites is due to the fact that many streams in southern Idaho and eastern Oregon had a period of above-average streamflow during water years 1980-85; the Salmon River (site 52, table 1) is representative of these streams.

Two-year moving averages and cumulative departures for water-year values of the Salmon River, the average geopotential height field, and the resultant of the westerly- and northerly-flow components (total geostrophic flow) (fig. 37) identify the difference between the 1977 shift (represented in the resultant) and a later change displayed by some of the streamflow data and the principal components time series. The temporal complexity in even these two regional atmospheric measures is highlighted by the differences between the height field and the resultant component—the four values used to calculate height field are also used to calculate the resultant. The phase locking between the streamflow and height field after 1977 shows that the height field is a dominant factor in the linkage of circulation to the HM regime in the southeastern part of the Pacific Northwest and to other HM data, as described previously. On a water-year basis, the height field is the only atmospheric-circulation measure analyzed in this study with a POST-period peak during water year 1982. However, note that the 1982 peak also was contained in the April 1 swc series and the October-March averaged precipitation series (see fig. 25), and the average of the standardized precipitation series for the 29 climate divisions showed above-average precipitation from about 1979 to 1985, with a peak in 1982. The evolving prominence of the height field tends to support the hypothesis of a continually evolving atmospheric circulation and SST regime.

Related Information

Several aspects of this study indicated the need to analyze additional information. First, except for the SOI, none of the atmospheric or SST information analyzed in this study was from the PRE period. Thus, it is of interest to determine if other, longer historical data series of relevant information contain the identified interdecadal shifts, especially the 1946-47 shift, which was not strongly displayed by the SOI. Next, although the interdecadal boundaries used in the study were defined using the HM data and previously published information, it is important to document that these boundaries not only are reasonable but also are contained in different, long-term, and influential (with respect to large-scale climatology) data. Last, given the regional-to-North Pacific extent of the HM, atmospheric, and SST regime changes, it is of practical importance to determine if these changes were hemispheric in nature. Thus, three additional geophysical data sets are examined; these data sets were selected to include important components of the ocean-atmosphere system in the Northern Hemisphere—the North Pacific, the North Atlantic, and the Arctic.

Data Sets and Background

The three data sets are (1) a sea-level pressure index, the Central North Pacific (CNP) index (Cayan and Peterson, 1989), provided by Cayan (U.S. Geological Survey, written commun., 1995), which is representative of a broad area of the North Pacific (35-55°N,150°W-170°E); (2) a sea-level pressure index based on the large-scale features of the July-August North Atlantic Oscillation (NAO) pattern (a large-scale north-south dipole) of Barnston and Livezey (1987)—calculated for each month as the difference between the standardized anomalies at 45°N,85°-105°W and 70-75°N,60°-70°W; and (3) Arctic ice concentrations (National Snow and Ice Data Center, written commun., 1995; provided to NSIDC by J. Walsh, University of Illinois; see Walsh and Johnson, 1979). For this analysis, ice-concentration values are presented for the water year (average of 12 months), April, and May periods. The water-year periods of record for the CNP index, NAO index, and ice-concentration data analyzed are 1900-94, 1900-93, and 1902-90, respectively. Selected aspects of these data sets are described below.

The CNP index has been shown to be related to the HM regime and to be representative of the PNA index (Cayan and Peterson, 1989)—probably related to the fact that much of the atmospheric flow near the Pacific Northwest coastline approximates both geostrophic and generally barotropic flow. However, because the sea-level pressure CNP index reflects a large area of only the North Pacific, it should not only be more directly linked to SSTs but also be representative of large-scale circulation features throughout the year and not just during the winter months.
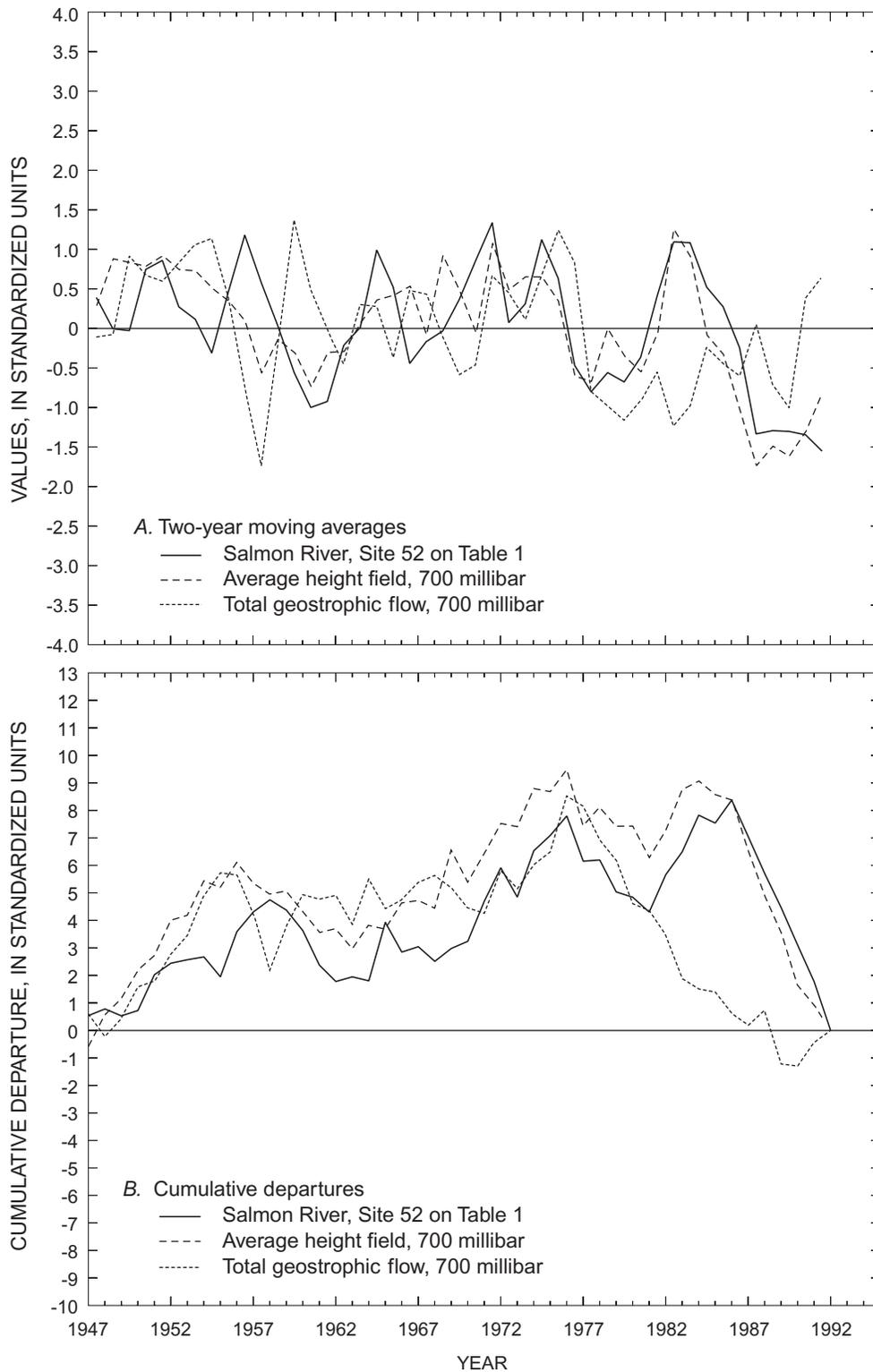
Figure 37. Two-year moving averages and cumulative departures for water-year values of the Salmon River, the average geopotential height field centered near the northern Washington coastline, and the resultant or total geostrophic-flow component.

The average height field has been reversed in sign for comparison.

In contrast to the CNP-PNA indices, there are differences between the NAO index and the same index calculated using the 700-mb data—probably related to more complex dynamics. For example, instead of upper-level pressures, Hurrell (1995) used sea-level pressures at two locations (Portugal and Iceland) to construct a NAO index because the upper-level data are not as related to the near-surface climatology as are the sea-level data. Hurrell's index was based on anomalies for the December-March winter season when the NAO is a dominant mode of interannual variability for both the North Atlantic and the Northern Hemisphere (Barnston and Livezey, 1987). An index based on the centers during the summer was chosen for this study not only because the NAO is the dominant mode during summer but also to isolate the potential effects of the PNA pattern, which is an important winter mode of circulation in the North Pacific. However, for the 1900-92 period, Hurrell's index is significantly correlated at the 0.01 level to the NAO index of this study for each month from December through March and to the index averaged over these months. At the decadal scale, 9-year moving averages of the December-March average index and Hurrell's index are also significantly correlated, with a correlation coefficient of 0.72. The reason the two different indices are related in the winter and not in the summer is that the winter pressures at the northern center (sometimes called the Icelandic Low) are correlated, although not as strongly, to an additional center, a continental-pressure center located near the southern center of NAO index employed in this study.

The Arctic data set consists of gridded data (1° latitude) of the end-of-month ice extent (as concentration; for example, 0/10 to 10/10) for the water-covered areas. The ice-concentration data are presented for the marginal ice zone for regions in the North Atlantic (East Greenland Shelf and Fram Strait) and the Bering Sea. Previous studies have shown the influence of atmospheric circulation on ice cover in the Bering Sea and other Arctic areas (Walsh and Johnson, 1979; Johnson, 1980; Niebauer, 1980; Rogers, 1981; Walsh and Sater, 1981; Kelly and others, 1987; Ikeda and others, 1988; Chapman and Walsh, 1991). In addition, annual ice-drift patterns are generally consistent with annual sea-level pressure patterns, and differences in drift patterns are consistent with interannual variations in sea-level pressure (Chapman and Walsh, 1991). Thus, ice cover and ice drift, which

affect SSTs, both should reflect interdecadal regime shifts in atmospheric-circulation patterns, especially the 1946-47 and 1976-77 shifts. In particular, ice cover in the Bering Sea region should reflect shifts in the CNP and PNA indices because of the proximity of the center of anomalously low (high) pressures associated with the PNA (reverse-PNA) pattern near the Bering Sea. Note that low pressures are generally associated with higher temperatures and less precipitation in the Pacific Northwest and that this hydroclimatology is generally reversed for anomalously high pressures (reverse-PNA pattern) in the Bering Sea region. Last, because the ice-cover extent in the Bering Sea is generally out of phase with the ice-cover extent in the North Atlantic region (Walsh and Johnson, 1979) for which the data are analyzed, there should be some coherency in interdecadal regime shifts in the ice-cover extent for these two areas.

The NAO index and the North Atlantic ice-concentration data are also analyzed because of the previous work in identifying changes in climate regimes for the North Atlantic region, in particular, with respect to temperature, precipitation, and oceanic parameters. These changes should be represented in the NAO index because of the dominance of this pattern: it is the only atmospheric-circulation pattern that is '"found unambiguously in all 12 months" (Barnston and Livezey, 1987) and is also seen in both the winter and the summer patterns of hemispheric climate variability of Barnett and Preisendorfer (1978). Hurrell (1995) shows that during years of small or negative values of the NAO index, winters in the European region are generally colder, and when values of the NAO index are positive and large, winters generally are warmer than normal. These results are consistent with those of Van Loon and Rogers (1978). For precipitation, European sites south of about 50°N are significantly negatively correlated to the NAO index, and northern sites are significantly positively correlated (Hurrell, 1995). In addition, because the northern center of the NAO pattern dipole is located at about 70°N near Greenland, the North Atlantic ice-concentration data analyzed in this study should closely follow variations in the NAO index, and because the southern center of the NAO index used in this study is near the southeastern center of the PNA index, there should be some relation between the NAO and PNA indices.

Hurrell (1995) also describes three broad interdecadal periods for the North Atlantic region—from the turn of the century to about 1930, from the early 1940's to the early 1970's, and from about 1980 to the end of the record, during which time the NAO index had the largest positive values. Levitus (1989a) summarizes much of the previous work on the temporal variability of oceanic measures as part of a series of papers on interpentadal changes in the North Atlantic circulation regime (Levitus, 1989a,1989b, 1989c, 1990). These papers concentrate on differences between 1970-74 and 1955-59, periods of large differences in many oceanic measures. Additionally, between 40°-60°N, a large decrease in salinity (the Great Salinity Anomaly) was observed during the period 1967-72 (Dickson and others, 1975; Dickson and others, 1988). Levitus (1989a) also identifies the 1977 boundary as a period of change in some oceanic measures such as selected water masses. For the early

period of record, Rogers (1985) discusses significant atmospheric circulation changes that occurred in the early 1920's for the North Atlantic, and the NAO index of Hurrell (1995) shows the initiation of about a 20-year downward trend at about this time. Thus, years of regime changes may be reflected in years indicated in the North Atlantic analyses—early 1920's, 1930, early 1940's, late 1950's (1957), 1967, 1972, and late 1970's, which are consistent with some of the years of change already identified in this study.

Central North Pacific Index

The CNP index for January contains both the 1946-47 and 1976-77 shifts (fig. 38), and values also indicate several other boundaries that define episodes of trends or shifts. There are some distinct differences between the CNP and the PNA indices, but the times of the major regime changes are consistent with those of the Pacific Northwest.
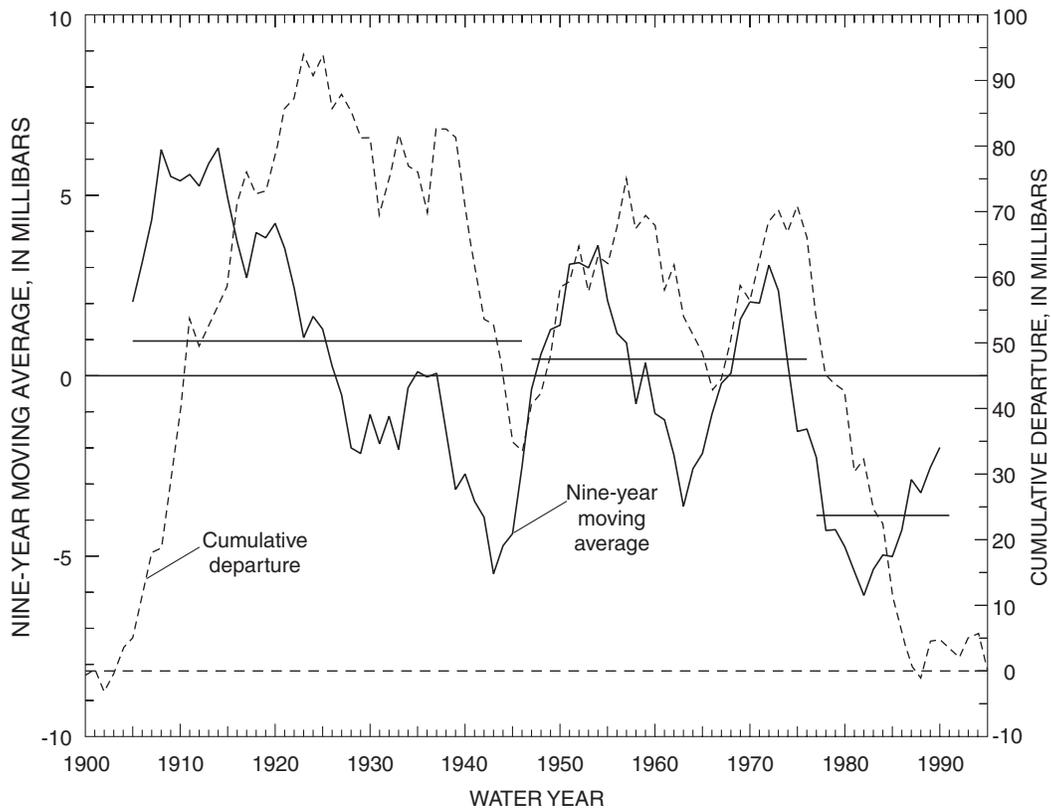

Figure 38. Nine-year moving averages and cumulative departures for the Central North Pacific (CNP) index for January. Horizontal lines, from left to right, are means, calculated using the 9-year moving averages, for the PRE, BASE, and POST periods.

The CNP index is calculated from sea-level pressures.

Thus, although site-specific variations in the HM data would not be fully captured by the CNP index because it represents a broad area of the North Pacific and its attendant circulation regime, it should be linked to regionalized HM data and those site-specific data that reflect regionalized interannual variations. The cumulative departures for the CNP index for January and the April 1 swc (also shown previously on figure 25) for the period BASE-POST period (fig. 39*A*) indicate this North Pacific-Pacific Northwest linkage.

For the Pacific Northwest, the most significant changes in the divisional temperature data were increasing temperatures during the POST period for the months of March-April, especially for the western slope of the Cascade Range and northeastern Washington divisions. Nine-year moving averages of the average values for the March-April temperature for the western Cascade division, January-March CNP index, and March-April CNP index (fig. 39*B*, air temperatures have been reversed in sign for comparison) indicate the linkage described above. However, distinct variations are also seen, both with respect to the decoupling of winter and spring transition circulation patterns and decoupling of temperatures and circulation patterns. This decoupling may be related to the apparent decoupling of circulation patterns and SSTs in the spring transition period. There are large differences between the presented data from about the turn of the century to about 1915, with a transition to a strong linkage and coherency from about 1920 to 1947. Thereafter, the decoupling of the circulation patterns occurs, with the spring transition air temperatures continuing to be strongly linked to winter circulation patterns until about the mid-1950's. For the remaining period of record, temperature is weakly linked to the winter CNP pattern from about 1960 to about 1973 and becomes more strongly related over the next 10 years. From about 1983, the three series are poorly related.

Nine-year moving averages of water-year values for the temperatures of the western Cascade division in Washington, the precipitation of the coastal Oregon division, and the CNP index (fig. 39*C*) also indicate linkages and shifts. An initial decoupling in the 1920's is seen, with a transition to out-of-phase relation between precipitation and temperature starting in about 1935. This out-of-phase relation is strongly established in 1947, ends about 1977, and restarts about 1983. Correspondingly, there are large changes in the phase relations between the North Pacific circulation patterns and divisional precipitation and temperature data. The lack of a relation between the CNP index and the HM data from about 1967 to 1977 further suggests that the previously described changes at 1967 reflect some type of a large-scale change in the circulation regime, with its attendant climate forcing. Also note the lack of a relation to the HM data during the 1900-20 period, a period when the precipitation and temperature were in phase. For this early period, decadal variations in the monthly means of the daily maximum and minimum temperature at Olga 2SE, Washington (site listed in table 3) are distinctly out of phase, and from about 1920 on slowly evolve to being phase locked starting in the mid-1930's. Correspondingly, the CNP index becomes phase locked with the maximum temperatures in the early 1920's and the minimum temperatures in the mid-1930's. This hydroclimatological coupling then follows the same pattern as that of the winter and spring transition CNP index described above. Obviously, there have been large shifts in the North Pacific climate regime that have been translated to the HM regime with the major interdecadal boundaries being clearly defined. However, both the linkages and the circulation regime are quite complex, as indicated by the information shown on figures 39*B, C*.
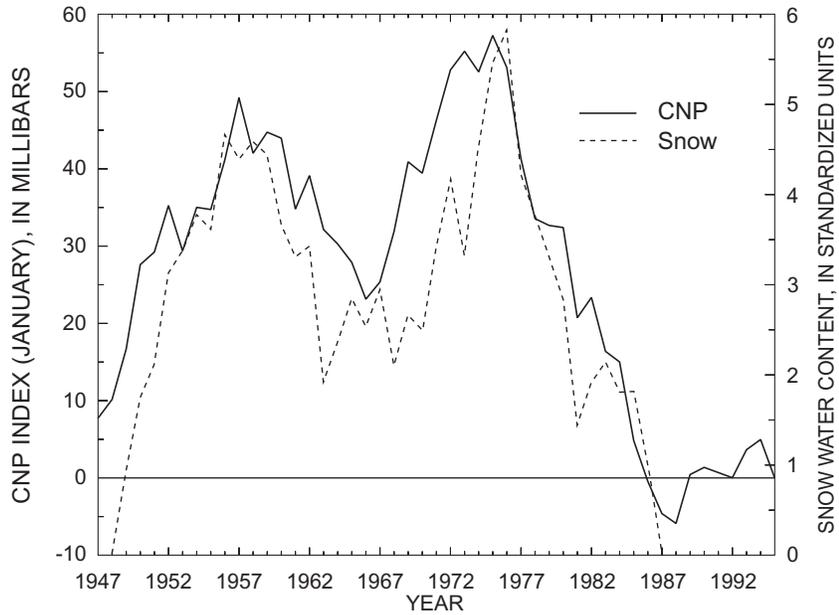
A. Cumulative departures for the Central North Pacific (CNP) for January and the April 1 snow-water content for 69 sites in the Pacific Northwest. The CNP index values are calculated on the basis of water years 1947-95, and the snow-water content values are based on water years 1948-87.
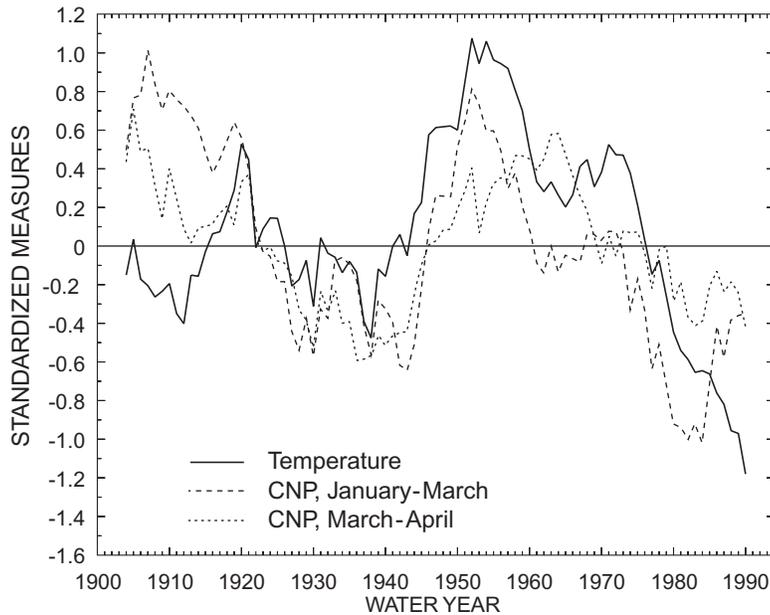
B. Nine-year moving averages of the average March-April temperature for the western Cascade Range climate division, the January-March CNP index, and the March-April CNP index. Air temperature has been reversed in sign for comparison.

Figure 39. Cumulative departures and 9-year moving averages that demonstrate the linkage between the North Pacific Ocean and the hydrometeorological regime in the Pacific Northwest.
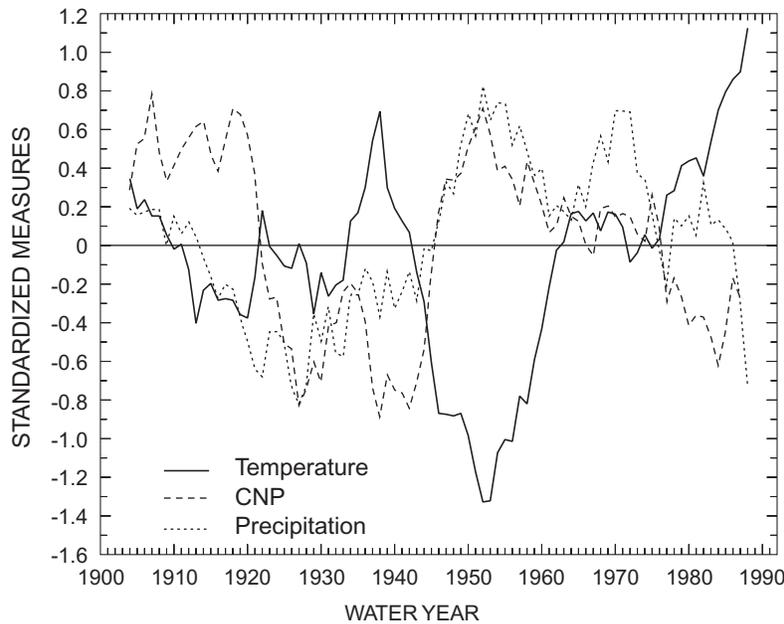
C. Nine-year moving averages of the water-year values for air temperature for the western Cascade Range climate division, precipitation for the coastal Oregon climate division, and the CNP index.

Figure 39. *—Continued.*

North Atlantic Oscillation Index

The water-year values for the NAO index had one major shift within the 94-year period of record near the 1946-47 boundary (fig. 40), and there was no shift in the first 35 years of record. The shift is represented by a significant downward trend and a change in mean. The fall and winter NAO-index values had a maximum annual departure in 1935, with a shift to persistent below-average values at about 1942 that ended about 1977. Although the downward trend started in the late 1930's, values were above average and did not significantly affect the mean. Of importance is the fact that, on an annual basis, the North Atlantic circulation regime displays the 1946-47 shift, but not a strong shift in 1977.

Although there was no clearly defined shift in 1957, a significant increasing trend "started" in 1957 (but with still consistently below long-term average values), "ending" a strong 10-year downward trend. The overall reversal of declining values in 1957 corresponds to the 1957 water-year shift in values for the southeastern center of the PNA index (see fig. 23).

Dunn (1957) describes major changes in hemispheric circulation patterns occurring in December of 1957 that would be consistent with the changes displayed by the NAO index for 1957, and a shift in 1957 boundary also is clearly defined in winter temperature for three sites in the eastern United States separated by thousands of kilometers (Dickson and Namias, 1976). However, most of the trend from 1957-93 is accounted for by a large change in winter-season values from 1972-73 that probably reflects the end of the salinity anomaly and the initiation of a strong upward trend in the winter NAO index of Hurrell (1995). Thus, with respect to persistent periods of below- or above-average values, the NAO index displays one major shift, with the annual values indicating several boundaries that represent large excursions from past values (fig. 40). Thus, the mid-1940's shift appears to have been hemispheric with respect to atmospheric-circulation features, whereas the 1977 shift, although likely hemispheric in nature, is mainly displayed in the North Pacific and Pacific Northwest information.
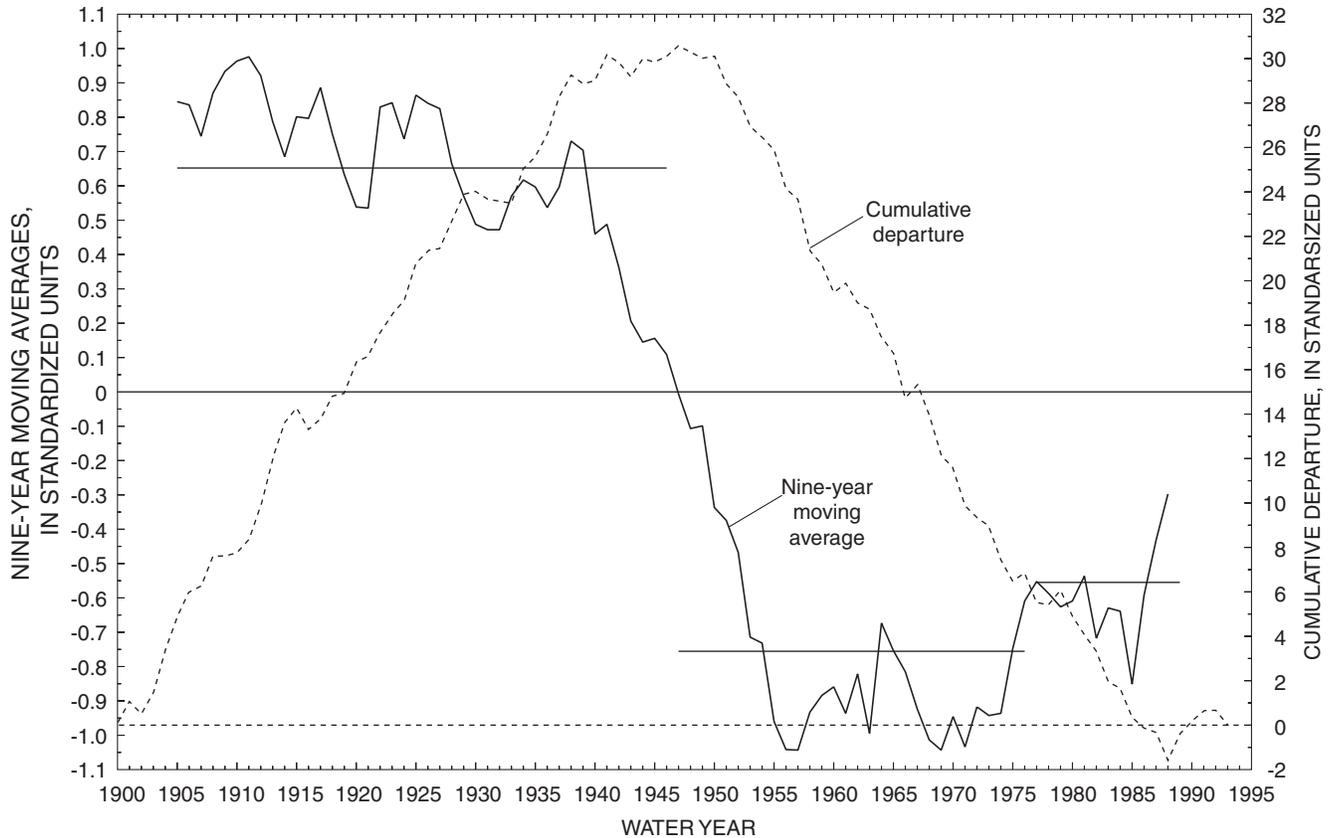
Figure 40. Nine-year moving averages and cumulative departures of water-year values for the North Atlantic Oscillation (NAO) index.

Horizontal lines are, from left to right, means for the PRE, BASE, and POST periods, calculated using the 9-year moving averages. The NAO is the dominant northern hemispheric circulation pattern, and its index was calculated using sea-level pressure data based on the summer patterns of Barnston and Livezey (1987).

Potential hemispheric linkages to the HM regime are shown by water-year anomalies for the NAO index and the Spokane River (site 27, table 1) (fig. 41; the values for the Spokane River have been reversed in sign for comparison). Although there is poor correlation between interannual variations of the two series, the overall trends and periods of departures from long-term means match reasonably well. Additionally, at the decadal scale, the correlation is -0.70 between 9-year moving averages of these two series for the period 1901-91. The cumulative departures for these two series (not shown) indicate this match and also show that the major difference between the series occurs after 1977, again suggesting the importance of the tropics as measured by the SOI and the North Pacific region in mediating the 1977 shift in the HM regime,

consistent with the fact that SSTs in the tropical Pacific are poorly linked to the NAO pattern and to the climatology of the North Atlantic region in general (Hurrell, 1995).

Nine-year moving averages of water year values of the Salmon River (site 52, table 1), the NAO index for October-March, and the October-March precipitation for the northeastern Washington climate division, which contains part of the drainage of the Spokane River, (fig. 42, NAO index reversed in sign for comparison) also suggest potential linkages to the HM regime. The correlation coefficients between the NAO index series and the Salmon River and precipitation series are -0.86 and -0.82, respectively, with the latter reflecting that of the Spokane River.
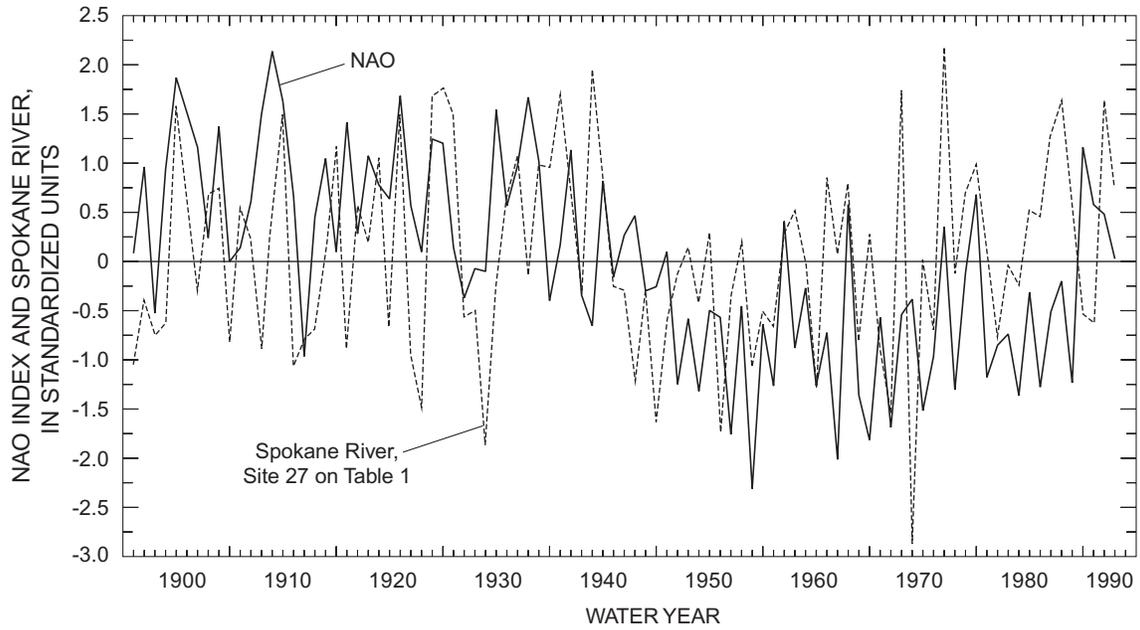
Figure 41. Water-year anomalies for the North Atlantic Oscillation (NAO) index and the Spokane River.
The values for the Spokane River have been reversed in sign for comparison.
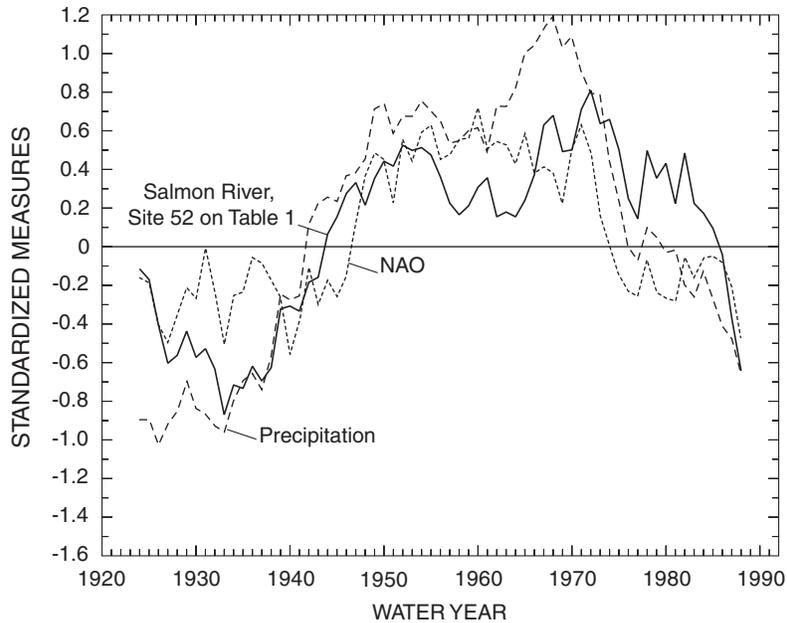
Figure 42. Nine-year moving averages of water-year values for the Salmon River, the
October-to-March North Atlantic Oscillation (NAO) index, and the October-to-March
precipitation for the northeastern Washington climate division.

The values for the NAO index have been reversed in sign for comparison.

Also note that, for the first 20 years of record, values for the Salmon River were generally in phase with the NAO index values but not with the winter divisional precipitation data; in the early 1940's the precipitation and the streamflow values became phase locked, suggesting an evolutionary shift in climatic forcing. The linkages suggested by figure 42 information are consistent with the contemporaneous winter patterns of Barnett and Preisendorfer (1978), which show both a PNA and a NAO type of pattern.

Ice-Concentration Data

Cumulative departures of the ice concentration for the East Greenland Shelf and Fram Strait (fig. 43A,B) show distinct changes with respect to shifts and their intermonthly variations in concentrations. The water-year values for the East Greenland Shelf display a minor shift at about 1917 and two major shifts at 1947 and 1972. Although the monthly data display the same major change near 1946-47 as the water-year values, there are distinct differences between April and May, especially between about 1920-30. The monthly data also contain a change to below-average ice concentrations after 1969. Mardsen and others (1991), using the same data set, show a distinct peak about 1969 for monthly ice-area anomalies for a region between about 62° to 72°N,5° to 22°W. In addition, winter concentrations suggest a shift in 1977. There is some consistency between the East Greenland Shelf water-year data and the NAO index, but with inconsistencies beginning about 1967-72. This period was one of persistent above-average ice extent for the complete Arctic region, and in about 1973 below-average ice extent began (Walsh and Johnson, 1979; Chapman and Walsh, 1991). The latter aspect appears to reflect the 1972-73 changes in the NAO index and the end of the salinity anomaly. Nine-year moving averages of the March-May ice concentration for the Shelf and the March-May and water year values of the NAO index (fig. 43C) show similarities on the decadal scale from the early 1930's (described previously as reflecting the initiation of a shift in the North Atlantic climatic regime) to about 1967.

For the Fram Strait, the water-year values (fig. 43B) retain the 1946-47 shift and resemble a subdued and reversed NAO index (compare to fig. 40).

The apparent earlier and later shifts in ice concentration for the Shelf are not contained in the Fram Strait information, but the winter ice concentrations contain a shift in 1977. Although the May concentration data are consistent with the water-year data (including an earlier shift which would be expected to occur in the summer marginal ice zone), the April data are not consistent with either water-year or May data, which may be attributed to the large change in the marginal ice zone in the Fram Strait from March through May. These intermonthly differences probably represent the response to intermonthly differences in both the regional oceanography and atmospheric-circulation patterns. For example, decadal-scale linkages to the NAO circulation pattern are reasonably strong, with 9-year moving averages of the April and May NAO index values being correlated with the May ice-concentration values at a 0.01 level, with correlation coefficients of -0.70 and -0.59 respectively. These linkages are stronger than those of the East Greenland Sea.

Ice concentrations in the Bering Sea generally followed three temporal patterns of periods with above- or below-average ice concentrations, which in turn, vary by location. Cumulative departures at 65°N,179°W (fig. 44A, the Bering Strait-Gulf of Anadyr) display the first pattern—one of above-average values until 1952 (or later for the summer-transition months) and below-average values for the remaining period of record. The differences between April and May curves (fig. 44A) also show the effects of temporal variations in warming on ice cover. May, with a smaller end-of-month extent, is more affected by persistent changes in atmospheric circulation and temperature (air and sea) and is less affected by ice drift from the Chukchi Sea, which is ice covered from December through March (Chapman and Walsh, 1991). The later shift, 1952 in contrast to 1947, is probably related to this flux. Thus, assuming the 1946-47 boundary is valid for ice concentration, there appears to have been about a 5-year time lag to the hemispheric change that occurred in 1946-47 before a response in the Chukchi Sea began. The lag can also be seen in the April-June concentration data for the 1947-90 period (fig. 44B), which follow the ice-cover relations in the Bering Sea (Cavalieri and Parkinson, 1987).
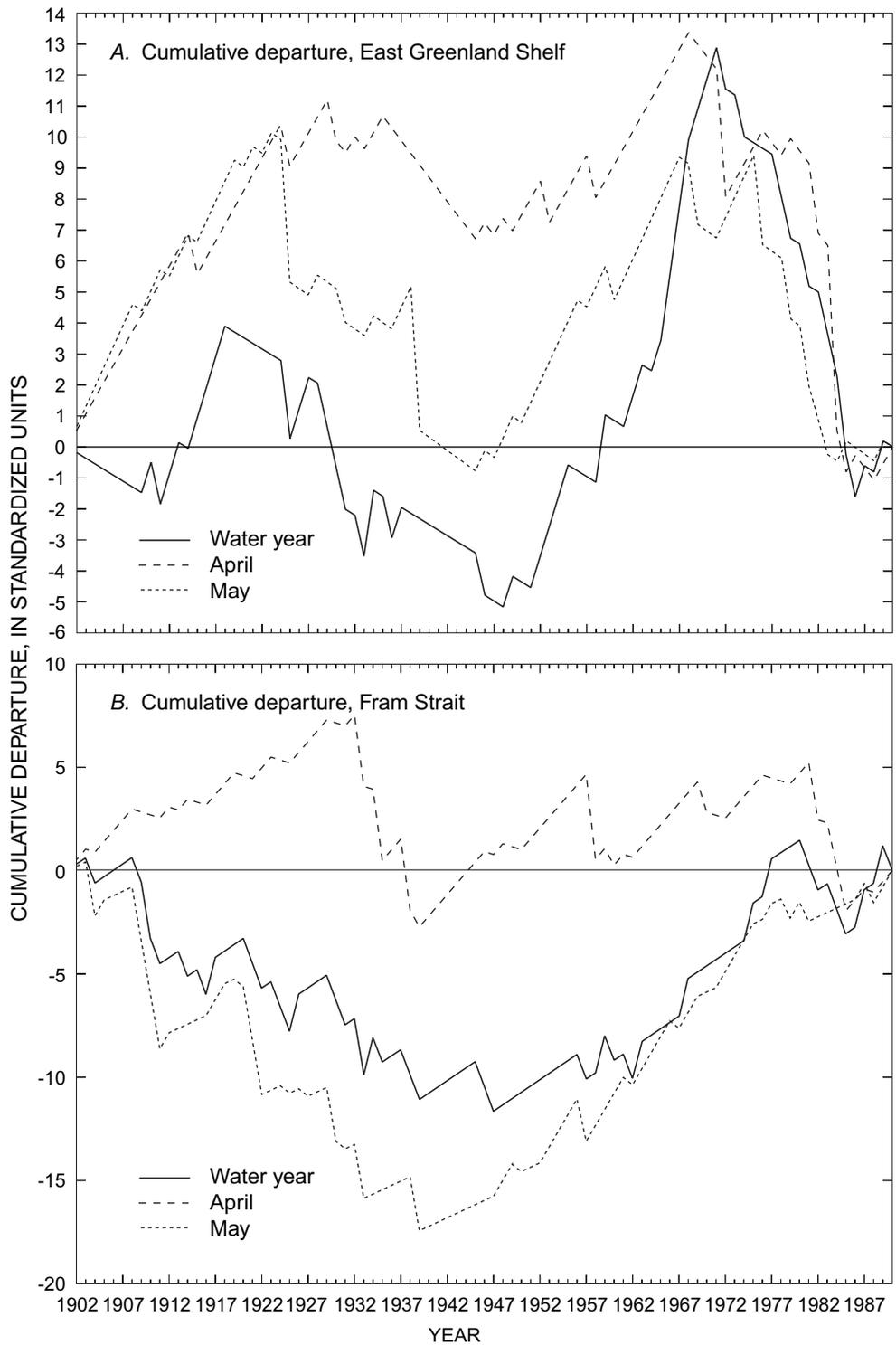
Figure 43. Cumulative departures for water year, April, and May sea-ice concentrations for the East Greenland Shelf (76°N,10°W) and for Fram Strait (78°N,4°W), and 9-year moving averages of values for the March-May ice concentration for the Shelf, and for the March-May and water-year North Atlantic Oscillation (NAO) index.

The sea-ice concentrations are monthly values for the end of a month. Grid locations are rounded to nearest whole degree. The values for the NAO index have been reversed in sign for comparison.
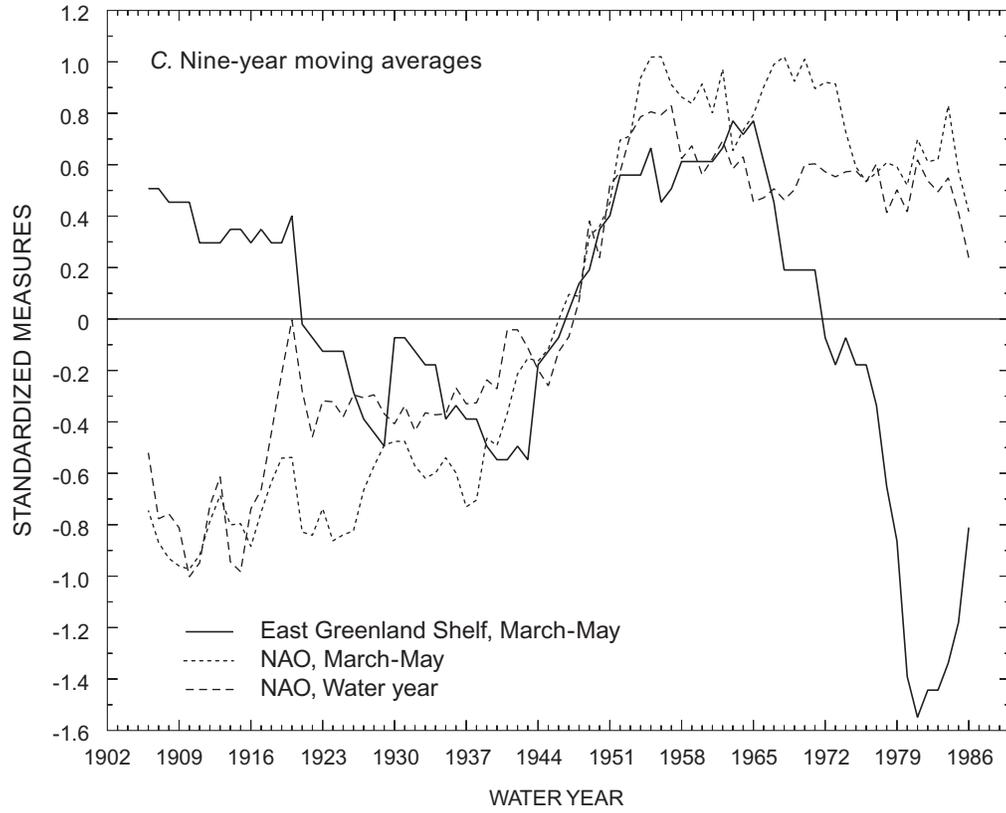
Figure 43. —*Continued.*
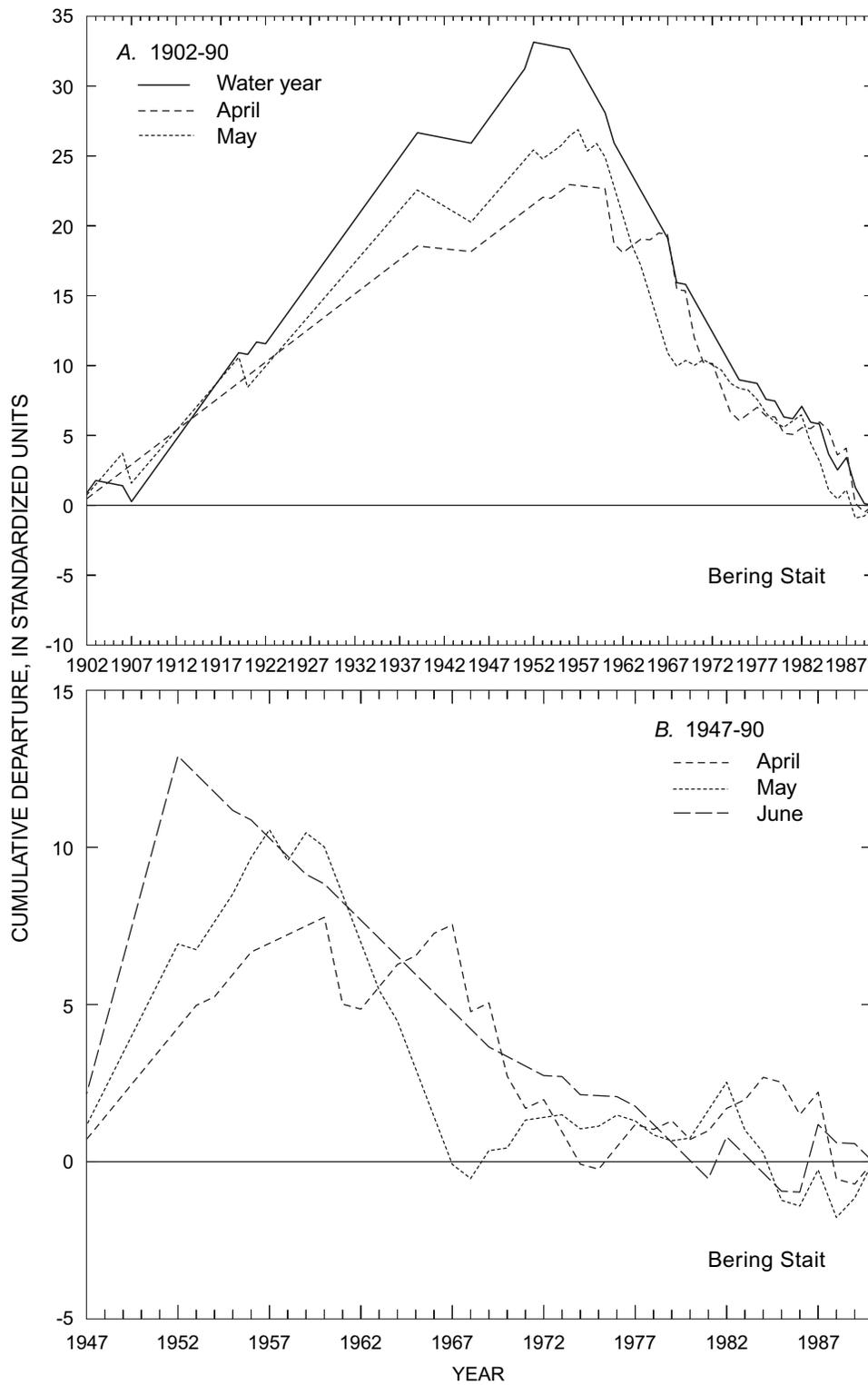
Figure 44. Cumulative departures for the sea-ice concentrations for an area near the Bering Strait (65°N,179°W) for the water year, April, and May for water years 1902-90, and for April, May, and June for water years 1947-90.

The sea-ice concentrations are monthly concentration values for the end of a month. Grid location is rounded to nearest whole degree.

The next Bering Sea pattern is displayed by the concentrations at 57°N,165°E, a grid point in the western Bering Sea (fig. 45A). This grid point was chosen because it lies near a center of low-pressure that occurs when January Aleutian temperatures are above average (Rogers, 1981). Thus, concentrations should be strongly related to circulation features, in particular the location of the Aleutian Low (Cavalieri and Parkinson, 1987), which, in turn, profoundly influences the HM regime. This grid point is also located near the northern winter center of the Western Pacific Oscillation of Barnston and Livezey (1987). Ice concentrations in this area are more affected by the ice drift from the Chukchi Sea than from the eastern Bering Sea (Walsh and others, 1985), and during the summer this area contains a strong western component of flow (Brasseur, 1991). In addition, ice cover in this area occurs only during February through May (only four May occurrences), and except for 1934, there was no ice cover from the 1902-45 period and from the 1960-74 period (for the 1975-90 only 3 years had ice-cover). Thus, ice cover at this location should be strongly related to climatic forcing.

The data contain two major shifts (fig. 45A), the first at 1946 and the second at 1952 or 1959, depending on the season (spring transition or water year, respectively). Comparison of figures 44A and 45A shows that the concentrations are out of phase for the first 46 years of record and generally in phase for the remaining period of record. Because ice cover in the western Bering Sea is influenced more by atmospheric-circulation features and regional oceanography than in the Strait, the abrupt change to ice-cover conditions after 1945 suggests an equally abrupt (and persistent) change in high-latitude circulation features. Differences between the western Bering Sea (fig. 45A) and the Fram Strait (fig. 43B) data suggest not only out-of-phase relations but also North Pacific and not hemispheric forcing. Cumulative departures of the water-year ice concentrations at this grid, an October-March index for the West Pacific Oscillation based on the winter centers of Barnston and Livezey (1987), and the simulated January-March snowpack for Cedar Lake (fig. 45B) indicate distinct decadal-scale phase changes in coherency between the circulation pattern and the ice and temperature data, and the apparent North Pacific forcing. The temporal variations in the values for each variable over their selected averaging periods (fig. 45B)

reflect (1) the temperature changes indicated by the climate division data for January through March, (2) the simulated snowpack for Cedar Lake containing a major change in the mid-1950's, and (3) the lack of ice cover after 1960.

Ice concentrations at 60°N,180°W for the northeastern Bering Sea (fig. 46) contain the third pattern of change. The data reflect three major regime changes that occurred at 1946, 1952, and 1970, mainly owing to intermonthly variations, including occurrence of ice cover. However, after 1977, there was no ice cover for 4 of the 6 months when cover occurs, indicating a rather abrupt change. The differences between the northeastern Bering Sea (fig. 46) and the Bering Strait (fig. 44A) indicate the effect of ice drift from the Chukchi Sea and regional oceanography /climatology on the ice concentrations for these two areas. The extended period of below-average values (lack of ice cover) for the first half of the record for the northeastern Bering Sea is not reflected in the Bering Strait data. The two areas are more in phase from 1952-70, after which there are again large differences. Note that this was not true for the western Bering Sea which, like the Strait, had consistent below-average water year values for the later period of record. The period of above-average values (existence of ice cover) from 1972-76 (fig. 46) suggests a regional forcing rather than a broader North Pacific forcing. This out-of-phase relationship forced by circulation has been described by Rogers (1981).

The ice-concentration data show large spatial and temporal variability due to the many physical factors. However, there are several aspects that stand out, the first of which is the general hemispheric coherency of the 1946-47 boundary. This boundary was also consistent with that of the two sea-level pressure indices. For the indices, the NAO index did not contain a major regime shift at 1977, but the CNP index did. The lack of a strong 1977 shift for the NAO index suggested that the shift would not be contained in the North Atlantic ice-concentration data. The 1977 shift, however, was expected to be strongly represented in all the Bering Sea data because of (1) the shift in the CNP index, (2) the known large-scale influence of atmospheric circulation on the extent of ice cover in the Bering Sea, and (3) the existence of the shift in most of the North Pacific/Pacific Northwest information analyzed in this study.
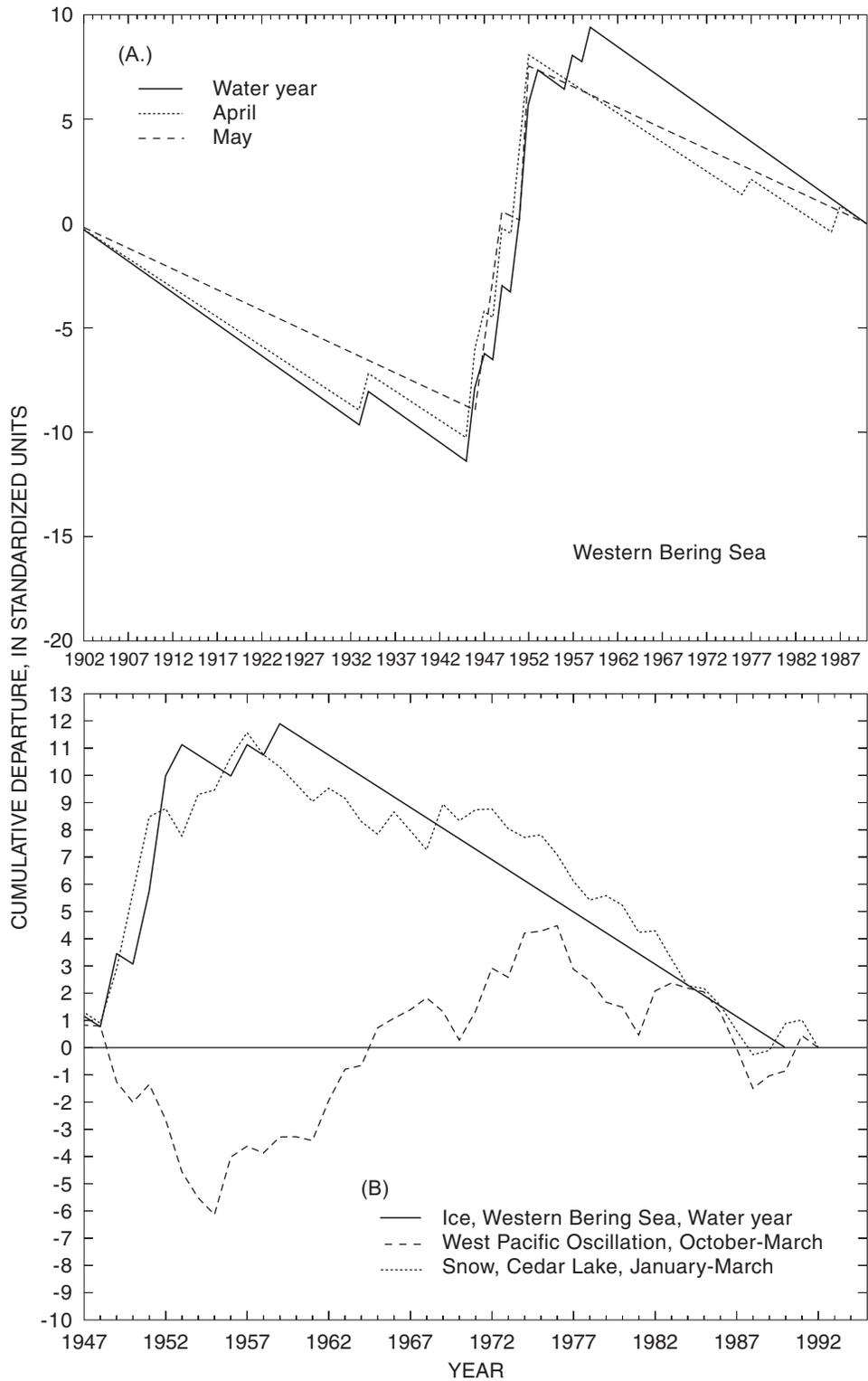
Figure 45. Cumulative departures for the water year, April, and May sea-ice concentrations for the western Bering Sea (57°N,165°E), and for water-year sea-ice concentrations in the western Bering Sea, the October-March index for the West Pacific Oscillation, and simulated January-March snowpack for Cedar Lake, Washington.

The sea-ice concentrations are monthly values for the end of a month. Grid location is rounded to nearest whole degree.
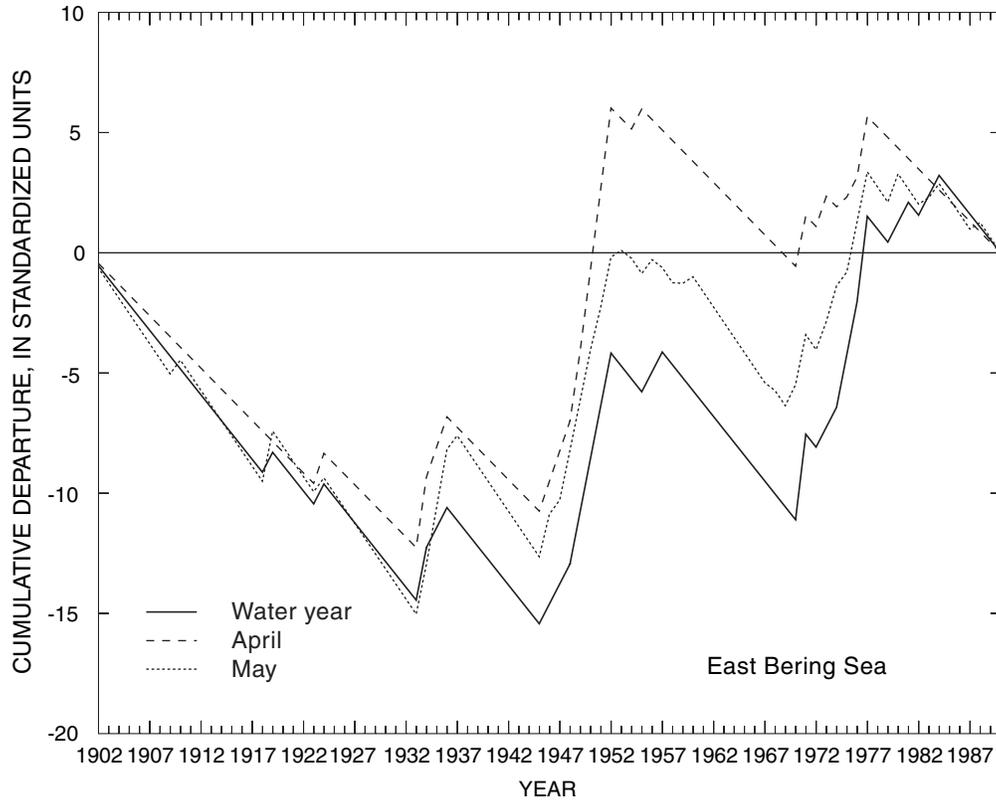
Figure 46. Cumulative departures for the water year, April, and May sea-ice concentrations for the northeastern Bering Sea (60°N,180°W).

Monthly values are for the end of a month. Grid location is rounded to the nearest whole degree.

The 1977 boundary did not define a major regime change in the water-year and spring-transition periods of the ice-concentration data, but a change was estimated to occur during the winter season for the North Atlantic data. For the North Pacific data for 1977, regime shifts are displayed by the concentration data for the northeastern Bering Sea, with no occurrences of ice cover after 1977 for December-

February and May, and with declining ice cover during March and April. These results suggest that, unlike in 1946-47, the effects of climate forcing, which so dramatically altered the HM regime in 1977, were not large enough to clearly affect or initiate a significant regime change in the ice cover throughout the Bering Sea.

CONCLUSIONS

Over the twentieth century, the hydrometeorological (HM) regime in the Pacific Northwest has experienced large interdecadal regime changes. These changes reflect large shifts in the mean in comparison to the climatological mean during the 1947-76 base period, appear to be continually evolving, and are forced by atmospheric circulation and oceanic factors (sea-surface temperatures (SSTs), and although not analyzed in this study, current patterns). Although the relations between the data series are complex, there is a strong linkage between the HM regime in the Pacific Northwest and atmospheric pressures and SSTs over the North Pacific.

The interdecadal periods chosen for study were defined by boundaries that were based on analysis of the HM data and previous studies. It was determined that shifts generally occurred at the pre-defined 1946-47 and 1976-77 boundaries. These shifts reflect transitions to periods of generally persistent above- and below-average values of precipitation and streamflow. In comparison to the 1947-76 period, the pre-1947 and the post-1976 periods exhibited dryer conditions. However, differences in precipitation, streamflow, and air temperature between the PRE and POST periods show that the HM and climatic regimes during the pre-1947 and post-1976 periods were different. The effects of these shifts have large implications for water resources in the Pacific Northwest. This is especially true of the 1977 shift because it is associated with a HM-regime change that appears to be continuing as of 1994.

The changes were caused by adjustments in hemispheric-global atmospheric circulation and are consistent with SST anomaly patterns on a regional-basin scale. The measures of atmospheric-circulation forcing generally show regime shifts at the same boundaries as the HM data, and this also was found to be true for the SST data. The shifts in the atmospheric-circulation measures and SSTs generally reflect significant changes in the mean for the different seasons and months analyzed. The 700-millibar data indicate that there has been a distinct strengthening or weakening of selected, dominant hemispheric circulation patterns, in many cases reflecting a rather striking shift to a more or a less persistent state; the latter aspect was shown to be especially true for the Pacific/North America (PNA) pattern. This abrupt change also is displayed by tropical Pacific anomaly behavior as indicated by the Southern Oscillation Index (SOI). When the SOI is in its negative state (warm central-eastern tropical SSTs), conditions generally are warm and dry in the Pacific Northwest, and the opposite occurs when the SOI is in its positive state. The concurrency of SST shifts and their associated significant trends indicate the importance of the ocean-atmosphere coupling. In the North Pacific, this coupling is strongest during October-March, and a decoupling in the spring-transition season of April-May is suggested. This apparent decoupling was also seen in divisional temperature data, winter and spring circulation indices, and in the response of snowpack and precipitation. Together, the analysis of atmospheric and SST data identifies a strong linkage to the HM regime in the Pacific Northwest.

Regional measures of atmospheric circulation also indicate this linkage, and generally provide more information in explaining the changes in the HM regime than the North Pacific measures; that is, on a monthly basis the HM regime is directly influenced by regional atmospheric-circulation and SST patterns. Although hemispheric measures do not explain as much of the change as the North Pacific/Pacific Northwest measures, on a decadal scale the coherency of the hemispheric North Atlantic Oscillation (NAO) pattern and selected HM data suggests a reasonable linkage. The importance of the hemispheric information appears to be a function of its coherency with the North Pacific and the tropical regions, the latter because of the influence of the El Niño/Southern Oscillation phenomenon.

The apparent evolutionary nature of changes in the HM regime also is displayed by the atmospheric and SST data—the nature of their changes is complex because of their temporal and spatial variations caused by complex dynamics that are further influenced by the pronounced seasonality in the North Pacific. Depending on the season or month analyzed, several other temporal boundaries appear to define important regime shifts, in particular, 1957, 1967, and 1982. The analyses of this study's data suggest that 1957 and 1967 were times of hemispheric changes that were, in some way, translated through the ocean-atmosphere system such that only selected data series for selected seasons or months contain a shift at these times.

Only the 1946-47 shift appears to have been both coherent and strong throughout the Northern Hemisphere and, on a decadal scale, throughout the tropics as measured by the SOI. The 1977 climate shift does not appear to have been hemispheric in nature, at least within the framework of the North Atlantic information analyzed, but appears to be mainly related to tropics-North Pacific dynamics. However, although the sea-level pressure NAO index and a 700-mb NAO index based on March centers did not exhibit a shift in 1977, the difference in composites (POST minus BASE) of the 700-mb data for March indicate a strengthening of the NAO, but with a reasonably large eastward translation of the centers of its dipole. This strengthening, suggesting a 1977 shift, would not have been captured by the NAO indices. In contrast, the North Atlantic ice-concentration data did not contain a clear shift in 1977.

The differences between the 1946-47 and 1976-77 shifts indicate the larger control atmospheric circulation in the North Pacific region, in contrast to hemispheric and tropical, on the HM regime. The SST data and the atmospheric measures further suggest that the 1977 shift in the HM regime was mainly mediated by changes over the North Pacific, which in turn were strongly influenced by changes in the tropics, in particular by persistent changes in SSTs associated with the Southern Oscillation (SO). Additionally, the 1977 shift appears to have been more evolutionary in nature, perhaps representing the combination of several modes or frequencies of variability in the ocean-atmosphere system in the North Pacific, with the system evolving to some new state.

The evolutionary nature of the changes in the HM regime and the profound effects of the major climate shifts on the regime identify an important component of climate variability that needs to be analyzed—the cause of the shifts and how they transfer through the ocean-atmosphere system (including time scales) on through the hydrologic system. Although these have been analyzed diagnostically to explain the atmospheric-circulation features that led to "abnormal" hydrologic conditions (see, for example, Namias, 1978), their underlying cause and subsequent persistence have not been analyzed. Dynamic models may elucidate underlying factors and have been used as such, but the recent abrupt shifts in this century have not been explicitly analyzed. Although much larger shifts have occurred historically in the Pacific

Northwest (Graumlich, 1985), it is only in this century that consistent and plentiful oceanic, atmospheric, and HM data have become available. The hemispheric nature, abruptness, and magnitude of the 1946-47 shift suggest that improved understanding of it, in contrast to the 1977 shift, may lead to an improved ability to describe the global-climate system. In addition, understanding the mechanism and persistence of the 1977 climate shift would allow for improved understanding of the tropical-North Pacific-Pacific Northwest linkage. Because water resources are important to the economy of the Pacific Northwest, the analysis of these recent shifts can provide valuable information for future planning and management of these resources.

An additional and important consideration of changes in the HM regime is how the historical data can be used in the management of resources. This would include deciding which "piece" of the historical data record to use in developing management tools such as models and management strategies. Based on the concept of three major interdecadal regimes, the HM data are essentially the outcome derived from three different climatic states, each with its own characteristics (persistence of circulation modes-SSTs and their associated statistics). That is, because of the combined influence of both water input (precipitation) and temperature on land-surface processes, the net outcome (streamflow) consists of at least three populations, the characteristics of which are retained by precipitation. Thus, to estimate characteristics of such hydrologic aspects as the length of consecutive wet or dry periods (floods-droughts), the mean prevailing ocean-atmosphere forcing occurring during some defined period needs to be determined. These concepts have large implications for managing water resources in the Pacific Northwest. For example, in the 14,374 square kilometers of the Yakima River Basin in eastern Washington (output measured by site 112, table 1), more recent "normal" precipitation and April 1 snow-water content are yielding less streamflow than that produced under these same "normal" conditions in earlier time-periods (D. Schram, U.S. Bureau of Reclamation, 1994, oral commun.). Thus, given the available length of record for most HM data in the Pacific Northwest, normals may best be defined by the BASE period (floods) and POST period (floods, droughts, water availability).

This is especially true because running means of precipitation and streamflow (not shown) do not become stable until about 40-60 years (depending on the site) due to the documented shifts. The temporal variations in the mean for precipitation and streamflow indicate that the inclusion of the PRE period in this and other analyses also is important for proper interpretation of HM variability and its regime changes and attendant climate forcing.

REFERENCES CITED

Aguado, E., Cayan, D.R., Riddle, L., and Roos, M., 1992, Climatic fluctuations and the timing of West Coast streamflow: Journal of Climate, v. 5, p. 1468-1483.

American Geophysical Union, 1987, El Niño: Journal of Geophysical Research, v. 92(C13), p. 14,187-14,479.

Angell, J.K., and Korshover, J.,1981, Comparison between sea surface temperature in the equatorial eastern Pacific and United States surface temperatures: Journal of Applied Meteorology, v. 20, p. 1105-1110.

Barnett, T.P., and Preisendorfer, R.W., 1978, Multifield analog prediction of short-term climate fluctuations using a climate state vector: Journal of Atmospheric Sciences, v. 35, p. 1771-1787.

Barnston, A.G., and Livezey, R.E., 1987, Classification, seasonality and persistence of low-frequency atmospheric circulation patterns: Monthly Weather Review, v. 115, p. 1083-1126.

Bauer, H.H., and Vaccaro, J.J., 1986, Model estimates of climatological variability on ground water:— Conference on climate and water management, A critical era: Ashville, NC, American Meteorological Society, August 4-7, 1986, p. 45-49.

Bauer, H.H., and Vaccaro, J.J., 1990, Estimates of ground-water recharge to the Columbia Plateau region aquifer system, Washington, Oregon, and Idaho, for predevelopment and current land-use conditions: U.S. Geological Survey Water-Resources Investigations Report 88-8108, 37 p.

Bjerknes, J.H., 1969, Atmospheric teleconnections from the equatorial Pacific: Monthly Weather Review, v. 97, p. 162-172.

Brasseur, P.J., 1991, A variational inverse method for the reconstruction of general circulation fields in the northeastern Bering Sea: Journal of Geophysical Research, v. 96(C3), p. 4891-4907.

Cane, M.A., 1986, El Niño: Annual Review of Earth Planet Science, v. 14, p. 43-70.

Cane, M.A., and Zebiak, S.E., 1985, A theory for El Niño and the Southern Oscillation: Science, v. 228, p. 1085-1087.

Cavalieri, D.J., and Parkinson, C.L., 1987, On the relationship between atmospheric circulation and the fluctuations in the sea ice extents of the Bering and Okhotsk Seas: Journal of Geophysical Research, v. 92(C7), p. 7141-7162.

Cayan, D.R., and Peterson, D.H., 1989, The influence of North Pacific atmospheric circulation on streamflow in the west, in Peterson, D.H., ed., Aspects of climate variability in the Pacific and Western Americas: Geophys. Mono. v. 55, Washington, D.C., American Geophysical Union, p. 375-397.

Cayan, D.R., and Webb, R.H., 1992, El Niño/Southern Oscillation and streamflow in the western United States, in Diaz, H.F. and Markgraf, V.M., eds., El Niño, Historical and paleoclimatic aspects of the Southern Oscillation: Cambridge, England, Cambridge University Press, p. 29-68.

Chapman, W.L., and Walsh, J.E., 1991, Long-range prediction of regional sea ice anomalies in the Arctic: Weather and Forecasting, v. 6, p. 271-288.

Christensen, R.A., and Eilbert, R.F., 1985, Seasonal precipitation forecasting with a 6-7 month lead time in the Pacific Northwest using an information theoretic model: Monthly Weather Review, v. 113, p. 502-518.

Dettinger, M.D., Cayan, D.R., and McCabe, G. J., 1993, Decadal trends in runoff over the western United States and links to persistent North Pacific sea-surface-temperature and atmospheric-circulation patterns: Boulder, Colo, Proceedings of the 18th Annual NOAA Climate Diagnostics Workshop, November 1993.

Dettinger, M.D., and Cayan D.R., 1995, Large-scale atmospheric forcing of recent trends toward early snowmelt runoff in California: Journal of Climate, v. 8, p. 606, 623.

Diaz, H.F., and Markgraf, V.M., eds., 1992, El Niño, Historical and paleoclimatic aspects of the Southern Oscillation: Cambridge, England, Cambridge University Press, 479 p.

Dickson, R.R., and Namias, J., 1976, North American influences on the circulation and climate of the North Atlantic sector: Monthly Weather Review, v. 104 (10), p. 47-57.

Dickson, R.R., Lamb, H.H., Malinberg, S.A., and Colebrook, J.M., 1975, Climatic reversal in the northern North Atlantic: Nature, v. 256, p. 479-482.

Dickson, R.R., Meinke, J., Malinberg, S.A., and Lee, A.J., 1988, The great salinity anomaly in the northern North Atlantic, 1968-1982: Progressive Oceanography, v. 20, p. 103-151.

Douglas, A.V., Cayan, D.R., and Namias, J., 1982, Large-scale changes in North Pacific and North American weather patterns in recent decades: Monthly Weather Review, v, 110, p. 1852-1862.

Dunn, C.R., 1957, The weather and circulation of December, 1957: Monthly Weather Review, v. 85, p. 409-416.

Ebbesmeyer, C.C., Coomes, C.A., Cannon, G.A., and Bretschneider, D.E., 1989, Linkage of ocean and fjord dynamics at decadal period, *in* Peterson, D.H., ed., Aspects of climate variability in the Pacific and Western Americas: Geophys. Mono. 55, Washington, D.C., American Geophysical Union, p. 399-417.

Francis, R.C., Hare, S.R., Hollowed, A.B., and Wooster, W.S., 1995, Effects of interdecadal climate variability on the oceanic ecosystems of the Northeast Pacific Ocean: Asilomar, Calif., Abstracts, Twelfth Annual Pacific Climate (PACLIM) Workshop, May 2-5, 1995.

Gladwell, J.S., 1970, Runoff generation in western Washington as a function of precipitation and watershed characteristics: Seattle, Wash., Washington State University, Bulletin 319, College of Engineering Research Division, R.L. Albrook Hydraulic Lab, 341 p.

Graumlich, L., 1985, Long-term records of temperature and precipitation in the Pacific Northwest derived from tree rings: Seattle, Wash., University of Washington, Ph.D. thesis, 198 p.

Horel, J.D., and Wallace, J.M., 1981, Planetary-scale atmospheric phenomena associated with the Southern Oscillation: Monthly Weather Review, v. 109, p. 813-829.

Hurrell, J.W., 1995, Decadal trends in the North Atlantic Oscillation—Regional temperatures and precipitation: Science, v. 269, p. 676-679.

Ikeda, M., Symonds, G., and Yao, T., 1988, Simulated fluctuations in the Labrador sea-ice cover: Atoms. Oceans, v. 26(1), p. 16-39.

Johnson, C.M., 1980, Wintertime Arctic sea ice extremes and the simultaneous atmospheric circulation: Monthly Weather Review, v. 108, p. 1782-1791.

Jones, P.D, Raper, S.C., Bradley, R.S., Diaz, H.F., Kelly, P.M., and Wigley, T.M., 1986, Northern Hemisphere surface air temperature variations—1851-1984: J. Clim. Appl. Meteor., v. 25, p. 161-179.

Julian, P.R., and Chervin, R.M., 1978, A study of the Southern Oscillation and Walker Circulation phenomenon: Monthly Weather Review, v. 106, p. 1433-1451.

Kahya, Ercan, and Dracup, J.A., 1992, Streamflow and La Nina event relationships in the ENSO-streamflow core areas, *in* Redmond, K.T., and Tharp, V.L., eds., Proceedings of the Ninth annual Pacific climate (PACLIM) workshop, April 21-24, 1992: California Department of Water Resources Interagency Ecological studies program, Technical Report 34, p. 89-96.

Kelly, P.M., Goodess, C.M., and Cherry, B.S., 1987, The interpretation of the Icelandic sea ice record: Journal of Geophysical Research, v. 92(C10), p. 10,835-10,843.

Kresch, D.L., 1994, Variability of streamflow and precipitation in Washington: U.S. Geological Survey Water-Resources Investigations Report 93-4132, 32 p.

Levitus, S., 1989a, Interpentadal variability of temperature and salinity at intermediate depths of the North Atlantic Ocean, 1970-1974 versus 1955-1959: Journal of Geophysical Research, v. 94(C5), p. 6091-6131.

———1989b, Interpentadal variability of salinity in the upper 150 m of the North Atlantic Ocean, 1970-1974 versus 1955-1959: Journal of Geophysical Research, v. 94(C7), p. 9679-9685.

———1989c, Interpentadal variability of temperature and salinity in the deep North Atlantic, 1970-1974 versus 1955-1959: Journal of Geophysical Research, v. 94(C11), p. 16,125-16,131.

———1990, Interpentadal variability of steric sea level and geopotential thickness of the North Atlantic Ocean, 1970-1974 versus 1955-1959: Journal of Geophysical Research, v. 95(C4), p. 5233-5238.

Leytham, K.M., 1982, Physical considerations in the analysis and synthesis of hydrologic sequences: Seattle, Wash., University of Washington, College of Engineering, Department of Civil Engineering Technical Report No. 76, Charles W. Harris Hydraulics Laboratory, 238 p.

Markham, C.G., 1979, Pacific sea-surface temperatures related to rain in California: Journal of Climate and Applied Meteorology, v. 18, p. 1369-1370.

Marsden, R.F., Mysak, L.A., and Myers, R.A., 1991, Evidence for stability enhancement of sea ice in the Greenland and Labrador Seas: Journal of Geophysical Research, v. 96(C3), p. 4783-4789.

Mayo, L.R., and March, R.S., 1990, Air temperature and precipitation at Wolverine Glacier, Alaska—glacier growth in a warmer, wetter climate: Annuals of Glaciology, v. 14, p. 191-194.

McDonald, C.C., and Riggs, H.C., 1948, Annual runoff in the Columbia River Basin in percent of the mean, 1928-45: U.S. Geological Survey Circular 36, 2 p., 19 plates.

McGuirk, J.P., 1982, A century of precipitation variability along the Pacific coast of North America and its impact: Climatological Change, v. 4, p. 41-56.

Miller, A.J., Cayan, D.R., Barnett, T.P., Graham, N.E., and Oberhuber, J.M., 1992a, The 1976-77 climate shift of the Pacific Ocean: Oceanography, v. 7, p. 21-25.

———1992b, Interdecadal variability of the Pacific Ocean: model response to observed heat flux and wind stress anomalies: Climate Dynamics, v. 9, p. 287-302.

Namias, J., 1959, Recent seasonal interactions between North Pacific waters and the overlying atmosphere circulation: Journal of Geophysical Research, v. 65(6), p. 631-646.

———1965, Macroscopic association between mean monthly sea-surface temperature and the overlying winds: Journal of Geophysical Research, v. 70(10), p. 2307-2318.

———1969, Seasonal interactions between the North Pacific Ocean and atmosphere during the 1960's: Monthly Weather Review, v. 97, p. 173.

———1975, Stabilization of atmospheric circulation patterns by sea surface temperatures: Journal of Marine Research, v. 33, p. 53-60.

———1976a, Some statistical and synoptic characteristics associated with El Niño: Journal of Physical Oceanography, v. 6, p. 130-138.

———1976b, Negative ocean-air feedback systems over the North Pacific in the transition from warm to cold seasons: Monthly Weather Review, v. 104 (9), p. 32-46.

———1978, Multiple causes the North American abnormal winter 1976-77: Monthly Weather Review, v. 106 (3), p. 67-82.

———1980, Some concomitant regional anomalies associated with hemispherically averaged temperature variations: Journal of Geophysical Research, v. 85 (C3), p. 1585-1590.

———1981, Teleconnections of 700 mb height anomalies for the northern hemisphere: La Jolla, Calif., CALCOFI Atlas 29, Scripps Inst. of Oceanogr. v. 265 p.

———1988, Persistence of North Pacific sea surface temperature and atmospheric flow patterns: Journal of Climate, v. 1, p. 682-703.

Niebauer, H.J., 1980, Sea ice and temperature variability in the eastern Bering Sea and the relation to atmospheric fluctuations: Journal of Geophysical Research, v. 85, p. 7507-7515

Quinn, W.H., Neal, V.T., and Antunez de Mayolo, S.E., 1987, El Niño occurrences over the past four and half centuries: Journal of Geophysical Research, v. 92 (C13), p. 14, 449-14,461.

Rasmusson, E.M., Wang, X., and Ropelewski, C.F., 1990, The biannual component of ENSO variability: Journal of Marine Systems, p. 71.

Redmond, K.T., and Koch, R.W., 1991, Surface climate and streamflow variability in the Western United States and their relationship to large-scale circulation indices: Water Resource Research, v. 27(9), p. 2381-2399.

Rogers, J.C., 1981, The North Pacific Oscillation: Journal of Climatology, v. 1, p. 39-57.

———1985, Atmospheric circulation changes associated with the warming over the northern North Atlantic in the 1920's: Journal of Climate and Applied Meteorology, v. 24, p. 1303-1310.

Ropelewski, C.F., and Halpert, M.S., 1986, Global and regional scale precipitation patterns associated with El Niño/Southern Oscillation (ENSO): Monthly Weather Review, v. 114, p. 2352-2362.

Ropelewski, C.F., and Jones, P.D., 1987, An extension of the Tahiti-Darwin Southern Oscillation Index: Monthly Weather Review, v. 115, p. 2161-2165.

Schermerhorn, V.P., 1967, Relations between topography and annual precipitation in western Oregon and Washington: Water Resource Research, v. 3(3), p. 707-711.

Speers, P., and Mass, C.F., 1986, Diagnosis and prediction of precipitation in regions of complex terrain: Washington State Deptartment of Transportation, WA-RD 91.1, 166 p.

Torranin, P., 1972, Applicability of canonical correlation in hydrology—Hydrology papers, No. 58: Fort Collins, Colo., Colorado State University, 30 p.

U. S. Department of Agriculture, 1916-1940, Climatological Data, Washington Section: Weather Bureau.

———1936, Climatic Summary of the United States, Section 1. Western Washington, inclusive through 1930: Weather Bureau.

U. S. Department of Commerce, 1940-1965, Climatological Data, Washington: Weather Bureau, July 1940-December 1965.

———1956, Climatography of the United States, Climatic Summary of the United States-Supplement for 1931 through 1952, Washington: Weather Bureau, No. 11-39.

———1966-1970, Climatological Data, Washington: Environmental Science Services Administration, January 1966-September 1970.

———1970-1988, Climatological Data, Washington: National Oceanic and Atmospheric Administration, September 1970-December 1988.

Vaccaro, J.J., 1992a, Plan of study for the Puget-Willamette Lowland regional aquifer system analysis, western Washington and western Oregon: U.S. Geological Survey Water-Resources Investigations Report 92-4189, 41 p.

———1992b, Sensitivity of groundwater recharge estimates to climate variability and change, Columbia Plateau, Washington: Journal of Geophysical Research, v. 97 (D33), p. 2821-2833.

van Heeswijk, M., Kimball, J.S., and Marks, D., 1996, Simulation of water available for runoff in clearcut forest openings during rain-on-snow events in the western Cascade Range of Oregon and Washington: U.S. Geological Survey Water-Resources Investigations Report 95-4219, 67 p.

Van Loon, H., and Rogers, J.C., 1978, The seesaw in winter temperatures between Greenland and Northern Europe, Part I—General description: Monthly Weather Review, v. 106, p. 296-310.

Wahl, K.L., 1991, Is April to July runoff really decreasing in the western United States: Juneau, Alaska, Proceedings of the Western Snow Conference, p. 67-68.

———1992, Evaluation of trends in runoff in the western United States. Managing Water Resources during Global Change: Reno, Nev, Proceedings, 28th Annual Conference and Symposium, American Water Resources Association, p. 701-710.

Wallace, J.M., and Gutzler, D.S., 1981, Teleconnections in the geopotential height field during the northern hemisphere winter: Monthly Weather Review, v. 109, p. 784-812.

Walsh, J.E., and Johnson, C.M., 1979, An analysis of Arctic Sea ice fluctuations, 1953-77: Journal of Physical Oceanography, v. 9, p. 580-591.

Walsh, J.E., and Sater, J.E., 1981, Monthly and seasonal variability in the ocean-atmosphere systems of the North Pacific and North Atlantic: Journall of Geophysical Research, v. 86 (C8), p. 7425-7445.

Walsh, J.E., Richman, M.B., and Allen, D.W., 1982, Spatial coherence of monthly precipitation in the United States: Monthly Weather Review, v. 110, p. 272-286.

Walsh, J.E., Hibler, W.D., and Ross, B., 1985, Numerical simulation of Northern Hemisphere sea ice variability, 1951-80: Journal of Geophysical Research, v. 90 (C3), p. 4847-4865.

Walters, R.A., and Meier, M.F., 1989, Variability of glacier mass balances in western North America, in Peterson, D.H., ed., Aspects of climate variability in the Pacific and Western Americas. Geophys. Mono. v. 55: Washington, D.C., American Geophysical Union, p. 375-397.

White, W.B. and Walker, A.E., 1973, Meridional atmospheric teleconnections over the North Pacific from 1950 to 1972: Monthly Weather Review, v. 101, p. 817-822.

Wyrtki, K., 1984, The slope of the seas level along the equator during the 1982-83 El Niño: Journal of Geophysical Research, v. 89(C8), p. 10,419-10,424.

———1985, Water displacements in the Pacific and the genesis of El Niño cycles: Journal of Geophysical Research, v. 90(C4), p. 7129-7132.

Yarnal, B., and Diaz, H.F., 1986, Relationships between extremes of the Southern Oscillation and the winter climate of the Anglo-American Pacific coast: Journal of Climatology, v. 6, p. 197-219.

≋USGS

Vaccaro

Interdecadal Changes in the Hydrometeorological Regime of the Pacific Northwest

WRIR 02-4176